Published January 26, 2015

New method for determining total calcium content in tissue applied to skeletal muscle with and without calsequestrin

Cédric R.H. Lamboley,[1] Sandrine A. Kake Guena,[2] Fatou Touré,[2] Camille Hébert,[2] Louiza Yaddaden,[2] Stephanie Nadeau,[2] Patrice Bouchard,[3] Lan Wei-LaPierre,[4] Jean Lainé,[2] Eric C. Rousseau,[2] Jérôme Frenette,[3] Feliciano Protasi,[5] Robert T. Dirksen,[4] and Paul C. Pape[2]

[1]Institute of Sport, Exercise and Active Living, Victoria University, Melbourne, Victoria 8001, Australia
[2]Département de physiologie et biophysique, Université de Sherbrooke Faculté de Médicine et des Sciences de la Santé, Sherbrooke, Québec J1H5N4, Canada
[3]Département de Réadaptation, Université Laval, Québec G1K 7P4, Canada
[4]Department of Pharmacology and Physiology, University of Rochester Medical Center, Rochester, NY 14642
[5]Center for Research on Aging and Department of Neuroscience, Imaging and Clinical Sciences, "*G. d'Annunzio*" University of Chieti-Pescara, I-66100 Chieti, Italy

We describe a new method for determining the concentration of total Ca in whole skeletal muscle samples ($[Ca_T]_{WM}$ in units of mmoles/kg wet weight) using the Ca-dependent UV absorbance spectra of the Ca chelator BAPTA (1,2-bis(2-aminophenoxy)ethane-*N*,*N*,*N*′,*N*′-tetraacetic acid). Muscle tissue was homogenized in a solution containing 0.15 mM BAPTA and 0.5% sodium dodecyl sulfate (to permeabilize membranes and denature proteins) and then centrifuged. The solution volume was adjusted so that BAPTA captured essentially all of the Ca. $[Ca_T]_{WM}$ was obtained with Beer's law from the absorbance change produced by adding 1 mM EGTA to capture Ca from BAPTA. Results from mouse, rat, and frog muscles were reasonably consistent with results obtained using other methods for estimating total [Ca] in whole muscles and in single muscle fibers. Results with external Ca removed before determining $[Ca_T]_{WM}$ indicate that most of the Ca was intracellular, indicative of a lack of bound Ca in the extracellular space. In both fast-twitch (extensor digitorum longus, EDL) and slow-twitch (soleus) muscles from mice, $[Ca_T]_{WM}$ increased approximately linearly with decreasing muscle weight, increasing approximately twofold with a twofold decrease in muscle weight. This suggests that the Ca concentration of smaller muscles might be increased relative to that in larger muscles, thereby increasing the specific force to compensate for the smaller mass. Knocking out the high capacity Ca-binding protein calsequestrin (CSQ) did not significantly reduce $[Ca_T]_{WM}$ in mouse EDL or soleus muscle. However, in EDL muscles lacking CSQ, muscle weights were significantly lower than in wild-type (WT) muscles and the values of $[Ca_T]_{WM}$ were, on average, about half the expected WT values, taking into account the above $[Ca_T]_{WM}$ versus muscle weight relationship. Because greater reductions in $[Ca_T]_{WM}$ would be predicted in both muscle types, we hypothesize that there is a substantial increase in Ca bound to other sites in the CSQ knockout muscles.

INTRODUCTION

This Methods and Approaches article describes a new method for determining the concentration of total calcium in a tissue sample. The technique involves releasing Ca into a solution containing the Ca chelator 1,2-bis (2-aminophenoxy)ethane-*N*,*N*,*N*′,*N*′-tetraacetic acid (BAPTA), present at a concentration severalfold greater than that needed to capture all of the released Ca. The amount of Ca bound by BAPTA is determined by the Ca-dependent change in BAPTA's UV absorbance spectrum.

One motivation for this study was to determine the physiological concentration of total Ca in whole skeletal muscles including fast- and slow-twitch muscles from mice and rats and twitch muscles from frog. Because experiments aimed at understanding excitation–contraction coupling and its regulation and other questions involving Ca homeostasis are often performed with isolated single muscle cells or portions of such cells, such as cut fibers or skinned fibers, one reason for these measurements was to establish to what extent the range of total Ca concentrations previously published for some of these isolated preparations (e.g., Pape et al., 1995, and Fryer and Stephenson, 1996) agree with the physiological range in whole muscle reported here. As shown in the Discussion, the results with whole twitch muscles from

C.R.H. Lamboley and S.A. Kake Guena contributed equally to this paper. Correspondence to Paul C. Pape: Paul.Pape@USherbrooke.ca

Abbreviations used in this paper: AAS, atomic absorption spectroscopy; BAPTA, 1,2-bis(2-aminophenoxy)ethane-*N*,*N*,*N*′,*N*′-tetraacetic acid; CSQ, calsequestrin; EDL, extensor digitorum longus; KO, knockout; SERCA, sarcoplasmic/endoplasmic reticulum Ca^{2+}-ATPase; TCA, trichloroacetic acid.

The Rockefeller University Press $30.00
J. Gen. Physiol. Vol. 145 No. 2 127–153
www.jgp.org/cgi/doi/10.1085/jgp.201411250

Supplemental Material can be found at:
http://jgp.rupress.org/content/suppl/2015/01/21/jgp.201411250.DC1.html

Published January 26, 2015

frog in this study are in close agreement with the total amount of releasable Ca from the SR in cut fibers under nominally physiological conditions. However, in contrast to an earlier report that less than half of the total Ca in whole muscle from frog is intracellular, indicating a very large amount of bound Ca in the extracellular space (Kirby et al., 1975), results in this study indicate a relatively small extracellular Ca component.

A second motivation for this study relates to the current understanding of the role of calsequestrin (CSQ) as a high capacity Ca-binding protein in skeletal muscle. Starting with the discovery of CSQ by MacLennan and Wong (1971), almost all researchers have suggested that this protein acts as a major buffer of total Ca in the SR. In support of this view, based on experiments with Ca indicators introduced into voltage-clamped cut fibers from frog, Pape et al. (2007) reported that almost all of the Ca in the SR is in the bound form in resting muscle; similarly, almost all of the Ca released by a voltage-clamp step comes from the bound pool (Fénelon et al., 2012). Further, the Ca-binding curve relating bound to free Ca in the SR is largely consistent with a single, cooperative Ca-binding component. This curve was interpreted as indirect evidence that a single Ca-binding entity, presumably CSQ, is responsible for 80% or more of the Ca binding in the SR (Fénelon et al., 2012). This possibility is consistent with earlier, more direct evidence indicating that the maximal Ca-binding capacity of the SR in skinned mammalian muscle fibers is accounted for by CSQ (Murphy et al., 2009). These findings—combined with the knowledge that CSQ is localized near the SR Ca^{2+} release channels in the luminal SR, tethered there by triadin and junctin (Zhang et al., 1997)—strongly suggest that CSQ plays an important role in SR Ca^{2+} release. In apparent contradiction to this idea, the amplitude of the twitch response is about the same or slightly greater in both fast- and slow-twitch muscle with CSQ knocked out (Paolini et al., 2007, 2011).

Another question arising from studies of muscles with the skeletal isoform of CSQ (type 1 CSQ, CSQ1) knocked out is whether or not the loss of CSQ results in the expected large reduction in the Ca content in muscle. One indirect approach for assessing total releasable Ca in permeabilized single extensor digitorum longus (EDL) fibers indicated an ∼70% decrease in readily releasable Ca in CSQ1-knockout (KO) fibers compared with control fibers (Fig. 8, B and E, of Paolini et al., 2007; discussed further in the Discussion). In contrast, results for EDL muscle in Table 1 of Sztretye et al. (2011) indicated only a modest (∼25%) decrease in the total SR Ca in fibers from CSQ1-KO versus WT mice. A main motivation for developing the new technique described in this Methods and Approaches article was to try to help resolve this controversy.

We found that knocking out CSQ had little effect on the concentration of total Ca in whole muscles, providing a full or partial explanation for the lack of effect of CSQ KO on the twitch response. Decreases in negative feedback mechanisms controlling SR Ca^{2+} release, in particular Ca inactivation, would also help explain the mostly unaltered twitch response (in a manner well explained in Discussion section in Posterino and Lamb, 2003). Even with the apparently contradictory result with the twitch response, CSQ is still expected to play an important role on SR Ca^{2+} release as evidenced, in part, by faster fatigue development with CSQ knocked out (Paolini et al., 2011). In regards to the Ca-storage function of CSQ and its loss with CSQ KO, we hypothesize that this function is replaced by the up-regulation of one or more other Ca-binding proteins and/or other Ca-binding sites in the SR.

One unexpected new finding in this study was the observation of significant increases in the concentration of total Ca content with decreasing muscle weight in both fast- and slow-twitch muscles from mice. This result suggests the presence of a physiological mechanism that increases the concentration of Ca in the SR in response to increased specific work demands, thereby increasing the specific force that the muscle can generate with a twitch.

The technique described here should be useful for determining total Ca levels in almost any tissue.

A preliminary report of some of these results was presented to the Biophysical Society (Kake-Guena et al., 2014).

MATERIALS AND METHODS

Absorbance measurements (250–340 nm) were made at room temperature (22–23°C) with a spectrophotometer (Ultraspec 2000; Pharmacia). The quartz cuvette generally used had 1-cm path length, a height of 2.5 cm, and a chamber width of 3 mm, allowing a somewhat small sample volume, typically 0.45 ml. Unless indicated, experiments were performed in a solution containing 120 mM KCl and 2 mM HEPES, pH 8.0, and a nominal concentration of 0.15 mM BAPTA. The value of pH 8.0 was chosen to give a negligible value for the protonated form of BAPTA (see Fig. S1 and Sections 1 and 2 of the supplemental text). This solution is referred to as the "usual measurement solution" or the "measurement solution." The only other solution used for the measurements was one that contained 2 mM [Mg] in addition to the constituents of the usual measurement solution (see last section of Results). The term "final solution" refers to the measurement solution with SDS and muscle added and processed as described below; muscle-sample absorbance values were obtained with this final solution.

All absorbance values shown in this Methods and Approaches article were corrected for the blank, i.e., by taking the difference between the sample absorbance and that measured with distilled water in the same cuvette. (There was no detectable difference between the absorbance values with just water and those with a solution that was the same as the usual measurement solution but without BAPTA.)

Composition of solutions other than the measurement solutions

Muscle samples were generally placed in a physiological or modified physiological solution for some period of time (usually just

Published January 26, 2015

briefly) before being blotted dry and weighed (see below). The mammalian Ringer's solution used for the mammalian muscle samples contained 146 mM NaCl, 5 mM KCl, 2 mM $CaCl_2$, 1 mM $MgCl_2$, and 10 mM HEPES titrated with NaOH to pH 7.4.

The composition of the normal Ringer's solution used for frog muscle is given in Table 1 of Irving et al. (1987); this solution contained 1.8 mM Ca. The 0 Ca Ringer's solution for the frog muscle contained (mM): 107 NaCl, 2.5 KCl, 2.15 Na_2HPO_4, 0.85 NaH_2PO_4, and 10 $MgCl_2$, pH 7.1.

Properties of Ca binding to BAPTA

The experiment described in this section gives properties of the lot of BAPTA used in this study, done in part to confirm that these properties agree with published values. Fig. 1 plots BAPTA-related absorbance at 292 nm versus different concentrations of total Ca (denoted "[Ca_T]") in addition to the usual constituents of the usual measurement solution. The different values of [Ca_T] were obtained by adding Ca from another solution containing the usual measurement solution with a known amount of total Ca (to give 100 mM $CaCl_2$) added from a known $CaCl_2$ standard. The red (solid) curve in Fig. 1 shows the least-squares best fit to the data of predicted absorbance values assuming a one-to-one binding reaction between Ca and BAPTA. The adjustable parameters for this fit were the K_d, the concentration of total BAPTA ([B_T]; total defined as the sum of Ca-free plus Ca-bound forms of BAPTA), and the absorbance values with no Ca present (A_{zero}) and with infinite Ca (A_{inf}), i.e., with all of the BAPTA in the Ca-bound form. An intermediate step of the fitting process was to determine values of [Ca^{2+}] from the known values of [Ca_T] and the adjustable parameters [B_T] and K_d; the nonlinear, horizontal axis at the top of Fig. 1 shows the values of [Ca^{2+}] corresponding to those of [Ca_T] shown on the bottom axis. The good fit of the red solid curve to the data in Fig. 1 is consistent with the conclusion of Tsien (1980) of a simple 1:1 stoichiometry, which he observed for the full tested ranges of BAPTA concentrations (0.01–1 mM) and concentrations of free Ca^{2+} (up to 1 mM). As [B_T] was <0.15 mM for all of the experiments reported here, the simple 1:1 stoichiometry should apply to all of the results reported in this Methods and Approaches article, assuming the addition of tissue does not affect this Ca-BAPTA reaction. The extinction coefficients at 292 nm of the Ca-free and Ca-bound forms of BAPTA, ε_B and ε_{CaB}, were obtained with Beer's law from the best-fit values of A_{zero} and A_{inf}, respectively, and [B_T]. The best-fit values of K_d, [B_T], ε_B, and ε_{CaB} were, respectively, 0.22 µM, 0.127 mM, 5,009 M^{-1} cm^{-1}, and 320 M^{-1} cm^{-1}. This value of K_d, which applies to the ionic strength of this study (0.12 M), is reasonably close to the value of 0.18 µM estimated from data in Harrison and Bers (1987). Because the nominal concentration of total BAPTA was 0.15 mM, the value of 0.127 mM for [B_T] indicates a purity of 85% (100 × 0.127 ÷ 0.15). This lack of 100% purity is probably caused by the presence of water, as Harrison and Bers (1987) reported a purity of 79% and determined that the impurity was caused by the presence of water. Our estimated values of 320 and 5,009 M^{-1} cm^{-1} for ε_{CaB} and ε_B, respectively, are in very good agreement with the values of 339 and 5,052 M^{-1} cm^{-1} at 292 nm estimated from Fig. 1 of Tsien (1980). Of particular interest for this Methods and Approaches article is the difference in extinction coefficients between the Ca-bound and Ca-free forms at 292 nm, denoted "$\Delta\varepsilon$," given by the value −4,689 M^{-1} cm^{-1} (−4,689 = 320 − 5,009). In conclusion, the properties of BAPTA estimated in this study agree with published values, and the reaction of Ca with BAPTA follows a simple 1:1 stoichiometry, at least in the absence of tissue.

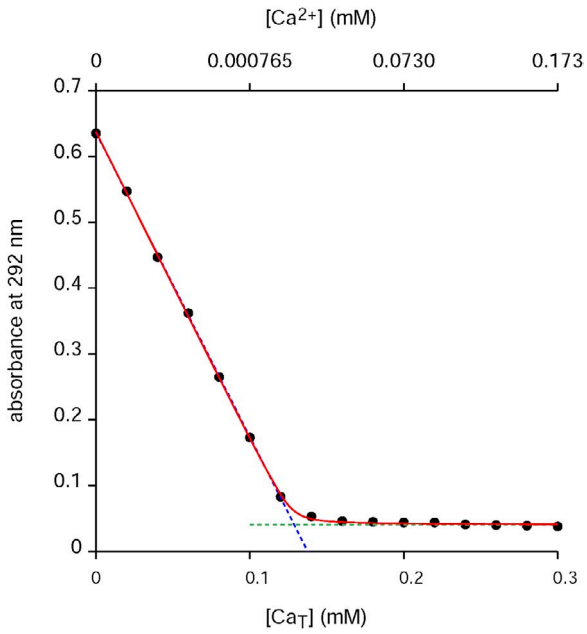

Figure 1. BAPTA absorbance at 292 nm versus [Ca_T]. See the description of this figure in the text for details of the experimental results and how the measured absorbance values were obtained. The text also describes how the solid red curve was obtained based on a 1:1 binding relationship for Ca to BAPTA. The best-fit value of A_{zero} associated with the red curve was 0.6375. The best-fit value of A_{inf} associated with the red curve was 0.0407, plotted as the horizontal hashed line (in green). The sloped hashed line shown (in blue) gives the least-squares best fit to the first six points. The slope and y intercept for this line are −4.625 mM^{-1} and 0.6362, respectively. The experiment ID was 821131. Experiment IDs are provided as an aid to the authors should access to the data and associated material be required.

The sloped dashed line shown in blue in Fig. 1 gives the least-squares best-fit line to the first six points, and the horizontal dashed line in green reflects the best-fit value of A_{inf}. As expected from the underlying relationships (not depicted), the value of [Ca_T] at the intersection of these two lines is very close to the best-fit value of [B_T]. It is clear that the relationship between BAPTA absorbance and [Ca_T] is essentially linear over the range of [Ca_T] values from zero to ∼0.11 mM, which is ∼87% of the best-fit (measurement-derived) value of 0.127 mM for [B_T] given above. With the exception of the intentional addition of higher saturating levels of [Ca_T], the total concentration of Ca from all sources (calcium from the muscle, the background solution, and the known amount from a Ca standard) was generally <75% of the measured concentration of BAPTA in the muscle experiments, so that the relationship between absorbance and total Ca concentration should be approximately linear for wavelengths such as 292 nm once background absorbance from muscle components is subtracted. Although the relationships derived below for determining [Ca_T] in a tissue sample do not assume a linear relationship between [Ca_T] and BAPTA absorbance for this range of [Ca_T] values, the final results presented for [Ca_T] do neglect any contribution of [Ca^{2+}] to [Ca_T]. This is justified because the calculated values of [Ca^{2+}] were no more than 0.4% of [Ca_T] over this range of [Ca_T] values, this maximum value occurring when [Ca_T] was 62% of [B_T] (from results associated with Fig. 1).

Processing of muscle samples

A whole muscle (from tendon to tendon) was removed from the animal. Unless indicated, the sample was placed in the mammalian Ringer's solution (for mice or rat) or normal Ringer's solution (for frog) for a short period (generally <10 min), and then gently blotted dry and weighed. Because most experiments did not require living tissue, muscle samples were often weighed and

Published January 26, 2015

then frozen before further processing. The solution used in the further processing was either the usual measurement solution or the measurement solution with Mg added. For both mice and rats, soleus (slow-twitch) and EDL (fast-twitch) muscles were used. For frog, the muscles used were semitendinosus (all twitch fibers) and ileofibularis, with the latter composed of almost all twitch fibers with a very small fraction of slow fibers. Care was taken to take as little tendon as possible without damaging the muscle.

Much or all of the processing of the samples described below was performed with the samples in the tubes used for centrifugation, using weight to keep track of the total volume of measurement solution added. In the case of frog and rat muscles (ranges of muscle weights: 60–120 mg and 120–300 mg, respectively), the high density polyethylene centrifuge tubes (Sarstedt) used had volumes of 15 and 50 ml, respectively. In the case of mouse muscles (4–13 mg), 1.5-ml Eppendorf tubes (made from "homo-polymer"; MCT-150-C; Axygen) were used. As described below, background levels of Ca were determined in the same manner as described here, except with no muscle present. Early studies with polycarbonate centrifuge tubes gave background Ca levels that differed from tube-to-tube, consistent with Ca leaching from the tubes at different rates. If Ca leaching did occur with the centrifuge tubes described above used for this study, these rates were small and, more importantly, there was no detectable tube-to-tube variability so that any contribution of Ca leaching to background Ca would have been correctly estimated and subtracted.

After weighing, a muscle was homogenized in a centrifuge tube with either an electrical homogenizer (PowerGen 125 grinder with a 10 × 95–mM saw tooth stator; Thermo Fischer Scientific) or a manual tissue grinder (Kontes Duall Tissue Grinder with PTFE pestle of appropriate size for the centrifuge tube; Thermo Fischer Scientific). For a muscle sample from a frog, rat, or mouse, homogenization was typically performed with, respectively, 1, 1, or 0.2 ml of measurement solution added to the muscle. In the case of frog muscle, the muscle was ground with the electric homogenizer running for 1 min at 14,000 rpm and 20 s or more at 8,000 rpm. For a rat or mouse muscle, the muscle was ground manually for 3–5 or 1–2 min, respectively. In every case, the aim was to completely homogenize the non-tendon part (i.e., fleshy part) of the muscle. After homogenization, additional measurement solution was added to give a final volume of 10 or 14 ml for frog (for ileofibularis or semitendinonus muscles, respectively), 40 ml for rat, and 0.5–1.2 ml for mouse muscle samples. For the most common muscle weights from mice, 7–13 mg, the final volume was generally 1.2 ml. For mouse muscles weighing <7 mg, the final solution volume was 0.5 or 0.6 ml, in which case the A_∞ and the optional A_S aliquots were not done. As described below for this case, a very close estimate of the concentration of total Ca in the muscle sample could still be obtained, with an error generally <2%. Much of the measurement solution added to reach the final volume was used to rinse the material off of the grinding instrument into the centrifuge tube. The detergent SDS was added to give a concentration of 0.5% (wt/vol) in the final solution. In the case of the electric grinder, the SDS was added after the grinding to avoid excessive foaming. For the manual homogenization, 0.5% SDS was present throughout. In addition to dissolving the surface and T-system membranes, SDS greatly reduced the intrinsic absorbance associated with proteins, presumably by its ability to denature the proteins so that they were more readily removed with the next step, centrifugation. The volume of the final solution including the added SDS (denoted "$V_{solution}$" below) was determined by weight (subtracting off the previously measured weight of the centrifuge tube), assuming a density of 1 g/ml for the mostly aqueous solution at this point.

To remove proteins and other insoluble muscle components that would produce unwanted absorbance or light scattering, samples were centrifuged at 14,000 rpm for 45 min at 6°C. The supernatant was then transferred to another tube for later use in the different aliquots described below.

It is noted that it was not considered necessary to correct $V_{solution}$ for the part of the processed sample in which BAPTA might be excluded, namely the solid part of the muscle in the pellet after centrifugation. This excluded volume is negligible as indicated by the following calculation. Considering typical values of a mouse muscle sample weighing 10 mg and 1.2 ml for $V_{solution}$ and assuming that ~80% of a muscle is water (Baylor et al., 1983), the pellet would contain ~2 mg of solids, giving an excluded volume of ~0.002 ml, which is <0.2% of $V_{solution}$.

The method assumes that BAPTA was able to complex all of the Ca, leaving none bound to muscle components and none in the pellet except for that present in any aqueous part of the pellet. Although no attempt was made to measure Ca in the pellet, calculations discussed later indicate that BAPTA should have been able to compete Ca off all muscle components with the possible exception of Ca/Mg-binding sites on parvalbumin, troponin, and myosin. Experiments to be discussed—with 2 mM Mg to mostly eliminate Ca binding to such sites—indicate that BAPTA was able to compete Ca off these sites probably because of decreases in the affinities of these proteins for Ca binding caused by the denaturing effect of SDS on proteins.

Absorbance measurements used to determine the amount of total Ca in a tissue sample

Four absorbance measurements, A_M, A_0, A_S, and A_∞, were generally made with the supernatant solution after the centrifugation step described above. A_M was determined with the supernatant alone, i.e., with no further processing. For the A_0 measurement, EGTA was added to an aliquot of supernatant solution (usually added to the quartz cuvette with the same aliquot used for the A_M measurement) to capture the Ca from BAPTA. With the nominal concentration of 1 mM EGTA used for A_0, calculations indicate that EGTA should complex >99.5% of the total Ca present (second to last section of the Appendix). For the A_S measurement, a known amount of Ca from a calcium standard was added to another aliquot of the supernatant solution (i.e., the A_M solution). A_∞ was obtained by adding excess Ca (to give a concentration of 1 mM Ca) to another aliquot of the supernatant or to the A_S aliquot so that essentially all of the BAPTA present was in the Ca-bound form.

Assumptions and equations used for interpreting absorbance data

This section gives the equations used to analyze the absorbance data, equations based on the following assumptions:

Assumption 1. BAPTA binds essentially all of the Ca initially present in the muscle sample and any background Ca present in the solution, which includes possible Ca leached from the centrifuge tubes. We denote the corresponding concentrations of CaBAPTA from these sources as "$[CaB]_M$" and "$[CaB]_{background}$," respectively. As justified above, the level of free [Ca] is negligible compared with the Ca bound to BAPTA. In addition, with its high affinity and relative large concentration (~0.13 mM), BAPTA should be able to capture Ca from essentially all of the large-capacity, Ca-binding proteins in the muscle, including CSQ, sarcoplasmic/endoplasmic reticulum Ca^{2+}-ATPase (SERCA), and the Ca-regulatory sites on troponin (see Table 2 in the first section of the Appendix and its associated text). A possible exception to this was Ca bound to the Ca/Mg-binding sites on parvalbumin and the high affinity Ca/Mg-binding sites on troponin and myosin. As shown in the last section of Results, experiments with added Mg indicate that Ca was not lost by this route, so that BAPTA did apparently capture almost all of the Ca initially present in the muscle samples.

Published January 26, 2015

Assumption 2. Binding of ions other than Ca to BAPTA is negligible because of the binding properties of BAPTA and the maximum expected concentration of other ions (e.g., Mg^{2+}) present in the muscle sample. This assumption is justified for protons at the value of 8 for the pH for the measurement solution (Section 1 of the supplemental text) and for Mg (last section of the Appendix, "The contribution of Mg from muscle samples is negligible"). The contribution of other possible ions should also be negligible.

Assumption 3. The reaction of Ca with BAPTA has a simple 1:1 stoichiometry in the concentration range of interest for BAPTA, i.e., 0.04–0.15 mM. (The justification for this assumption is given above.)

Assumption 4. The intrinsic absorbance of the sample (denoted "A_{INTR}"; see below)—defined as non-BAPTA–related absorbance—is not affected by changes in the concentration of free Ca^{2+} or by the addition of EGTA. It will be seen that A_{INTR} becomes quite pronounced at shorter wavelengths and that almost all of it is caused by muscle components remaining in the solution after the centrifugation.

Assumption 5. BAPTA and CaBAPTA do not bind to the intrinsic muscle components or any other components in the solution (specifically the pH buffer, HEPES), or such binding, if it does occur, does not affect the results.

With these assumptions, the equation for A_M is given by

$$A_M = A_{INTR} + \left\{ \begin{array}{l} \varepsilon_{CaB}\left([CaB]_M + [CaB]_{background}\right) + \\ \varepsilon_B\left([B_T] - [CaB]_M - [CaB]_{background}\right) \end{array} \right\} \cdot l, \quad (1)$$

where the contributions of Ca-free and Ca-bound BAPTA are given by the Beer–Lambert law, where l is the path length in the cuvette (always 1 cm), and ε_{CaB} and ε_B are the extinction coefficients of the Ca-bound and Ca-free forms of BAPTA, respectively. Likewise, with all of the BAPTA in the Ca-free form,

$$A_0 = A_{INTR} + \varepsilon_B[B_T] \cdot l, \quad (2)$$

With all of the BAPTA in the Ca-bound form

$$A_\infty = A_{INTR} + \varepsilon_{CaB}[B_T] \cdot l. \quad (3)$$

The absorbance value of the aliquot with the added standard is given by

$$A_S = A_{INTR} + \left\{ \begin{array}{l} \varepsilon_{CaB}\left([CaB]_M + [CaB]_{background} + [CaB]_S\right) + \\ \varepsilon_B\left([B_T] - [CaB]_M - [CaB]_{background} - [CaB]_S\right) \end{array} \right\} \cdot l, \quad (4)$$

where $[CaB]_S$ denotes the increase in the concentration of total Ca caused by the addition of Ca from the standard. With A_{INTR} assumed to be the same for all four absorbance values (Assumption 4), one obtains the following relationships:

$$\frac{A_M - A_0}{\Delta\varepsilon \cdot l} = [CaB]_M + [CaB]_{background}, \quad (5)$$

$$\frac{A_\infty - A_0}{\Delta\varepsilon \cdot l} = [B_T], \quad (6)$$

and

$$\frac{A_S - A_M}{\Delta\varepsilon \cdot l} = [CaB]_S, \quad (7)$$

where $\Delta\varepsilon \equiv \varepsilon_{CaB} - \varepsilon_B$. It is noted that $A_S - A_M$ in combination with the amount of Ca added from the standard can be used as a check on the product $\Delta\varepsilon \cdot l$. Therefore, the method does not require the use of the standard measurement. In particular, the essential value $[B_T]$ can be determined from Eq. 6 or from the following relationship obtained by combining Eqs. 6 and 7:

$$[B_T] = \frac{A_\infty - A_0}{A_S - A_M}[CaB]_S. \quad (8)$$

It is useful to express binding in terms of the fraction of BAPTA bound with Ca, denoted "f," and given by

$$f \equiv \frac{[CaB]_M + [CaB]_{background}}{B_T}. \quad (9)$$

The value of f can be considered as the sum of two parts depending on the source of Ca, i.e., muscle (M) or background, given by the following relationships:

$$f = f_M + f_{background}, \quad (10)$$

where

$$f_M \equiv \frac{[CaB]_M}{[B_T]} \quad (11)$$

and

$$f_{background} \equiv \frac{[CaB]_{background}}{[B_T]}. \quad (12)$$

From Eqs. 5, 6, and 9, f is determined from the absorbance values by

$$f = \frac{A_M - A_0}{A_\infty - A_0}. \quad (13)$$

The value of $f_{background}$ was determined in the same way as f, except that muscle was not present, using the relationship

$$f_{background} = \frac{S_M - S_0}{S_\infty - S_0}, \quad (14)$$

where S (which designates solution only) replaces A to denote absorbance values with no muscle present. Because the background Ca could come from one or more of several sources—including the KCl used for the measurement solution, the detergent (SDS), and possibly the HEPES buffer and from Ca leaching from the centrifuge tubes—the absorbance measurements without muscle were obtained from solutions treated the same way as the muscle samples, including the addition of SDS followed by centrifugation. From Eqs. 10, 13, and 14,

$$f_M = f - f_{background} = \frac{A_M - A_0}{A_\infty - A_0} - \frac{S_M - S_0}{S_\infty - S_0}. \quad (15)$$

The value of $[CaB]_M$ was obtained from the relationship

$$[CaB]_M = f_M \cdot [B_T], \quad (16a)$$

Published January 26, 2015

where $[B_T]$ can be determined by Eq. 6 or by Eq. 8, as indicated above. Substituting Eqs. 6 and 15 into Eq. 16a gives:

$$[CaB]_M = \left[(A_M - A_0) - (S_M - S_0)\left(\frac{A_\infty - A_0}{S_\infty - S_0}\right)\right] \cdot \left(\frac{1}{\Delta\varepsilon \cdot l}\right). \quad (16b)$$

As indicated later, with Eq. 18 in Results, the ratio $(A_\infty - A_0)/(S_\infty - S_0)$ gives the ratio of $[B_T]$ in the solution with the muscle sample to that without the muscle sample. As shown in Results shortly after Eq. 18, the average value for this ratio was 0.961, which is close to 1, indicating that there was almost no loss of BAPTA caused by interaction with muscle components. The main things to note from this are: (a) the $A_M - A_0$ and $S_M - S_0$ are the most important measurements, (b) A_S and S_S are not needed, and (c) A_∞ and S_∞ are almost not important at all. In fact, as seen next, a very good approximation of $[CaB]_M$ can be made without A_∞ and S_∞.

If one assumes a value of 1 for $(A_\infty - A_0)/(S_\infty - S_0)$, a very good approximation of $[Ca_B]_M$ is given by

$$[CaB]_M \cong \left[(A_M - A_0) - (S_M - S_0)\right] \cdot \left(\frac{1}{\Delta\varepsilon \cdot l}\right). \quad (16c)$$

This approximation was used for some measurements with small muscle samples where enough supernatant was not available to make the A_S and A_∞ measurements (see above). The degree to which this approximation agrees with Eq. 16b can be assessed by dividing Eq. 16c by Eq. 16b, giving:

$$\frac{[CaB]_{M\_from\_eqn\_16c}}{[CaB]_{M\_from\_eqn\_16b}} = \frac{1 - \dfrac{S_M - S_0}{A_M - A_0}}{1 - \dfrac{S_M - S_0}{A_M - A_0} \cdot \dfrac{A_\infty - A_0}{S_\infty - S_0}}. \quad (16d)$$

Because the ratio $(A_\infty - A_0)/(S_\infty - S_0)$ was generally <1, the approximation generally results in an underestimation. As an example of the error, with a value of 0.3 for the ratio $(S_M - S_0)/(A_M - A_0)$, which is near the maximum measured, and with the value above of 0.961 for the ratio $(A_\infty - A_0)/(S_\infty - S_0)$, Eq. 16d gives a value of 0.984 ($(1 - 0.3) \div (1 - (0.3 \times 0.961))$), i.e., only a 1.6% error. Because the error is almost negligible, no attempt was made to correct for it, for example by assuming a value of 0.961 instead of 1 for the ratio $(A_\infty - A_0)/(S_\infty - S_0)$.

The main value of interest is the concentration of total Ca from the muscle in units of mmoles/kg (denoted "$[Ca_T]_{WM}$", where the subscript "WM" refers to whole muscle):

$$[Ca_T]_{WM} = \frac{V_{solution}}{W_{muscle}}[CaB]_M, \quad (17)$$

where $V_{solution}$ is the volume of the solution and muscle combined before the centrifugation step (see description of $V_{solution}$ above), and W_{muscle} is the wet weight of the muscle in grams (muscles blotted dry and weighed).

Correcting for small differences in BAPTA concentration in the different samples

Unless indicated, all of the absorbance values (except A_M) were corrected for small differences in BAPTA concentration, so that all of the absorbance values refer to the concentration of BAPTA in the A_M solution. As an example, for the results from muscles from mice, A_M was measured first with 0.45 ml in a cuvette followed by A_0 obtained with 9 µl of 50 mM EGTA added to the same solution to give a final concentration of 1 mM EGTA. The A_0 data were therefore scaled by 1.02 (1.02 = (0.45 ml + 0.009 ml) ÷ 0.45 ml), so that the corrected A_0 value refers to the concentration of BAPTA that was present in A_M. When comparing absorbance measurements with muscle samples present to those without muscle samples present (Eqs. 13 and 14), a similar correction was made for the fact that the BAPTA was diluted by the volume of the muscle added. For example, with a mouse muscle weighing 8 mg added to a volume 1.2 ml of measurement solution, the volume of the muscle added is assumed to be 0.00755 ml (0.008 g divided by the assumed density of muscle, 1.06 g/ml; Mendez and Keys, 1960). To refer to the concentration of BAPTA present in the A_M measurement, the absorbance values with no muscle present (S values) were scaled by 0.994 (0.994 = 1.2 ml ÷ (1.2 ml + 0.00755 ml)).

A model protocol with practical suggestions for adapting it to other tissues

The first part of this section summarizes the protocol currently used in our laboratory for a 7–13-mg mouse muscle sample (referred to below as the ~10-mg tissue sample). This protocol could serve as a model for adapting the BAPTA method to other size tissue samples, a process that would likely require scaling some of the variables involved if tissue samples are outside of the 7–13-mg range. Some practical suggestions are given for this process and for some of the steps in the method.

After extraction and weighing of the ~10-mg tissue sample, the tissue is put into a 1.5-ml Eppendorf tube. The sample is optionally frozen for later processing, with the latter all done on the same day to minimize possible slow leaching of Ca into the sample once aqueous solution has been added. For the same reason, the measurement solution with 2 mM Mg is made on the same day, and 0.5% SDS is added. About 0.2 ml of this solution is added to the Eppendorf tube, and the tissue is manually homogenized. After homogenization, more of the measurement solution with Mg and SDS is added to give a volume of ~1.2 ml, the actual volume ($V_{solution}$) determined by weight as described above. After a period of ~30 min to assure complete redistribution of Ca to BAPTA (no tests were performed to establish this waiting period, and it is unknown if any time beyond a few minutes is actually required), the sample is centrifuged and the supernatant is removed and placed in another Eppendorf tube. For the A_M measurement, 0.45 ml of this supernatant is introduced into the quartz cuvette (see above). For the A_0 measurement, 9 µl of a 50-mM EGTA solution is added to the cuvette to give 1 mM EGTA. For the A_S measurement, the quartz cuvette is then thoroughly rinsed and dried, and another 0.45 ml of the supernatant is added followed by the addition of 9 µl of a 1.5-mM $CaCl_2$ standard solution (made by multiple dilutions from a 0.1-M $CaCl_2$ standard) to give an additional 0.03 mM of Ca ($[CaB]_S$). (For reasons described later, glass Pasteur pipettes should not be used for mixing the A_s aliquot, as these introduce Ca. Our current method for mixing is to cover the cuvette with a small square of Parafilm, grasp the cuvette between fingers on the top and bottom of the cuvette, and turn it over several times. The finger pressure on the Parafilm helps seal the cuvette.) For the A_∞ measurement, 9 µl of a 50-mM $CaCl_2$ standard solution is added to the cuvette with the A_S aliquot to give an additional 1 mM of Ca. Glass Pasteur pipettes can be used for mixing the A_0 and A_∞ aliquots because the Ca contamination would not be a problem for these aliquots.

Although absorbance measurements made over a range of wavelengths have the advantage of confirming well-behaved spectral properties (see Figs. 3–5), measurements are only needed at one wavelength. A wavelength of 292 nm would be a good choice because: (a) information about Δε is provided in this Methods and Approaches article for this wavelength, (b) a local peak in the difference spectra occurs near this wavelength, and (c) there should be relatively little intrinsic absorbance at this wavelength (Figs. 2–5).

The main variables when considering modifying the protocol and/or adapting it to different tissue masses are the concentration

Published January 26, 2015

of BAPTA in the measurement solution, the volume of measurement solution added (a value very close to $V_{solution}$), and the size of the cuvette. (The size of the centrifuge tubes used would depend on $V_{solution}$.) With a 1-cm path length for the quartz cuvette, the nominal BAPTA concentration of 0.15 mM should provide reasonably high maximum absorbance values without being too high. If smaller tissue samples are required, one option would be to decrease the cuvette volume by using a quartz cuvette with a shorter path length, in which case the BAPTA concentration can be proportionally increased. Otherwise, the BAPTA concentration can be considered as a fixed variable. The only other main variable is $V_{solution}$. As a first estimate, $V_{solution}$ could be chosen to give 1.2 ml per 10 mg of tissue, with $V_{solution}$ adjusted for each tissue sample or kept constant over a range of perhaps ±30% as done above (we use $V_{solution}$ values of ~1.2 ml for samples ranging from 7 to 13 mg). The aim would be for f_M values to be somewhere in the range of 0.1 to 0.5. The low end of the range is to provide resolution above $f_{background}$, which was typically 0.06 or less. The high end is to keep the absorbance measurements in the linear range of BAPTA absorbance versus $[Ca_T]$, as seen with Fig. 1.

Statistical significance

The difference between two sets of results was considered statistically significant if P was <0.05 with the Student's two-tailed *t* test. For least-squares best-fit lines, the slopes were considered significantly different from zero with p-values <0.05 (determined with GraphPad software package).

Online supplemental material

Section 1 of the supplemental text gives the relationships used for assessing Ca^{2+}, Mg^{2+}, and proton binding to BAPTA and EGTA. Section 2 shows the absorbance spectra of BAPTA at different pH values. In addition to yielding information about how protons interact with BAPTA, the results led to our choice of pH 8.0 for the measurement solution. Section 3 gives the relationship used for assessing stray light in the spectrophotometer and the relationship used to correct for this stray light component. Section 4 gives evidence of Ca leaching from some of the labware used in the study and results indicating that this leaching does not affect $[Ca_T]_{WM}$ values reported in this study. Section 5 gives results for the one set of mice for which dried muscle weights were determined in addition to the usual measurements. Mouse weights were also recorded with this set of mice. Unless indicated, these results were not included in the main text. Results in Section 5a indicate that the inverse relationships between $[Ca_T]_{WM}$ and wet muscle weight in Fig. 6 are not caused by differences in the fractional water content. Results in Section 5b indicate that smaller muscles are associated with fractionally greater mouse body weights. Results in Section 5c indicate that an apparent non-reproducibility in $[Ca_T]_{WM}$ results was almost certainly caused by contamination by aluminum ions as a result of the fact that the muscles were dried on aluminum foil. Section 6 describes criteria used to reject the outlier points in this study and possible explanations for these outlier points. (Only 2 out of the almost 200 data points in this study were rejected, neither of which was in the main set of results.) Section 7 gives predicted values for $[Ca_T]_{WM}$ with CSQ KO in EDL and soleus muscles if the only effect of the KO was to remove Ca bound to CSQ. The online supplemental material is available at http://www.jgp.org/cgi/content/full/jgp.201411250/DC1.

RESULTS

The Materials and methods section describes how the concentration of total Ca in a muscle sample can be determined from the four absorbance measurements with the following solutions: (a) the processed muscle sample itself (A_M), the same A_M solution with (b) EGTA added so that essentially all of the Ca is displaced from BAPTA (A_0), (c) a known amount of Ca from a Ca standard added (A_S), and (d) enough Ca added so that essentially all the BAPTA is in the Ca-bound form (A_∞). Although this determination only requires information at a single wavelength, it is of interest to make measurements over a range of wavelengths to confirm that assumptions made for the determination of Ca content are valid. For example, problems with the spectra could be indicative of various possibilities including a Ca/BAPTA stoichiometry other than 1:1 (invalidating Assumption 3 in Materials and methods) and/or a substantial interaction of BAPTA with muscle components (invalidating Assumption 5), and/or Ca dependence of the absorbance of residual muscle components, components not removed by the centrifugation procedure (invalidating Assumption 4). These issues are addressed in the Figs. 2–5 by assessing UV absorbance spectra measured between 250 and 340 nm.

Test of Assumption 4 that A_{intr} is constant and EGTA lacks absorbance

Fig. 2 A shows the four absorbance spectra (A_M, A_0, A_S, and A_∞) with an EDL muscle from a mouse processed

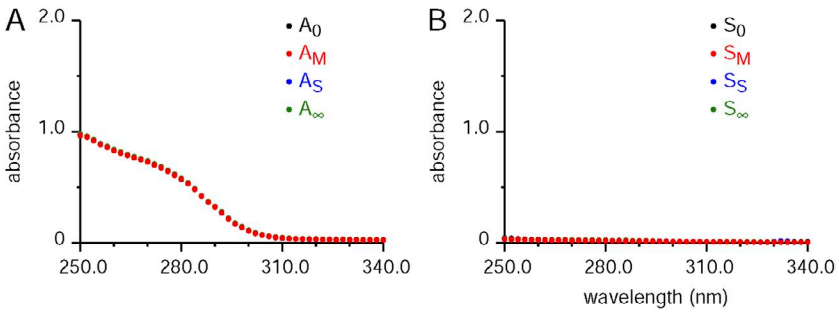

Figure 2. Absorbance spectra with no BAPTA present: justification of the assumption of constant "intrinsic" absorbance, A_{intr}. (A) Plots of the absorbance spectra for the A_0, A_M, A_S, and A_∞ aliquots for an 8.9-mg EDL muscle from a mouse in 1.2 ml of final solution volume (including homogenized muscle) processed in the usual way, except that BAPTA was not present in the usual measurement solution. In this and B, only one set of values is visible, as the other points are covered by the last spectrum plotted (the A_M values in red for A). (B) The same format as A, with the results processed in the same way (including the addition of SDS and centrifugation), except that muscle was not present. The experiment IDs for A and B were, respectively, 310131_E2noBall and 310131_LnoBall.

Published January 26, 2015

and measured in the usual way, except that no BAPTA was present. The purpose of this experiment was to test Assumption 4 that the intrinsic absorbance (A_{intr})—arising mainly from "intrinsic" muscle components still present after the centrifugation step—was unchanged in the four conditions. Only one spectrum is clearly visible because all four spectra were almost identical. The results from this and similar experiments with muscle from other species (frog and rat) indicate that the intrinsic absorbance does not depend on the presence of EGTA used for A_0 or the presence of saturating Ca used for A_∞, thereby verifying Assumption 4. It is noted that this result does not rule out the possibility that BAPTA interacts somehow with the remnant muscle components, a possibility that is evaluated below.

In Fig. 2, B is identical to A, except that no muscle sample was present. There was a small, nonzero absorbance at shorter wavelengths of unknown origin, but overall the absorbance values are essentially negligible compared with those attributable to muscle in A. Because the S_0 spectrum was not different from the others, the results indicate that EGTA does not exhibit absorbance over the full spectral range measured. Our unpublished results suggest that the EGTA does have significant absorbance between 250 and 280 nm when pH is close to 7, which is one reason for carrying out the experiments at pH 8.

The shapes of the uncorrected difference spectra with BAPTA present do not match over the full spectral range

Fig. 3 shows typical spectra with BAPTA present. A and B were obtained with an EDL mouse muscle sample, and C and D were obtained in the same way but without muscle. The spectra of A_M, A_0, A_S, and A_∞ are shown in A. Fig. 3 B plots the following difference spectra: $A_0 - A_\infty$ (black circles), $A_M - A_S$ (blue circles), and $A_0 - A_M$ (red circles). (Note that for clarity, absorbance differences in equations and associated text in Materials and methods were given by the absorbance with the greater level of Ca present minus that with the lower amount of Ca, whereas the inverse was used here and elsewhere in Results to give positive values. For example, $A_M - A_0$ is used in Materials and methods, whereas $A_0 - A_M$ is used in Results. This small inconvenience is because the Ca-free form of BAPTA has a higher absorbance than the Ca-bound form.) In Fig. 3 B, the $A_0 - A_\infty$ difference spectrum between 282 and 340 nm (black circles) has been least-squares best fitted with a scaled version of the $A_0 - A_M$ difference spectrum; this scaled spectrum is shown as the superimposed solid red curve. The hashed curve (between 250 and 282 nm) shows the same scaling factor applied to the rest of the $A_0 - A_M$ spectrum, i.e., from the data not included in the least-squares best fit. (This convention of solid and hashed lines, respectively, for the fitted and nonfitted parts applies to similar such fitted spectra shown in the rest of this article.)

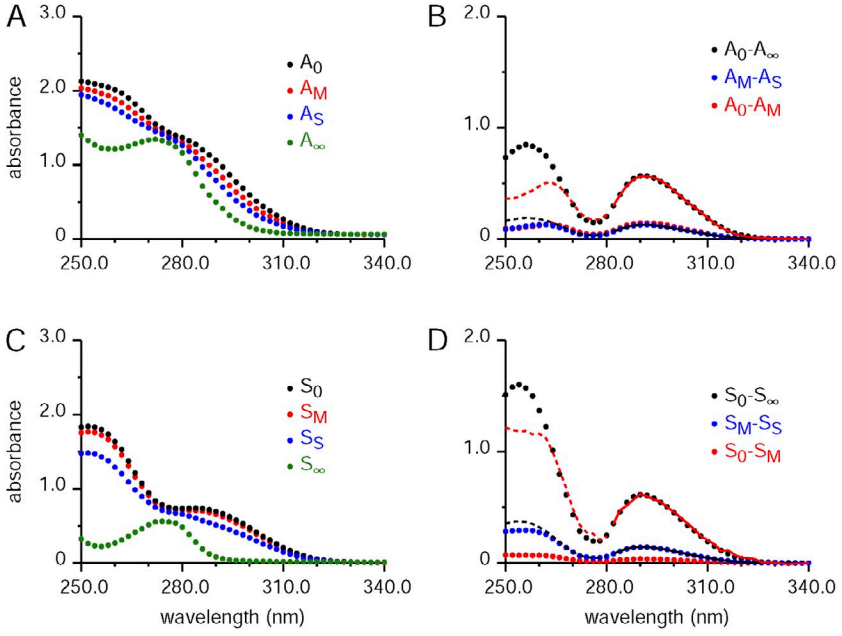

Figure 3. Absorbance spectra for a muscle sample and associated spectra without muscle for determining background Ca. The format of panels A and C is the same as Fig. 2 (A and B, respectively), except that BAPTA was present at the usual, nominal concentration of 0.15 mM. A and B were obtained with a 9.8-mg EDL muscle from a mouse in 1.36 ml of final solution volume. The Ca standard aliquot (A_S) was obtained in the usual way of adding 9 µl of a solution containing 1.5 mM $CaCl_2$ made from a 1-M $CaCl_2$ standard to 0.45 ml of the supernatant (or A_M aliquot), giving a concentration of added standard of 0.03 mM (concentration referred to volume before adding standard). (A) As indicated, the highest to the lowest spectra for the four aliquots are in the order A_0, A_M, A_S, and A_∞; this is the order because the absorbance of the Ca-free form of BAPTA is higher than that of the Ca-bound form. (B) Shows differences of spectra in A. As indicated in the text describing this figure, the solid red curve shows the least-squares best fit of the $A_0 - A_M$ difference spectra from 282 to 340 nm to the corresponding $A_0 - A_\infty$ data. The best-fit scaling factor for the ratio $(A_0 - A_\infty)/(A_0 - A_M)$ was 3.895. For the corresponding fit of the $A_0 - A_\infty$ data to the $A_M - A_S$ difference spectrum (solid black curve), the best-fit scaling factor for the ratio $(A_M - A_S)/(A_0 - A_\infty)$ was 0.2244. The hashed lines show the part of the scaled spectra from the wavelength range not used for the fit (i.e., wavelengths below 282 nm). (C and D) Obtained in the same way as A and B, except that muscle was not present. For D, the best-fit ratios $(S_0 - S_\infty)/(S_0 - S_M)$ and $(S_M - S_S)/(S_0 - S_\infty)$ were, respectively, 17.00 and 0.2339. The experiment ID for A and B was 012214_E6, and that for C and D was 012214_LnoMg.

Published January 26, 2015

Although the scaled $A_0 - A_M$ difference spectrum is close to that of $A_0 - A_\infty$ for the spectral region included in the fit, it is obviously a poor fit for much of the spectral region below 282 nm. A similar poor fit is seen with the corresponding difference spectra without muscle present, i.e., the fit of $S_0 - S_M$ to $S_0 - S_\infty$ in Fig. 3 D.

The difference spectra match if corrected for stray light component

Fig. 4 shows the same absorbance spectra from Fig. 3 corrected for stray light using the procedure described in Section 3 of the supplemental text. As in Fig. 3 B, the solid red curve shows the least-squares best fit of the $A_0 - A_M$ spectrum to the $A_0 - A_\infty$ spectrum over the wavelength range of 282 to 340 nm. In contrast to Fig. 3, the $A_0 - A_M$ difference spectrum matches well with that of $A_0 - A_\infty$ over the nonfitted region of the spectrum (250–282 nm). The solid and dashed black curves give the corresponding fit of $A_0 - A_\infty$ to the $A_M - A_S$ difference spectrum. These black curves are difficult to see because, again, the fit is excellent for the full wavelength range. Likewise, the corresponding fits without muscle present in Fig. 4 D are excellent for the full measured wavelength range. Similar good matches were obtained in other experiments with uncorrected spectra if the effects of stray light were greatly decreased by decreasing the magnitude of the absorbance signals. The lower absorbance values were achieved by either diluting the muscle and BAPTA concentrations by a factor of ~3 or by using quartz cuvettes with shorter path lengths (1 or 3 mm) compared with that used for all of the data given in this article (path length of 1 cm).

Similarly good fits were observed over the full wavelength range for all of the difference spectra used for the results in this article, with the exception of some small variation in the extrapolated fits near the peak at 254 nm. This variation is attributable to small variations in the stray-light component that plays a much larger role at the higher absorbance values near 254 nm. Whether the stray light component is mostly removed by reducing the overall absorbance or by the correction procedure, the good matches of the difference spectra over the measured full wavelength range indicate that the BAPTA spectra are not distorted as might occur if BAPTA were significantly bound to muscle components.

An example of the determination of the concentration of total Ca in a muscle sample

This section provides a specific example of how the concentration of total Ca in a mouse EDL muscle sample was obtained from the absorbance data with the BAPTA method, Fig. 4 (B and D) in this case. According to Eq. 13, the fraction of BAPTA complexed with Ca (f) is given by $(A_M - A_0)/(A_\infty - A_0)$ (which equals $(A_0 - A_M)/(A_0 - A_\infty)$), determined here by the reciprocal of the best-fit scaling factor relating the $A_0 - A_M$ difference spectrum to that of $A_0 - A_\infty$ in Fig. 4 B. The value of f in this case was 0.263. Correspondingly, the best fit of $S_0 - S_M$ to $S_0 - S_\infty$ in Fig. 4 D gives a value for $f_{background}$ (see Eq. 14) of 0.060. As seen in Eq. 15, the difference between f and $f_{background}$ gives f_M, the fraction of BAPTA with Ca that originated from the muscle sample, which has a value of 0.203 in this case.

The next step was to determine $[B_T]$ from Eq. 6 using the values of 1 cm for l and $-4{,}689\ M^{-1}\ cm^{-1}$ for $\Delta\varepsilon$ at 292 nm, as given in Materials and methods. The value of 0.6008 for $A_0 - A_\infty$ at this wavelength is from the point indicated by the top arrow in Fig. 4 B. The value

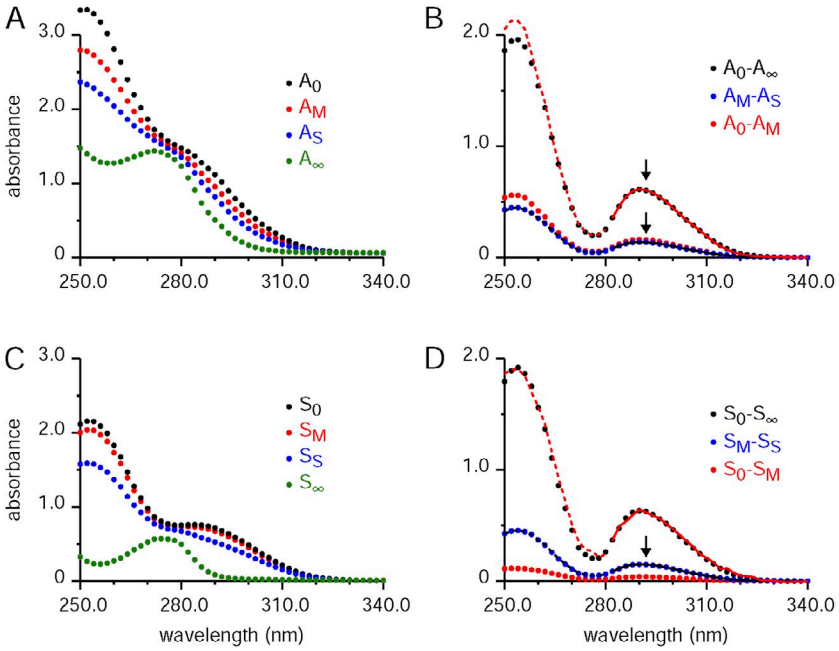

Figure 4. Absorbance spectra corrected for stray light used to determine $[Ca_T]_{WM}$ with the BAPTA method. (A–D) The absorbance spectra in this figure are from the same experiment shown in Fig. 3, except that they are corrected for the stray light component. Details of this correction are given in the text associated with this figure and Section 3 of the supplemental text. The format of the figure is the same as that used for Fig. 3. For B, the best-fit ratios $(A_0 - A_\infty)/(A_0 - A_M)$ and $(A_M - A_S)/(A_0 - A_\infty)$ were, respectively, 3.809 and 0.2275. For D, the best-fit ratios $(S_0 - S_\infty)/(S_0 - S_M)$ and $(S_M - S_S)/(S_0 - S_\infty)$ were, respectively, 16.73 and 0.2368.

Published January 26, 2015

of $[B_T]$ in this case is 0.128 mM ($-0.6008 \div (-4.689\ mM^{-1}\ cm^{-1} \times 1\ cm)$). The concentration of Ca bound to BAPTA, which originated from the muscle sample, $[CaB]_M$, is given by the product of f_M and $[B_T]$ (see Eq. 16a); $[CaB]_M$ in this case is 0.0260 mM (0.203×0.128 mM).

The estimated concentration of total Ca in the original muscle sample ($[Ca_T]_{WM}$; concentration referred to the whole-muscle mass) is given by Eq. 17. For this equation, the weight of the EDL muscle sample in this experiment, W_{muscle}, was 0.0098 g (9.8 mg), and the final volume of the solution with the homogenized muscle, $V_{solution}$, was 1.36 ml, giving a value for $[Ca_T]_{WM}$ of 3.61 mmoles/kg (3.61 mmoles/kg = $1.36\ ml \times 0.0260\ mM \div 0.0098$ g).

Difference spectra match with and without muscle

Fig. 5 plots difference spectra with (symbols) and without (curves) muscle present; these are the same as four of the difference spectra in Fig. 4 (B and D). The very close matches of the forms of the difference spectra indicate that BAPTA absorbance was not altered by possible binding to muscle components. With the exception of the problematic spectral region near the higher peak at 254 nm caused by stray light (see above), similar close matches were found for all of the experiments in this study. As described near the end of Materials and methods, the difference spectra without muscle were scaled by 0.995 to take into account the dilution of the BAPTA concentration by the muscle sample so that all absorbance values refer to the concentration of BAPTA in the A_M solution. Because no other scaling factor was applied, the very close match of the magnitude of the $A_0 - A_\infty$ difference spectrum to that of $S_0 - S_\infty$ indicates that the presence of muscle components did not significantly change the estimate of the concentration of total BAPTA, $[B_T]$, using Eq. 6 above and the analogous equation for solution-only measurements. Likewise, the very close match of the magnitude of the $A_M - A_S$ difference spectrum to that of $S_M - S_S$ indicates that the presence of muscle components did not significantly change the response to the same amount of Ca added, $[Ca_B]_S$, as seen by Eq. 7.

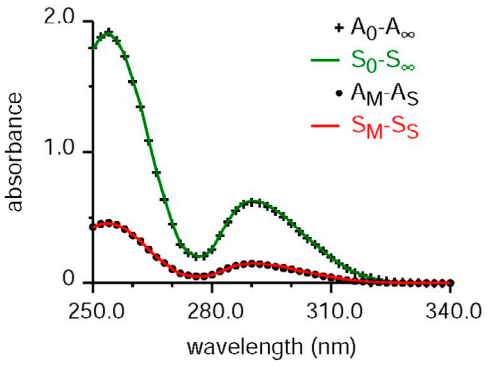

Figure 5. $[B_T]$ and the response of BAPTA to an added amount of known Ca were very similar with and without muscle present. The difference spectra plotted as symbols ($A_0 - A_\infty$ and $A_M - A_S$) were obtained with muscle present and are the same as those shown in Fig. 4 B. The difference spectra plotted as lines ($S_0 - S_\infty$ and $S_M - S_S$) were obtained without muscle present and are the same as those shown in Fig. 4 D.

The next two sections give additional details including quantification of the degree to which the magnitudes of $A_0 - A_\infty$ match $S_0 - S_\infty$ and those of $A_M - A_S$ match $S_M - S_S$ in all of the experiments in this study by comparing their values at 292 nm.

The presence of muscle has almost no effect on the measured value of $[B_T]$

From Eq. 6 and the analogous equation for solution-only measurements, the ratio of the estimated concentration of total BAPTA ($[B_T]$) with muscle present to that without muscle, denoted "γ," is given by

$$\gamma = \frac{A_0 - A_\infty}{S_0 - S_\infty}. \quad (18)$$

(Values of $S_0 - S_\infty$ used with this ratio were reduced to account for the reduction of BAPTA concentration caused by the addition of muscle to the measurement solution, as described in "Correcting for small differences in BAPTA concentration..." in Materials and methods.) A value of 1 for γ would indicate that $[B_T]$ is not affected by either of the following two cases: (1) loss of BAPTA caused by binding to muscle components in the pellet after centrifugation (which would result in a decrease in $[B_T]$ and a value of $\gamma < 1$), or (2) a combination of BAPTA binding to muscle components in the supernatant and changes in BAPTA's absorbance properties (which would also likely give a value of $\gamma < 1$). For the 148 mouse muscle samples reported in this article, the average value of γ was 0.961 (SEM = 0.002). Although significantly <1 ($P < 0.0001$), the results indicate only a loss of 3.9% on average of the reported BAPTA concentration. A loss of BAPTA caused by case 1 (loss in the pellet) would not present a problem for the method of detecting Ca in a tissue sample, as it depends on the value of $[B_T]$ present in the supernatant (see Eqs. 6 and 16a). However, binding of BAPTA to muscle components in the supernatant (case 2) could present a problem. For example, the 3.9% loss could be caused by a much larger percentage of Ca-free BAPTA bound to muscle components if this binding were accompanied by a partial loss of its ability to absorb light (e.g., the 3.9% loss could be caused by the binding of 39% of BAPTA to muscle components with a 10% decrease in absorptivity).

The presence of muscle has almost no effect on the responsiveness of BAPTA to Ca

This section considers the change in BAPTA absorbance ($A_M - A_S$ or $S_M - S_S$) upon the addition of a presumably known amount of Ca. The important question addressed

Published January 26, 2015

is whether the presence of muscle affects this response and, thereby, the ability of the method to accurately detect the concentration of Ca in a muscle sample. The measured value of $[CaB]_S$ is given by Eq. 7, reproduced here in slightly different forms:

$$[CaB]_S = \frac{A_S - A_M}{\Delta\varepsilon \cdot l} = -\frac{A_M - A_S}{\Delta\varepsilon \cdot l}, \quad (19a)$$

or, in the absence of muscle,

$$[CaB]_S = \frac{S_S - S_M}{\Delta\varepsilon \cdot l} = -\frac{S_M - S_S}{\Delta\varepsilon \cdot l}. \quad (19b)$$

As seen in Section 4 of the supplemental text, values of $[CaB]_S$ were always greater, both with and without muscle present, than the expected amounts, a problem attributable to Ca leaching from the labware used for the standard measurements. For the purposes of comparing whether muscle affects the response to Ca, the Ca-leaching problems can be ignored because the errors associated with the Ca leaching should have been the same with and without muscle present. For this purpose, it is helpful to define a parameter, denoted "ρ," that gives the ratio of the measured value of $[CaB]_S$ with muscle present to that measured with no muscle present, obtained by taking the ratio of Eqs. 19a and 19b and given by the relationship

$$\rho = \frac{A_S - A_M}{S_S - S_M} = \frac{A_M - A_S}{S_M - S_S}. \quad (20)$$

A value of 1 for ρ would indicate that muscle does not affect the responsiveness of BAPTA to Ca. It is noted that the values of $S_M - S_S$ should not be corrected for the small difference in BAPTA concentration in the solution compared with the muscle sample, as done with Fig. 5, as the change in absorbance upon the addition of the standard does not depend on $[B_T]$ (see Eq. 7). For the example in Figs. 4 and 5, the values of $A_M - A_S$ and $S_M - S_S$ were, respectively, 0.1371 and 0.1458 (from the points labeled with the bottom arrow in Fig. 4 B and the arrow in Fig. 4 D, respectively), giving a value for ρ of 0.940.

All of the data in this Methods and Approaches article were obtained in 11 sets of 8–20 samples with muscle present and an associated single sample with solution only; all samples in each set were processed and measured on the same day. The average value of ρ, including experiments with CSQ knocked out and their controls, was 0.967 (SEM = 0.004; n = 164). Although significantly <1, the difference is small (only 3.3%), indicating that possible binding of BAPTA to muscle components is small or, if a significant amount of such binding does occur, it has only a minor effect on the ability of BAPTA to detect Ca.

Values of $[Ca_T]_{WM}$ in mice increase with decreasing muscle weight

All four panels in Fig. 6 plot the concentration of total Ca in whole muscles ($[Ca_T]_{WM}$; determined with Eq. 17) versus muscle weight. All of the results were with control muscles from 3–6-mo-old mice. A and B show results with EDL muscle samples, and C and D show results with soleus muscle samples. All of the mice in A and C and most of the mice in B and D were C57BL/6 mice, whereas some of the mice in B and D were from hybrid mixes, as indicated in the figure legend. The results in A and C are from the largest set of control mice done with a single set of mice obtained in the same shipment and studied together over a 2-d period. In each of the panels, the line is the least-squares best fit to the $[Ca_T]_{WM}$ versus muscle weight results in that panel. The slopes of all of these lines were significantly different from zero with the exception of that in C, which was almost significantly different (P = 0.0539; this and the other p-values are given in the figure legend). The results in Fig. 6 indicate that $[Ca_T]_{WM}$ increases with decreasing muscle weight in both EDL and soleus muscles.

These inverse relationships suggest the existence of a physiological mechanism that up-regulates the cellular Ca load to somehow compensate for the lower muscle weights. In particular, if the lower muscle weights were required to move a heavier load (a greater weight of mouse) with respect to the size of the muscle, this could activate a signaling pathway that stimulates Ca entry into the cell, thereby increasing Ca storage in the SR to somehow increase the specific force generated by the muscle. We assessed the first part of this hypothesis, namely whether the smaller muscles were associated with a relatively greater load, using a parameter (denoted "R") given by the ratio of the weight of the mouse from which a muscle was taken to the weight of the muscle. As shown in Fig. S5 (E and F), R versus muscle weight values are well described by a linear, inverse relationship, i.e., confirming that R does, in fact, increase with decreasing muscle weight.

To show how $[Ca_T]_{WM}$ varies with R, the horizontal scales at the tops of the panels in Fig. 6 show R values corresponding to the muscle weights shown on the abscissa, generated using the equations for the least-squares best-fit lines of the R versus muscle weight data in E (EDL) or F (soleus) in Fig. S5. (As indicated in Section 5b of the supplemental text, the linear relations used for the R scales are expected to apply to the results in Fig. 6, even though mouse weights, and therefore R values, were not determined for most of the data in Fig. 6.) As seen in all of the panels in Fig. 6, $[Ca_T]_{WM}$ increases with increasing R values, results consistent with the idea that increasing the relative workload of a muscle increases Ca loading of the SR.

Knocking out CSQ reduced muscle weight and $[Ca_T]_{WM}$ in EDL but not soleus muscle

Fig. 7 plots measurements of $[Ca_T]_{WM}$ versus muscle weight from EDL (A) and soleus (B) muscle samples with either just the skeletal-muscle form of CSQ (CSQ1)

Published January 26, 2015

knocked out (red circles) or with both the skeletal and cardiac forms of CSQ (CSQ1 and CSQ2) knocked out (B, blue triangles). The associated control results measured at the same time are plotted as open triangles. The control results and the lines in A and B are the same as those shown in Fig. 6 (B and D, respectively). The lines indicate the expected average value of $[Ca_T]_{WM}$ for that particular muscle weight for control muscle samples. For both EDL and soleus muscle samples, there were no significant differences in the average values of $[Ca_T]_{WM}$ for both the single and double CSQ KOs.

It is evident from the results for EDL muscle samples in Fig. 7 A that the CSQ-KO muscles tended to weigh less than the control muscle, and that the values of $[Ca_T]_{WM}$ for 11 of the 12 KO muscles were significantly below the line for the control muscles. In the following assessment, the point indicated by the arrow in Fig. 7 A is not included; it is one of the two outlier points mentioned in Section 6 of the supplemental text that were rejected with the criterion that its value is more than three standard deviations above the mean of the other points in its group. The degree to which $[Ca_T]_{WM}$ is lower than the control muscles was assessed by taking the ratio, for each point, of the measured value of $[Ca_T]_{WM}$ and the expected control value for the muscle weight of the point, given by the value of the line. The average (SEM) values for this ratio for the EDL muscle results in Fig. 7 A are 0.559 (0.047; $n = 6$), 0.686 (0.043; $n = 5$), and 0.616 (0.037; $n = 11$) for, respectively, the CSQ1-KO muscles, double-KO muscles, and the combined data from both groups. All three averages are significantly <1. The mean for the CSQ1-KO muscles is not significantly less than that for the double-KO muscles,

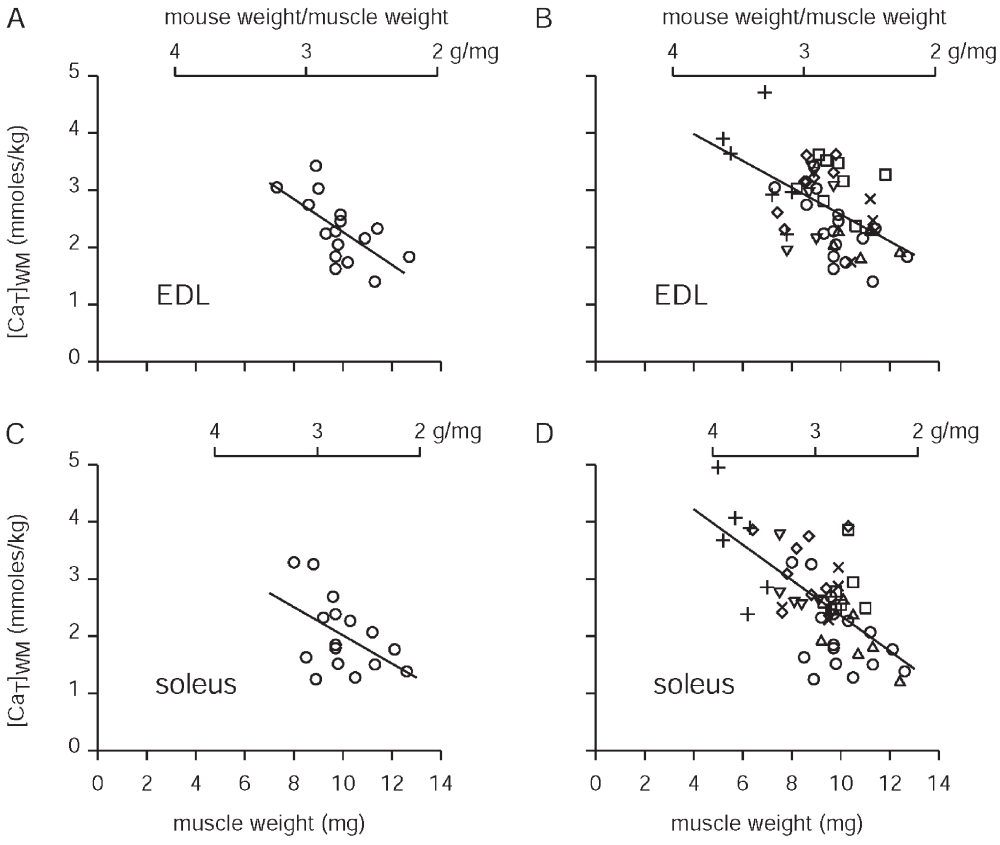

Figure 6. Inverse relationship between $[Ca_T]_{WM}$ and muscle weight in muscles from mice. (A–D) The open circles in A and C plot $[Ca_T]_{WM}$ versus muscle weight for EDL and soleus muscles, respectively, from a set of 4–6-mo-old C57BL/6 mice. B and D plot these same results in A and C, respectively, along with several other sets of muscles. Each set of muscles is plotted with a different symbol, and all muscles in a set were processed together on the same day or, in one case, a 2-d period. As for the set plotted with open circles from A and C, the sets plotted with open squares and open diamonds were also obtained with 4–6-mo-old C57BL/6 mice. All of the other four sets were genetically modified to allow for selective deletion of normally expressed genes. Because the genes function normally and because the mice were crossbred on background C57BL/6 or C57BL/6J mice, results for these other four sets would not be expected to differ from those with the C57BL/6 mice. For the two sets plotted with + and × symbols, the mice ($RANK^{floxed/floxed}$) were genetically modified to allow for deletion of the gene for the receptor activator of nuclear factor κB (RANK), an enzyme involved in regulating bone remodeling. These mice also underwent mock surgical experiments involving exposing the sciatic nerve without cutting it, and then closing the wound 2 wk before the measurements here. Because this would not be expected to alter $[Ca_T]_{WM}$, it seems reasonable to include these sets. For the two sets plotted with open triangles and open-inverted triangles, the mice were modified to allow for deletion of CSQ (results given in Fig. 7). The $RANK^{floxed/floxed}$ mice were 3–4 mo old, somewhat younger than the range of 4 to 6 mo for the mice in the other sets. The lines in each panel were obtained with least-squares best fits to the data. The best-fit slopes in units of millimoles/kilogram per milligram of muscle weight (y intercepts in millimoles/kilogram; p-values) for the lines in A–D are, respectively, −0.2866 (5.13; P = 0.0072), −0.2347 (4.92; P < 0.0001), −0.2489 (4.48; P = 0.0539), and −0.3102 (5.46; P < 0.0001). The average values (and n values) of $[Ca_T]_{WM}$ in A–D are, respectively, 2.30 (16), 2.71 (54), 2.02 (16), and 2.62 (54). For EDL muscles in A and B, the horizontal scales on top were calculated with the linear least-squares best-fit line of R versus muscle weight in Fig. S5 E given by $R = -0.187 \times$ muscle weight + 4.59. The corresponding relationship for soleus muscles in C and D is given by $R = -0.239 \times$ muscle weight + 5.14.

Published January 26, 2015

although the difference is close to significant (P = 0.082). In summary, taking into account the effect of muscle weight on $[Ca_T]_{WM}$ for the combined results, we conclude, in EDL muscle, that knocking out CSQ does decrease $[Ca_T]_{WM}$ by 38% on average compared with WT muscles. This decrease is significantly less than the >80% reduction expected as a result of the loss of Ca bound to CSQ (see Discussion).

$[Ca_T]_{WM}$ values in skeletal muscles from rats

Values for $[Ca_T]_{WM}$ were determined for whole skeletal muscle samples from rats and frogs, processed in essentially the same way as those from mice. For EDL muscle samples from Sprague-Dawley rats, the average value of $[Ca_T]_{WM}$ was 1.46 mmoles/kg (SEM = 0.09 mmoles/kg; $n = 8$). For soleus muscles from the same four rats, the average value of $[Ca_T]_{WM}$ was 1.26 mmoles/kg (SEM = 0.10 mmoles/kg; $n = 8$). Weights of the EDL muscles ranged from 0.135 to 0.296 g and averaged 0.199 g (SEM = 0.023 g). Weights of the soleus muscle ranged from 0.128 to 0.257 g and averaged 0.183 g (SEM = 0.016 g). Although there was no apparent dependence of $[Ca_T]_{WM}$ on muscle weight for the rat muscles, the sample size was too small to firmly establish a lack of effect. The values of $[Ca_T]_{WM}$ in rats given here are about half of those for mice (the average values for EDL and soleus muscles from mice given in the legend of Fig. 6 were 2.71 and 2.62 mmoles/kg, respectively).

$[Ca_T]_{WM}$ values in twitch skeletal muscles from frogs and assessment of whether or not there is a significant extracellular Ca component

Values for $[Ca_T]_{WM}$ were obtained for semitendinosus and ileofibularis skeletal muscles from frog. The semitendinosus muscles are composed of twitch fibers. For ileofibularis, almost all of the fibers are twitch fibers, with only a small fraction of slow fibers found mixed with twitch fibers in the "tonus bundle" (Peachey and Huxley, 1962), which is a small part of the whole muscle. The average values of $[Ca_T]_{WM}$ were about the same for the two groups, so the results for the two muscles are combined here. Three conditions were evaluated that differed by exposure to external solution of the whole muscles after they were removed. The first condition involved the usual procedure of an ~5-min exposure of the muscle to normal Ringer's solution, followed by gentle blotting dry and weighing of the muscle. Because of the brief exposure time and the nominally physiological level of Ca in the normal Ringer's solution, this condition should not have affected $[Ca_T]_{WM}$. For the second and third conditions, the muscles were exposed for periods of 1 h in, respectively, the 0-Ca Ringer's and normal Ringer's solution. For conditions 1, 2, and 3, the average (SEM) values in mmoles/kg for $[Ca_T]_{WM}$ were 1.88 (0.11; $n = 16$), 1.95 (0.25; $n = 8$), and 2.26 (0.27; $n = 7$). (An outlier point with a value of 5.25 mmoles/kg was excluded for condition 3. This was one of the two outlier points excluded in this study for the reasons given in Section 6 of the supplemental text.) There was no statistically significant difference between any of the three conditions. The average values for conditions 1 and 2 of 1.88 and 1.95 mmoles/kg were almost identical, indicating that there was not a significant extracellular Ca component in frog muscle. The slightly higher average value with exposure to the 0-Ca Ringer's is likely a result of random variation. As the two sets of muscles were processed on different days, this could have been caused by random errors affecting one or both of the background levels of Ca for the two sets. The similarity of the results for conditions 2 and 3 (which were from opposite leg muscles from the same frogs) provides additional evidence that there was not a large amount of Ca in the extracellular space. As discussed further in the Discussion, this contrasts with an earlier study with ^{45}Ca, which reported that more than half of the total Ca content of whole muscle from frog is extracellular, a result

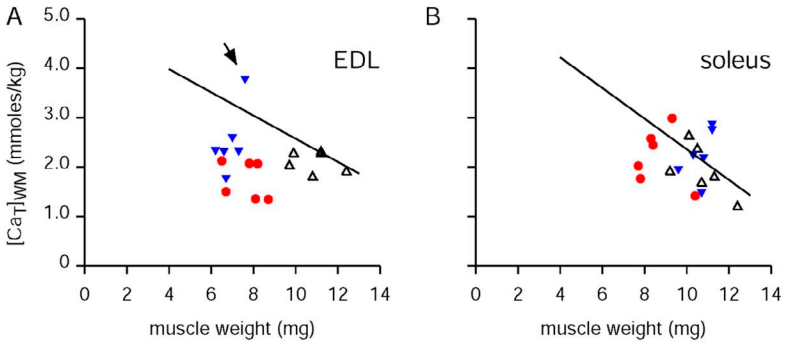

Figure 7. Effect of knocking out CSQ on $[Ca_T]_{WM}$. The solid lines in A and B for EDL and soleus muscles, respectively, are the same best-fit lines obtained for all of the control results shown in Fig. 6 (B and D, respectively). The red circles were obtained with muscles from mice with the skeletal muscle isoform of CSQ (CSQ1) knocked out, and the blue triangles were with both the skeletal and cardiac isoforms (CSQ1 and CSQ2) knocked out. The open triangles were from the control muscles processed at the same time; these were also plotted in Fig. 6. For EDL muscles ($n = 6$ for each case), the average (SEM) values of $[Ca_T]_{WM}$ in millimolars were 2.12 (0.09), 1.73 (0.16), and 2.54 (0.29) for, respectively, the controls, the CSQ1 KOs, and the double KOs. For soleus muscles ($n = 6$ for each case), the corresponding average (SEM) values were 1.95 (0.22), 2.24 (0.25), and 2.31 (0.22).

Published January 26, 2015

attributed to the binding of Ca to extracellular components (Kirby et al.,1975).

The presence of a relatively small amount of extracellular Ca indicates that all or most of extracellular Ca was present in the free form, an assumption used in the Discussion for assessing the intracellular component

Although the average value for $[Ca_T]_{WM}$ of 2.26 mmoles/kg with condition 3 (1 h in normal Ringer's solution) was not significantly greater than the average value of 1.88 mmoles/kg with condition 1 ($P = 0.131$), it was close to being significantly greater. (Inclusion of the outlier point above would result in the difference being significant.) Assuming it could be shown with more data points that the 1-h exposure to normal Ringer's solution with condition 3 does tend to increase $[Ca_T]_{WM}$, one possible explanation for this is that the concentration of Ca in the normal Ringer's solution (1.8 mM) is somewhat greater than the physiological extracellular fluid present in the freshly extracted muscle. In support of this possibility, the value of 1.8 mM generally used for frog muscle could be too high, as it is apparently based on limited measurements made almost 80 years ago and before. (Its apparent origin was the calculation of 1.8 mM by Fenn [1936] for a Ringer's solution that contains 0.2% [wt/vol] of $CaCl_2$. The origin of this percentage is unclear, as it is much greater than the 0.012% [wt/vol] reported by Ringer [1883] from his five parts of $CaCl_2$ solution in 100 cm^3 of saline and other components; the $CaCl_2$ solution contained 1 part of $CaCl_2$ in 390 parts water. The 1.8-mM value does, however, agree with Fenn's measured value of 2 mM for the concentration of Ca in plasma from frog.)

Summary of $[Ca_T]$ values from different species

For the purpose of a convenient reference, Table 1 gives average values for $[Ca_T]_{WM}$ determined in this study and the concentration (mM) of total intracellular Ca referred to the myoplasmic water volume for all of the muscle types and species evaluated in this study. The latter values are provided because they should be close to the concentration of total releasable Ca from the SR referred to the myoplasmic volume usually determined with a myoplasmic indicator. Considering total Ca in just the extracellular (EC) and intracellular (IC) compartments, the following mass balance for Ca should apply:

$$W_M\left[Ca_T\right]_{WM} = W_M \cdot 0.124 \cdot \left[Ca_T\right]_{EC} + 0.58 \cdot W_M\left[Ca_T\right]_{IC\_ref\_myo}, \quad (21)$$

where W_M is the weight of the muscle (in kg) and $[Ca_T]_{EC}$ is an assumed concentration (mM) of total Ca in the extracellular space. The factor 0.124 gives liters of extracellular water volume per kilogram of whole skeletal muscle and was determined for rat skeletal muscle (Cieslar et al., 1998). The factor 0.58 has units of liters of myoplasmic water per kilogram of whole muscle (Baylor et al., 1983). Both of these factors are assumed to apply for all of the muscle types given in Table 1. Eq. 21 can be rearranged to give

$$\left[Ca_T\right]_{IC\_ref\_myo} = 1.72 \cdot \left[Ca_T\right]_{WM} - 0.214 \cdot \left[Ca_T\right]_{EC}. \quad (22)$$

Values for $[Ca_T]_{EC}$ of 2 and 1.8 mM, corresponding to the concentrations of Ca generally used, respectively, in mammalian and frog Ringer's solutions, were assumed for mammalian and frog muscles in Table 1. It is noted that the values for $[Ca_T]_{IC\_ref\_myo}$ in Table 1 would overestimate total releasable Ca in the SR by the amount of nonreleasable Ca in the SR (if such a component exists) and by resting Ca outside the SR. Estimates of this latter component are given in the Discussion.

Evaluation of the possibility that Ca was "lost" to parvalbumin by adding Mg to the measurement solution

The myoplasmic protein parvalbumin is involved in rapid relaxation in twitch muscle from frogs and fast-twitch muscle from mammals (e.g., Heizmann et al., 1982; Baylor et al., 1983) and is either absent or at nearly undetectable levels in slow-twitch muscles (see, e.g., Heizmann et al., 1982). Each of two metal-binding sites on parvalbumin (formed by E-F hand motifs) binds Ca with very high affinity and Mg with moderate affinity. As shown in Table 2 and associated text in the first part of the Appendix, if parvalbumin maintained its high affinity for Ca after exposure to SDS (which denatures proteins), BAPTA would not have been able to capture Ca from parvalbumin when using our usual measurement solution, i.e., the measurement solution without Mg. If this was the case, the results with the BAPTA method reported thus far would have underestimated Ca by ~25%

TABLE 1
Average (SEM) values of $[Ca_T]$

	1	2	3	4
	Muscle type	$[Ca_T]_{WM}$ *mmoles/kg wet weight*	$[Ca_T]$ referred to myoplasm *mmoles/liter of myoplasmic volume*	*n*
1	Mouse EDL	2.71 (0.09)	4.23 (0.14)	54
2	Mouse soleus	2.62 (0.11)	4.08 (0.17)	54
3	Rat EDL	1.46 (0.09)	2.08 (0.13)	8
4	Rat soleus	1.26 (0.10)	1.74 (0.14)	8
5	Frog ileofibularis and semitendinosus	1.88 (0.11)	2.85 (0.17)	10

$[Ca_T]$ values for all of the muscle types used in this study. For column 2, the values for mouse EDL and soleus muscles were from the data plotted in Fig. 6 (B and D, respectively), and the values for rat and frog muscles were, respectively, from the third and second preceding sections giving results for these muscles. The values for frog twitch muscle were obtained with condition 1, i.e. with muscles blotted dry soon after extraction. See text associated with this table for the determination of values in column 3.

Published January 26, 2015

because of "loss" of Ca bound to parvalbumin, either in the pellet after centrifugation or with any parvalbumin still in the supernatant (see Tables 2 and 3 in the Appendix). However, results in Cox et al. (1979; their Table 1) showed that treatment of parvalbumin with 1% SDS resulted in loss of parvalbumin's metal-sensitive fluorescence. This strongly suggests that the denaturing of parvalbumin by SDS prevents metal binding to parvalbumin. Because the concentration of SDS was similar in this study (0.5 vs. 1%), it is likely that metal binding to parvalbumin was also eliminated or at least parvalbumin's affinity was reduced enough so that BAPTA was able to capture Ca from parvalbumin.

To assess whether or not Ca was lost to parvalbumin, Mg was added to the usual measurement solution to lower parvalbumin's apparent affinity for Ca (see Eq. A2 in the Appendix). Results are compared below with no added Mg in the measurement solution (the usual solution used for all of the results thus far) and with Mg added so that the modified measurement solution contained 2 mM [Mg] in addition to its usual constituents. Before presenting these results, it is useful to first consider simulations of the experiments with the BAPTA method using published values for the Ca- and Mg-binding constants of BAPTA, EGTA, and parvalbumin, performed with the following three sets of conditions (see Table 3 in the Appendix and associated text): condition 1: with a Mg-free measurement solution and with no binding of Ca or Mg to parvalbumin; condition 2: with a Mg-free measurement solution and now including metal binding to parvalbumin; and condition 3: with 2 mM Mg and also including metal binding to parvalbumin. As seen from the last row of Table 3 for conditions 1–3, the BAPTA method would have reported 99.6, 75.2, and 94.8%, respectively, of the total Ca present (ignoring the relatively small amounts of Ca that might be bound to other sites as seen in Table 2). Based on these simulations, if parvalbumin's metal-binding properties were not affected by SDS, the reported values of $[Ca_T]_{WM}$ with 2 mM Mg present (condition 3) would be greater on average than those without Mg present (condition 2) by a predicted 26.1% ($100 \times (94.8 - 75.2) \div 75.2$). If parvalbumin's ability to bind metals was lost because of the SDS treatment, the addition of 2 mM Mg is predicted to have a negligible effect, decreasing the percentage of total Ca reported by BAPTA from 99.6% (condition 1) to 99.4% (results for this condition are not depicted).

For muscles from eight mice, a value of $[Ca_T]_{WM}$ for EDL muscle with 2 mM Mg in the measurement solution was obtained from the muscle from one leg of a mouse (left or right), and the value with no Mg present (the usual measurement solution) was obtained from the muscle taken from the opposite leg. The average value of 3.194 mmoles/kg (SEM = 0.275 mmoles/kg) for $[Ca_T]_{WM}$ with 2 mM Mg present was almost the same as that without Mg present, 3.124 mmoles/kg (SEM = 0.180 mmoles/kg). These results support the idea that denaturation of parvalbumin by the SDS treatment occurred, thereby allowing BAPTA to capture Ca that might otherwise have been lost as a result of binding to parvalbumin. However, this conclusion is not certain because of unexpected results for the soleus muscles from the same eight mice. Soleus muscle contains little, if any, parvalbumin (Heizmann et al., 1982), so that one would not expect a difference in $[Ca_T]_{WM}$ with Mg added. Contrary to this expectation for the soleus muscles, the average of 2.418 mmoles/kg (SEM = 0.120 mmoles/kg) with 2 mM Mg present was significantly lower ($P = 0.015$; paired t test) than the average value of 3.268 mmoles/kg (SEM = 0.204 mmoles/kg) without Mg present in the measurement solution. We have no explanation for this difference other than random error or the possibility of some unexplained effect of Mg. Because of this unresolved problem, we can only tentatively conclude that the BAPTA method was able to record essentially all (within a few percent) of the Ca present in the muscle, a conclusion based on the lack of any effect of the added Mg on the reported $[Ca_T]_{WM}$ values in EDL muscle and the results from Cox et al. (1979) cited above.

DISCUSSION

Much of this Methods and Approaches article was devoted to verifying the reliability of a new method for measuring the total Ca content of a tissue sample based on BAPTA absorbance. The Discussion begins with an explanation of the need to measure background Ca, much of which may come from Ca leaching from labware. Results reviewed afterward indicate that the method does provide a reliable measure of total muscle Ca if the background level of Ca and the additional problem of stray light are properly addressed.

The problem of Ca leaching from labware

Results in Fig. S4 and Section 4 of the supplemental text show that Ca leaches slowly (over many days) from glass scintillation vials (used to store the 1.5-mM $CaCl_2$ standard solution) and very rapidly from the Pasteur pipettes used to mix all of the aliquots. The very rapid leaching from Pasteur pipettes is presumably caused by readily releasable Ca present on the surface of the glass. As explained with Fig. S4, because this Ca leaching only affected the Ca-standard aliquots (A_S and S_S), this did not impact the results reported in this article, as the Ca-standard measurements were not needed and not used for the determination of total Ca.

It has long been recognized by some researchers that leaching of divalent ions (Ca^{2+}, Mg^{2+}, Pb^{2+}) from some types of glass used for patch-clamp electrodes can affect ionic currents, and that chelating agents can minimize

Published January 26, 2015

such effects (Cota and Armstrong, 1988; Rojas and Zuazaga, 1988). We were unable to find any references addressing the problem of Ca leaching from other forms of labware, although anecdotal evidence suggests that at least some researchers are aware of the possibility. Given this background, we are not sure to what extent the problem of Ca leaching revealed here is a new finding. In any case, the results suggest that such Ca leaching could produce unexplained experimental results under some conditions if it is not recognized and addressed. The BAPTA method would be useful for assessing Ca leaching from labware, as done with Fig. S4.

For the purposes of this study, Ca leaching would not be a problem as long as the amount of Ca leached was the same for all of the labware. To highlight this point, it is noted that some initial, confounding results were later attributed to a variable degree of Ca leaching from polycarbonate centrifuge tubes initially used for the larger muscles from frogs and rats. These results are not reported here, and other types of centrifuge tubes were subsequently used that gave constant background Ca levels indicating either no leaching or about the same degree of Ca leaching from each tube. The reason a constant amount of leached Ca would not be a problem is that it would be included in the background Ca level, which is subtracted off. Therefore, in addition to making measurements in parallel without tissue present, application of the BAPTA method (and most other methods for assessing total Ca) should include confirmation of constant background Ca levels with the labware used.

The BAPTA method can reliably estimate the total Ca content of a muscle sample

In regards to the reliability of the BAPTA method, one major concern was the possibility that muscle components could somehow affect the results. One problem would be if remnant muscle components in the supernatant after centrifugation or substances in the solution (such as the pH buffer used or any remaining SDS) had a Ca-dependent absorbance in the UV. This possibility was discounted by results in Fig. 2 that showed no difference in the "intrinsic" absorbance of the four aliquots (A_M, A_0, A_S, and A_∞; measured without BAPTA present). This finding justified Assumption 4 in Materials and methods (so that A_{intr} was the same in all four aliquots).

Another key assumption, based on the relatively large concentration of BAPTA and BAPTA's high affinity for Ca, is that BAPTA captures essentially all of the Ca initially present in the muscle (Assumption 1 in Materials and methods). Calculations in Tables 2 and 3 indicate that BAPTA should, in fact, capture essentially all of the Ca on the major Ca-binding proteins in muscle, with the possible exception of Ca bound to the Ca/Mg sites on parvalbumin, troponin, and myosin. Based on experiments in the last section of Results with 2 mM Mg to greatly reduce possible Ca binding to these sites, we tentatively concluded that Ca was not lost to these sites. As mentioned, the most likely explanation for this is that SDS denatured parvalbumin and perhaps also troponin and myosin, thereby lowering their abilities to bind Ca, allowing BAPTA to capture all or most of the Ca that might otherwise have remained bound to the Ca/Mg sites. Even though the lack of added Mg in our basic measurement solution did not appear to have affected the results in this article, a Mg concentration of 2 mM or more in the measurement solution is recommended for future applications of the BAPTA method.

Results showed that $[B_T]$ with muscle present was, on average, ~96% of the value with no muscle present, indicating that very little BAPTA was lost in the pellet formed in the centrifugation step and/or by some interaction with soluble muscle components still present in the supernatant. More importantly, based on comparisons of BAPTA's response to the addition of a Ca standard in the presence and absence of muscle, the ability of BAPTA to detect Ca was not greatly affected by the presence of muscle, with the results indicating a possible underestimate of $[Ca_T]_{WM}$ of only 3.3% on average. This result largely justifies Assumption 5 in Materials and methods that binding of Ca-free or Ca-bound BAPTA to muscle components does not occur or, if it does, that it has little effect on BAPTA's response to total Ca.

This section covered three of the five assumptions for the BAPTA method given in Materials and methods. As indicated in Materials and methods, the other two assumptions should also be valid. We conclude that the five key assumptions are all valid and that the BAPTA method should provide a reliable measure of the total Ca content of a tissue sample.

Different components of total Ca in whole muscle

For discussions below, it is helpful to consider the following components of the concentration of total Ca in whole muscle: extracellular ($[Ca_T]_{EC}$), intracellular outside of the SR ($[Ca_T]_{NonSR}$), and intracellular inside the SR ($[Ca_T]_{SR}$). With these definitions,

$$[Ca_T]_{WM} = [Ca_T]_{EC} + [Ca_T]_{NonSR} + [Ca_T]_{SR}. \quad (23a)$$

It is useful to consider the different Ca components in fractional terms, obtained by dividing both sides of Eq. 23a by $[Ca_T]_{WM}$, giving

$$1.0 = f_{EC} + f_{NonSR} + f_{SR}. \quad (23b)$$

$$\text{EDL muscle: } 1.0 = 0.11 + 0.12 + 0.77 \quad (23c)$$

$$\text{soleus muscle: } 1.0 = 0.11 + 0.02 + 0.87 \quad (23d)$$

Published January 26, 2015

Eqs. 23c and 23d give estimates for the fractions of $[Ca_T]_{WM}$ associated with the different components in EDL and soleus muscles, respectively. The value of 0.11 for f_{EC} is from the value of 0.124 liters of extracellular water volume per kilogram of whole skeletal muscle determined for rat skeletal muscle (Cieslar et al., 1998), the concentration of 2 mM for Ca in the extracellular space (set by the concentration in the mammalian Ringer's solution), and the average value of $[Ca_T]_{WM}$ for the EDL muscles from C57BL/6 mice in Fig. 6 A of 2.30 mmoles/kg (0.11 = 0.124 × 2 mM ÷ 2.30). The value of 0.12 for f_{NonSR} in Eq. 23c is from the sum of values of 0.224 and 0.046 mmoles/kg of whole muscle for the estimated concentrations of Ca bound to the Ca/Mg sites on parvalbumin and troponin in the resting state (see "Estimation of Ca bound in the resting state..." in the Appendix; 0.12 = (0.224 + 0.046) ÷ 2.30). Because soleus muscle has little, if any, parvalbumin (Heizmann et al., 1982), the value of 0.02 for f_{NonSR} in Eq. 23d is that estimated for troponin only (0.02 =0.046 ÷ 2.30). As indicated in the second section of the Appendix, parvalbumin and the Ca/Mg sites on troponin are the only myoplasmic sites with a nonnegligible resting Ca level compared with the total Ca content of muscle. As also indicated, the resting Ca content of mitochondria should also be negligible. It is expected that other non-SR components of Ca are also negligible. The values of 0.77 and 0.87 for f_{SR} in Eqs. 23c and 23d, respectively, were calculated to balance the equations. We assume that the values in Eq. 23c also apply to twitch muscle from frog discussed in the next section.

The intracellular Ca content with the BAPTA method agrees with the SR Ca content in frog cut twitch fibers

As mentioned in the Introduction, one reason for obtaining information about the Ca content of whole tissue is to assess whether or not the Ca contents in isolated single-cell preparations under nominally physiological conditions are, in fact, physiological. As shown in this section, the values of Ca content in whole muscle reported in this study for frog muscle agree with the total amount of releasable Ca from the SR in cut twitch fibers from frog measured with the EGTA/phenol red method (same as $[Ca_T]_{SR}$ in Eq. 23a above; concentrations referred to myoplasmic water volume). Similar to the BAPTA method introduced in this study, with the EGTA/phenol red method, a relatively large concentration of a Ca buffer (EGTA in this case) is present, capturing almost all (>97%) of the released Ca. Cut fibers were equilibrated for a period of ~60 min with an internal solution (i.e., end-pool solution) that contained 20 mM EGTA and 1.76 mM of total Ca at pH 7, giving an estimated concentration of 36 nM for free Ca^{2+} in the end pools. Based on the active pH signal in response to a "fully depleting" train of action potentials, Pape et al. (1995; their Table 2) obtained an average value for $[Ca_T]_{SR}$ of 2.685 mM (SEM = 0.252 mM; n = 12; concentration referred to myoplasmic water volume) under current-clamp conditions (normal Ringer's external solution and K internal solution). The average value under voltage-clamp conditions of 2.544 mM (SEM = 0.070 mM; n = 11) was very similar to that obtained under current-clamp conditions. Two estimates for $[Ca_T]_{SR}$ from the results in this study are given next.

The first estimate of $[Ca_T]_{SR}$ is based on the average value of 1.96 mmoles/kg (SEM = 0.25 mmoles/kg; n = 8) for $[Ca_T]_{WM}$ for muscles exposed to the 0-Ca Ringer's solution for 1 h (condition 2 in "$[Ca_T]_{WM}$ values in twitch skeletal muscles from frogs..." in Results) and assumes that all of the extracellular Ca diffused out of the muscle during the 1-h period and that none of the intracellular Ca was lost. From Eq. 23b above with $[Ca_T]_{EC}$ = 0, the estimated fraction of $[Ca_T]_{WM}$ coming from the SR is 0.87 (0.87 = 0.77 ÷ (0.012 + 0.77)). With this fraction along with the value for $[Ca_T]_{WM}$ and the factor of 0.58 kg (or liter) of myoplasmic water per kilogram of whole muscle (Baylor et al., 1983), the first estimate of $[Ca_T]_{SR}$ is 2.94 mM (SEM = 0.38 mM; n = 8; the values 2.94 and 0.38 mM are given by 1.96 and 0.25 mmoles/kg, respectively, multiplied by 0.87 and divided by 0.58). This average value is not significantly different from the average value of 2.685 mM for $[Ca_T]_{SR}$ in cut fibers above (P = 0.47).

The second estimate of $[Ca_T]_{SR}$ is obtained from the average value of 1.88 mmoles/kg (SEM = 0.11 mmoles/kg; n = 16) for $[Ca_T]_{WM}$ for muscles quickly rinsed in normal Ringer's solution and blotted dry just after extraction, thereby minimizing any diffusional loss or gain from the extracellular space (condition 1 in "$[Ca_T]_{WM}$ values in twitch skeletal muscles from frogs..." in Results). This second estimate is 2.50 mM (2.50 = 1.88 × 0.77 ÷ 0.58), which is very close to the average value of 2.685 mM for $[Ca_T]_{SR}$ in cut fibers. Because the second estimate did not require an assumption concerning possible loss of Ca from the extracellular compartment, it should give the best estimate of $[Ca_T]_{SR}$ under physiological conditions. In summary, the nominally physiological values of $[Ca_T]_{SR}$ for cut fibers from frog twitch muscle in Pape et al. (1995) are, in fact, close to the physiological level estimated here.

Comparison with the SR Ca contents determined in mammalian skinned fibers

From Results, the average values of $[Ca_T]_{WM}$ from EDL and soleus muscles from rat (SEM; all units in mmoles/kg of muscle; n = 8 for each case) were 1.46 (0.09) and 1.26 (0.10), respectively. For comparison with results below, these values were multiplied by the assumed density of muscle (1.06 kg per liter) to give units in millimolar that referred to whole-muscle volume and then multiplied by the fractions of 0.77 and 0.87 for EDL and soleus muscles, respectively, from Eqs. 23b and 23c,

Published January 26, 2015

respectively. The resulting estimates of $[Ca_T]_{SR}$ that referred to whole-muscle volume are 1.12 (0.07) and 1.10 (0.09) mM (units of mmoles of Ca/L of muscle). These values are compared here with $[Ca_T]_{SR}$ values estimated in skinned fibers from EDL and soleus muscles from rat (Fryer and Stephenson, 1996). The somewhat involved approach consisted of mechanically skinning the fibers under oil, followed by a brief (∼1-min) "equilibrating period" in a solution containing BAPTA (in part to prevent saturation of the Ca-regulatory sites on troponin) and Ca with a Ca/BAPTA ratio giving a nominally physiological concentration of free Ca^{2+} of 71 nM (pCa = 7.15). The total Ca content was then determined by the integrated tension response after permeabilization of the SR membrane with triton, calibrated afterward with tension responses with different Ca/BAPTA ratios. The average values of total Ca from the SR that referred to the whole fiber volume for EDL (fast-twitch) and soleus (slow-twitch) fibers in Fryer and Stephenson (1996) were 1.32 mM (SEM = 0.02 mM) and 1.35 mM (SEM = 0.08 mM), respectively (values of n were not given, although they were apparently in the range of 20 to 65). The average value of 1.32 mM for EDL muscle was significantly greater than that of 1.12 mM estimated above from the value of $[Ca_T]_{WM}$ in this study, whereas the value of 1.35 mM for soleus muscle was not significantly greater than that of 1.10 mM from this study (regardless of the value of n assumed for the skinned-fiber results, assumed to be 20 or 65). Despite the significant difference for the EDL muscles, the average values are fairly close. Also, because whole-muscle volume contains interstitial space and whole fiber volume does not, the values of 1.12 and 1.10 mM for $[Ca_T]_{SR}$ from this study should be scaled up somewhat for the comparison with those estimated with skinned fibers. We conclude that the values with the two methods are in agreement. This agreement indicates that the total Ca content obtained in both fast-twitch and slow-twitch skinned fibers from rat by Fryer and Stephenson (1996) were very close to the physiological level, in support of the requirement of a minimal loss or gain of Ca during the equilibrating period of their protocol described above.

Using essentially the same approach for estimating $[Ca_T]_{SR}$ in skinned fibers from human skeletal muscle, Lamboley et al. (2013b) obtained average values of 0.85 and 0.76 mM (these referred to whole-fiber volume) for fast-twitch (type II) and slow-type (type I) fibers, respectively, both obtained from vastus lateralis muscle biopsies. These values are similar, although somewhat less than the average values above for rat muscle.

Agreement with earlier methods for measuring Ca content of mammalian whole muscle

The most common method previously used for determining total Ca content of whole muscle involved some type of treatment of the muscle sample, followed by measurement of total Ca with atomic absorption spectroscopy (AAS). The most common, and also most recent, pretreatment protocol was somewhat similar to that used in this study, involving homogenization of the sample and then exposure to trichloroacetic acid (TCA) to precipitate proteins, followed by centrifugation to remove muscle components. With this approach, Gissel and Clausen (1999) reported an average value of 1.21 mmoles/kg (SEM = 0.04 mmoles/kg; n = 10) for $[Ca_T]_{WM}$ in rat soleus muscle. This average value is not significantly different from the corresponding average value obtained for rat soleus muscle in this study of 1.26 mmoles/kg (SEM = 0.01 mmoles/kg; n = 8). With the same approach with TCA and AAS, Everts et al. (1993) reported an average value of 1.46 mmole/kg (SEM = 0.04; n = 3) for rat EDL muscle, which is the same value obtained in this study, 1.46 mmoles/kg (SEM = 0.09 mmoles/kg; n = 8). It is noted that the problem of possible loss of Ca to parvalbumin addressed in the last section of Results would also apply to the pretreatment protocol with TCA. The agreement of the total Ca contents in rat EDL muscle with the TCA-AAS approach with the results from this study suggests that the denaturing effect of TCA also reduced parvalbumin's apparent affinity for Ca.

There are only a few reports of total Ca content in whole muscles from mice. Our best estimates for this data, given in bar graphs for tibialis anterior in Yoshida et al. (2006) and gluteus and quadriceps muscle in Glesby et al. (1988), are 1.68, 1.68, and 1.77 mmoles/kg. These values are within the range but on the low side of values with EDL and soleus muscles in this study; the average values for $[Ca_T]_{WM}$ for EDL and soleus muscles given in Table 1 are 2.71 and 2.62 mmoles/kg, respectively.

Comparison of Ca content in frog whole-muscle samples with results from earlier methods

Kirby et al. (1975) estimated the concentration of total Ca in whole toe muscles from frog (also *Rana pipiens*) using a ^{45}Ca washout method and AAS. Their values for $[Ca_T]_{WM}$ with the two methods were, respectively, 1.96 and 2.00 mmoles/kg, values not significantly different from the average value in this study of 1.88 mmoles/kg for $[Ca_T]_{WM}$ for twitch muscle (the ileofibularis and semitendinosus muscles, which are leg muscles). In contrast to the results in this study, Kirby et al. (1975; see their Table 2) reported that only 0.83 of the 1.96 mmoles/kg Ca obtained with the ^{45}Ca method was intracellular, with the remaining 1.13 mmoles/kg coming from the extracellular compartment, i.e., only 42% was intracellular (42% = 100 × 0.83 mM ÷ 1.96 mM). They concluded that there must be a very large amount of bound Ca in the extracellular space, perhaps to proteins such as collagen and/or to the surface and T-system membranes. We have no plausible explanation for the fact that our results indicate a much larger amount of intracellular Ca (∼2.3-fold) and no bound pool in the extracellular

Published January 26, 2015

space. It seems unlikely that the difference is caused by the different muscles used, leg versus toe muscles.

When CSQ is knocked out, muscles compensate for the loss of Ca content associated with CSQ by increasing Ca at other sites

To help interpret the results with CSQ knocked out, Section 7 of the supplemental text gives predicted values of $[Ca_T]_{WM}$ with CSQ KO assuming that the only effect of the KO was to remove the Ca component bound to CSQ. With this assumption, CSQ KO is predicted to reduce $[Ca_T]_{WM}$ to 0.256 and 0.160, respectively, of the values for EDL and soleus muscles from WT mice. Because $[Ca_T]_{WM}$ with EDL muscles from mice with CSQ knocked out in EDL muscles was 62% on average of the value expected for control muscle (combined single- and double-KO results taking into account muscle weight; the 62% value is given in text associated with Fig. 7), the average value of $[Ca_T]_{WM}$ with CSQ KO muscles was 2.4-fold greater than predicted (2.4 = 0.62 ÷ 0.256). For soleus muscles, CSQ KO did not affect $[Ca_T]_{WM}$, so the values of $[Ca_T]_{WM}$ with the CSQ KO muscles were 6.3-fold greater than predicted (6.3 = 1.0 ÷ 0.160). Possible reasons are given below for why the measured value of $[Ca_T]_{WM}$ was so much greater than the predicted values.

As noted in the Introduction, apparently contradictory results have been reported as to whether knocking out CSQ results in a large reduction in total releasable Ca in the SR (which should be equivalent to $[Ca_T]_{SR}$ above). With the assumption that there was no change in the extracellular and intracellular non-SR Ca components, the modest decrease in $[Ca_T]_{WM}$ for CSQ1-KO EDL muscles relative to controls in this study is in agreement with the modest (25%) decrease in readily releasable total Ca in patch-clamped single EDL fibers from CSQ1-KO versus WT mice reported in Sztretye et al. (2011; their Table 1). This modest decrease contrasts with the ∼70% reduction in readily releasable Ca estimated in fibers from CSQ1-KO versus WT EDL muscle from mice (Paolini et al., 2007; their Fig. 8, B and E). One way to distinguish between the possibilities would be if one or the other method gave a more dependable estimate of $[Ca_T]_{SR}$. However, although both methods are indirect and can be challenged, they both appear, at first glance, capable of determining the degree to which $[Ca_T]_{SR}$ in KO muscle fibers might vary from that in WT fibers. For the following three reasons, we believe the most likely possibility is that the loss of Ca associated with the removal of CSQ was compensated for by an increase in SR Ca, probably Ca binding to some other protein in the SR. (1) It appears unlikely that the compensatory increase would have occurred outside the SR. A sufficiently large increase in Ca in the extracellular space seems unlikely, as $[Ca^{2+}]$ in the extracellular space was set by the experimental conditions. Also, because both approaches involved isolated single fibers, a difference in $[Ca_T]_{EC}$ would have required the expression of a previously unknown high capacity Ca-binding protein in the T-system when CSQ is knocked out (a possibility, although a seemingly remote one). In regards to the intracellular, non-SR possibility, parvalbumin is the only known candidate with both the required high capacity and high affinity Ca-binding sites (see second section of Appendix). One argument against an increase in parvalbumin concentration is that it would not explain the lack of a decrease in $[Ca_T]_{WM}$ in soleus muscle because parvalbumin is normally not present in soleus muscle from mice. Also, in EDL muscle, an increase in parvalbumin concentration would have tended to speed up relaxation (the primary function of parvalbumin), whereas relaxation was slower in fibers with CSQ knocked out compared with WT fibers (Paolini et al., 2007), although the somewhat slower relaxation could be caused by other factors. (2) At least in regards to the possibility of a large increase in Ca binding to a myoplasmic site, there would be no apparent physiological advantage, whereas restoring the CSQ's function of storing Ca in the SR would be advantageous. (3) And lastly, at least four Ca-binding protein components in the SR have already been identified that may serve to replace some of the Ca-storing function lost with CSQ KO (the four protein components including sarcalumenin and calreticulum are reviewed on p. 415 of Fénelon et al., 2012; to our knowledge, the other two are still unnamed).

Although arguments other than the difference in the two methods above favor the possibility of a compensatory increase in $[Ca_T]_{SR}$ as opposed to an increase in non-SR Ca, it seems worthwhile to discuss the methods used to understand why they may have given different results. Sztretye et al. (2011) estimated SR Ca content from the voltage-activated myoplasmic free Ca^{2+} transient with total Ca released derived from this transient and assumptions about the Ca-buffering properties of myoplasm including added Ca buffer. Importantly, much of the released Ca was captured by the relatively large concentrations of added Ca buffer in the myoplasm, either EGTA or BAPTA, reducing some of the uncertainty in the method and also preventing early termination of SR Ca^{2+} release caused by Ca inactivation so that a large fraction of the resting SR Ca content could be released. The approach of Paolini et al. (2007) was similar to the skinned-fiber approach described above (Fryer and Stephenson, 1996) in that the total Ca content was assumed to be proportional to the integrated tension signal in response to the maximal release of SR Ca (by caffeine in the case of Paolini et al., 2007). One potential problem with the approach of Paolini et al. (2007), however, was that excess Ca buffer was not added so that the tension response would tend to be saturated and, therefore, nonlinear with respect to total Ca released. Another important difference was that released Ca^{2+} would have been able to diffuse away from the fiber with the conditions used in Paolini et al. (2007), unlike

Published January 26, 2015

the approach with skinned fibers, as they were immersed in oil. Because results from several laboratories indicate, or at least suggest, that SR Ca^{2+} release is completed significantly earlier in fibers from muscles with CSQ knocked out compared with those from WT muscles (Paolini et al., 2007, 2011; Canato et al., 2010; Sztretye et al., 2011), the tension response should also be shorter if the released Ca is able to diffuse away from the fiber resulting in reduction in the integrated tension response. Any of these differences with the experimental approach of Paolini et al. (2007) may have resulted in a greater reduction in the apparent SR Ca content than what actually occurred with CSQ KO.

Given past results indicating that most of the Ca in muscle is bound to CSQ in WT muscle (see above), and because knocking out CSQ must have eliminated this large component, there must have been a large compensatory increase in Ca at some other site or sites.

As argued above, the SR is the most likely location for this compensatory increase. Paolini et al. (2007) and Protasi et al. (2009) reported several ultrastructural changes in EDL muscles with CSQ knocked out, including the presence of multiple T-tubular elements stacked between somewhat flattened junctional SR regions. Although an increase in SR volume was not observed, the increase in SR membrane area might result in increased Ca-binding sites to SR membrane or any associated protein. In addition, given the changes in the ultrastructure observed, it seems reasonable to suppose that other adaptations may have occurred to maintain normal SR Ca^{2+} release, including the up-regulation of one or more of the four previously identified Ca-binding proteins in the SR (see above) or some, as yet unidentified, Ca-binding protein. Because the concentration of free Ca^{2+} in the SR was apparently not significantly altered by CSQ KO (Canato et al., 2010; Sztretye et al., 2011), a compensatory increase in Ca bound to an alternate Ca-binding protein in the SR would almost certainly have had to involve up-regulation of the concentration and/or the Ca^{2+}-binding affinity of this alternate protein.

The possibility of a physiological mechanism that increases muscle Ca content with increased specific force requirements

As seen in Fig. 6, $[Ca_T]_{WM}$ increases substantially as muscle weight decreases in both fast-twitch and slow-twitch skeletal muscle from mice. As seen from the best-fit lines to the data, the Ca contents nearly doubled in both cases with a twofold decrease in muscle weight from 12 to 6 mg, close to the full range of whole-muscle weights for both types of muscle. The least-squares best-fit line in Fig. 6 B for EDL muscle gave values for $[Ca_T]_{WM}$ at 12 and 6 mg of 2.104 and 3.513 mmoles/kg, respectively, a 1.67-fold increase. For the same muscle weights for soleus muscle, the values of $[Ca_T]_{WM}$ were 1.739 and 3.600 mmoles/kg, respectively, a 2.07-fold increase. The $[Ca_T]_{WM}$ in Fig. 6 were also plotted as a function of R (the ratio of mouse weight to muscle weight), a parameter likely reflecting the relative workload or specific force associated with the muscle's contribution to mouse movements. For the decrease in muscle weights above of 12 to 6 mg, the value of R was expected to increase from 2.35 to 3.47 g/mg for EDL muscles and 2.27 to 3.71 in soleus muscle (values determined from linear relationships for R vs. muscle weight given in legend of Fig. 6). For EDL muscles, this means that the 1.67-fold increase in $[Ca_T]_{WM}$ was associated with a 1.48-fold estimated increase in R with the decrease in muscle weight from 12 to 6 mg. For soleus muscle, the 2.07-fold increase in $[Ca_T]_{WM}$ was associated with a 1.63-fold estimated increase in R. To our knowledge, the inverse relationship between $[Ca_T]_{WM}$ and muscle weight is a new finding.

Given the increase in $[Ca_T]_{WM}$ with increasing R values, it seems reasonable to hypothesize the existence of a physiological mechanism that somehow increases the Ca load in smaller muscles to maintain the specific force or some other contractile property required by the muscle. Moreover, because an individual muscle fiber would not know the size of the whole muscle, it seems likely that such a mechanism or mechanisms would be controlled by the force demands on individual fibers in the whole muscle.

There could be several explanations for the increase in $[Ca_T]_{WM}$ with decreasing muscle weight and increasing R. Although the results thus far do not rule out increases in Ca in non-SR locations, such as the extracellular space and/or mitochondria, the location of the increased Ca is most likely the SR. Such an increase would have to be caused by an increase in the volume fraction of SR in the muscle and/or an increase in the resting concentration of total Ca in the SR ($[Ca_T]_{SR,R}$). An increase in $[Ca_T]_{SR,R}$ could be caused by an increase in Ca bound to CSQ (and perhaps other Ca-binding proteins in the SR) either by increasing the concentration of CSQ and/or increasing the fraction of binding sites occupied by Ca by increasing the resting concentration of free Ca in the SR ($[Ca^{2+}]_{SR,R}$). (Because free Ca^{2+} is only a small fraction of total Ca in the SR, it is unlikely that the large increase in total SR Ca with decreasing muscle weight would be attributable to any significant extent to an increase in the pool of free Ca^{2+}.) The latter case of increasing Ca bound to CSQ by increasing $[Ca^{2+}]_{SR,R}$ probably does not occur with soleus muscle, as Fryer and Stephenson (1996) reported that bound Ca in the SR of soleus muscle is at a saturated level. (This was not the case for the fast-twitch muscles that had $[Ca_T]_{SR,R}$ values of about one third the saturating level.) Therefore, the large increase in $[Ca_T]_{WM}$ with decreasing muscle weight for soleus muscle in this study is presumably caused by increased fractional SR volume and/or an increased

Published January 26, 2015

concentration of CSQ and/or some other Ca-binding protein in the SR.

Could an increase in $[Ca_T]_{SR,R}$ result in an increase in the specific force generated by a muscle?

Because measurements combined with modeling results indicate that almost all of the Ca-regulatory sites on troponin are occupied by Ca in response to a single action potential in both fast-twitch and slow-twitch mammalian fibers (Baylor and Hollingworth, 2007; Hollingworth et al., 2012), one question is whether or not an increase in $[Ca_T]_{SR,R}$ could actually result in an increase in specific force generated by a muscle. One argument against the idea that the tension response to a single action potential (twitch response) is already maximal is that the peak of the twitch response is generally significantly less than the tetanic response (e.g., Caputo and Bolaños, 1994). The explanation for this is that maximum tension is only reached when elastic elements in the muscle (mainly the contractile proteins) are adequately stretched, which would usually take more than a single action potential (e.g., Celichowski and Grottel, 1993). In addition, an increase in the twitch response was actually observed after at least one type of increase in $[Ca_T]_{SR,R}$, namely an increase in $[Ca^{2+}]_{SR,R}$ with no change in the concentration of CSQ. Posterino and Lamb (2003) found that Ca overloading of skinned fibers from fast-twitch (rat) or twitch (toad) skeletal muscles resulted in a faster rise time and greater amplitude (by 50%; from their Table 1) of the twitch response. These effects and a much slower rate of relaxation were not caused by differences in the amount of Ca^{2+} released, which remained approximately constant, but rather by a greatly reduced rate of reuptake of Ca^{2+} into the SR by SERCA, presumably caused by a higher value of $[Ca^{2+}]_{SR,R}$. As far as we are aware, there are no reports of the effect on tension of an increase in the concentration of CSQ or any other Ca-binding protein without changes in $[Ca^{2+}]_{SR,R}$, so it is unclear whether such increases would also enhance the twitch response. Nevertheless, the results with Ca-overloading results indicate that the twitch can be significantly increased and prolonged with at least one type of increase in $[Ca_T]_{SR,R}$. As a result, it is possible, as hypothesized above, that a physiological mechanism exists that increases $[Ca_T]_{SR,R}$ to generate a greater twitch response.

Adapting the BAPTA method to other tissues

As noted in the Introduction, the BAPTA method should be useful for determining the concentration of total Ca in samples from most tissues. To help with the introduction of the method in other laboratories and possibly with different tissue types, a condensed version of the protocol and practical suggestions are provided in "A model protocol with practical suggestions..." in Materials and methods.

APPENDIX

BAPTA should capture most of the Ca on intracellular Ca-binding proteins with the possible exception of Ca/Mg-binding sites on parvalbumin, troponin, and myosin

This section assesses BAPTA' s ability to capture Ca from the main Ca-binding proteins in muscles. Toward this end, estimates are given for the amount of Ca expected to be bound to various Ca-binding proteins from the muscle compared with that bound to BAPTA, assuming that the Ca-binding properties of these proteins are not affected by the exposure to SDS, which denatures proteins. The Ca-binding sites considered here are troponin, SERCA, CSQ, myosin, and parvalbumin. The total amount of Ca bound to other muscle components is expected to be negligible because of their relatively low capacities compared with the proteins mentioned.

As a first approximation, the concentration of free Ca^{2+} ($[Ca^{2+}]$) is determined assuming a typical amount of Ca bound to BAPTA. This value of $[Ca^{2+}]$ is then used to estimate binding to the main Ca-binding protein components from muscle. As a typical example, we consider the case of a mouse whole muscle weighing 8 mg (8×10^{-6} kg; a typical weight for EDL and soleus muscles) that is homogenized and diluted into a final solution volume of 1.2 ml containing 120 µM BAPTA resulting in a measured concentration of 2,400 µmoles of total Ca per kilogram of muscle weight. The concentration of total Ca bound to BAPTA in the final solution ([CaB]) would be 16 µM (16 µM = 2,400 µmoles/kg × 8×10^{-6} kg ÷ 1.2 ml × 10^3 ml/L). Assuming a K_d of 0.22 µM for Ca binding to BAPTA (from Fig. 1) and a 1:1 binding reaction of Ca^{2+} with BAPTA, the concentration of free Ca^{2+} ($[Ca^{2+}]$) would be 0.034 µM. These results for BAPTA and free Ca^{2+} are given in the first two rows with data in Table 2. As seen in the column 6 in Table 2, the free form of Ca^{2+} is only 0.0021 of the Ca bound to BAPTA (0.0021 = 0.034 µM ÷ 16 µM), so that neglecting this amount results in an underestimation of total Ca by only ∼0.2%. Table 2 also gives the amount of Ca bound to the main high capacity Ca-binding proteins in muscle—including the Ca-regulatory sites on troponin, SERCA, and CSQ, and the Ca/Mg-binding sites on parvalbumin, troponin, and myosin—assuming values from the literature for the concentration of total binding sites on the proteins referred to the myoplasm and the apparent K_d for Ca binding. Column 3 in Table 2 gives the concentration of Ca-binding sites after dilution in the final volume (after homogenization and the addition of more solution). Column 5 gives the calculated concentration of Ca bound to the BAPTA and to the muscle proteins, and the column 6 gives the fraction of this amount to that bound to BAPTA. The next four paragraphs, in order, give details for the calculation for Ca binding to: (1) the Ca-regulatory sites on troponin, (2) CSQ, (3) parvalbumin, and (4) the Ca/Mg-binding sites on troponin and myosin.

Published January 26, 2015

From Table 1 in Baylor et al. (1983), the concentration of Ca-binding sites on the Ca-regulatory sites on troponin is 240 μM (column 2 of Table 2; concentrations referred to the volume of myoplasmic water in frog skeletal muscle fibers), which corresponds to a concentration of 139 μmoles/kg of whole-muscle weight using the factor of 0.58 given in Baylor et al. (1983) for this conversion (they estimated 0.58 kg myoplasmic water per kilogram of whole muscle; 139 = 0.58 × 240; the myoplasmic water is also assumed to have a density of 1 g/ml). With the dilution of the homogenized muscle in the measurement solution, the concentration of Ca-binding sites on the Ca-regulatory sites on troponin in the final measurement solution would be 0.93 μM (Table 2, column 3; 0.93 μM = 139 μmoles/kg × 8 × 10^{-6} kg ÷ 1.2 ml × 10^{3} ml/L). With the value of 0.2 μM for the K_d of Ca binding to these sites on troponin in a 1:1 reaction (Baylor et al., 1983), and the value from above of 0.034 μM for [Ca^{2+}], 0.145 of the Ca-regulatory sites on troponin would be occupied by Ca (0.145 = 0.034 μM ÷ (0.034 μM + 0.2 μM)), giving an estimated 0.135 μM of Ca bound to these sites (Table 2, column 5; 0.135 μM = 0.145 × 0.93 μM), which is only 0.0084 of the Ca captured by BAPTA (Table 2, column 6; 0.0084 = 0.135 μM ÷ 16 μM).

To obtain a rough estimate of possible Ca binding to SERCA, we assumed a value of 240 μM for the concentration of Ca-binding sites on SERCA referred to myoplasmic water volume (from the estimates from three different methods of 190–490 μM, 220 μM, and 260 μM for frog muscle given in Baylor et al., 1983) and an apparent K_d of 0.43 μM (from the value for the apparent association constant with 1:1 binding of 2.3 × 10^{6} M^{-1} given in Inesi et al., 1980; note that although Inesi et al. indicated that a cooperative reaction involving the binding of two Ca^{2+} ions per pump molecule better described their data, their K_d given here assuming 1:1 binding provided a rough match to their data and is adequate for the purpose here). As above, with the dilution of the homogenized muscle in the measurement solution, the concentration of Ca-binding sites on SERCA would be ∼0.93 μM (240 μM × 0.58 × 0.008 ml ÷ 1.2 ml), of which ∼0.073 would be occupied by Ca (0.073 = 0.034 μM ÷ (0.034 μM + 0.43 μM)), giving an estimated 0.068 μM of Ca bound to SERCA (0.068 μM = 0.073 × 0.93 μM) or ∼0.0043 of the amount of Ca bound to BAPTA (0.0043 = 0.068 μM ÷ 16 μM).

For CSQ, the value in Table 2 for the concentration of Ca-binding sites of 5,500 μM that referred to the myoplasm water volume was obtained from the value of 44,000 μM that referred to SR water volume for Case 1 in Table 1 of Fénelon et al. (2012) and the value of 8 for the ratio of myoplasmic water volume to SR water volume (Section 3

TABLE 2
Ca bound to BAPTA relative to other possible sites

1	2	3	4	5	6
Species	Concentration of Ca binding sites referred to				Fraction relative to CaBAPTA
	Myoplasm	Final solution	K_d	[CaX]	
	μM	*μM*	*μM*	*μM*	
BAPTA		120	0.22	16	1.0
Free Ca^{2+}				0.034	0.0021
Troponin	240	0.93	0.2	0.135	0.0084
SERCA	240	0.93	0.43	0.068	0.0043
CSQ	5,500	21.3	780 ($n = 3$)	1.7×10^{-12}	10^{-13}
		Ca/Mg-binding sites with [Mg^{2+}] = 0			
Parvalbumin	1,500	7.0	0.012	5.2	0.33
Troponin	240	0.93	0.002	0.88	0.055
Myosin	240	0.93	0.033	0.46	0.029
		Ca/Mg-binding sites with [Mg^{2+}] = 2 mM			
Parvalbumin	1,500	7.0	0.276	0.77	0.05
Troponin	240	0.93	0.202	0.134	0.0084
Myosin	240	0.93	18.4	0.002	0.0001

Ability of BAPTA to capture Ca from muscle components. Columns 2 and 3 give the concentrations of the Ca-binding sites associated with the substance in column 1. The concentrations in columns 2 and 3 refer to different volumes, the myoplasmic water volume of the muscle sample for column 2, and the volume of the final solution for the measurement (with the homogenized muscle) for column 3. Details for the conversion from column 2 to column 3 given in the text for troponin also apply to the other muscle components. Column 4 gives the K_d for the substance in column 1. Values in columns 2 and 4 were obtained from the literature as detailed in the text. Column 5 gives the concentration of Ca in the final solution (CaX) bound to BAPTA, present as the free form, or bound to muscle components. As indicated in the text, the assumed value of 16 μM for Ca bound to BAPTA is typical of the experimentally measured values. The concentration of free Ca^{2+} was determined from the relative concentrations of Ca-bound and Ca-free BAPTA and its K_d in column 4. Values for Ca bound to the muscle components were determined with this value for free Ca^{2+} using the values in columns 3 and 4. To assess how well BAPTA is expected to capture Ca from the different sites, column 6 gives the ratio of the values of [CaX] for the different components in column 5 to that for CaBAPTA. With the exception of the last three rows, it was assumed that no Mg was present. The last three rows were calculated with a free Mg^{2+} concentration of 2 mM. See text for additional details.

Published January 26, 2015

of the supplemental text for Fénelon et al., 2012; 5,500 μM = 44,000 μM ÷ 8). The value of the K_d and Hill coefficient for Ca binding to CSQ were also taken from Table 1 of Fénelon et al. (2012). The value of 10^{-13} for CSQ in column 6 of Table 2 indicates that BAPTA captures essentially all of the Ca from CSQ.

To summarize so far, the Ca in the free form and that possibly bound to troponin, SERCA, and CSQ amount to only 1.5% of the amount of Ca bound to BAPTA (1.5% = $100 \times (0.034 + 0.135 + 0.068 + 1.7 \times 10^{-12}$ μM) ÷ 16 μM).

Three proteins in fast-twitch skeletal muscle have binding sites that can bind either Ca or Mg to the same site (denoted "Ca/Mg-binding sites") with enough capacity and/or high affinity for Ca to make nonnegligible contributions to total Ca in resting muscles and to compete for Ca with BAPTA. These three proteins are parvalbumin, myosin, and sites on troponin different than the Ca-regulatory sites (Robertson et al., 1981). For each of these proteins, the concentration of Ca bound to the Ca/Mg-binding sites (denoted "CMBS") is given by the usual relationship for competing ligands, i.e.,

$$[CaCMBS] = [CaCMBS_T] \frac{[Ca^{2+}]}{[Ca^{2+}] + K_{Dapp,Ca}}, \quad \text{(A1)}$$

where the subscript "T" is for the total concentration of the sites, and $K_{Dapp,Ca}$ is the apparent K_d for Ca given by the usual relationship,

$$K_{Dapp,Ca} = K_{D,Ca}\left(1 + [Mg^{2+}] / K_{D,Mg}\right), \quad \text{(A2)}$$

where $K_{d,Ca}$ and $K_{d,Mg}$ are the K_ds for Ca and Mg binding, respectively, in the absence of the other divalent cation. Likewise for Mg binding,

$$[MgCMBS] = [MgCMBS_T] \frac{[Mg^{2+}]}{[Mg^{2+}] + K_{Dapp,Mg}}, \quad \text{(A3)}$$

where

$$K_{Dapp,Mg} = K_{D,Mg}\left(1 + [Ca^{2+}] / K_{D,Ca}\right). \quad \text{(A4)}$$

The parameters used for parvalbumin in Table 2 are the same as those given for mouse EDL muscle in Baylor and Hollingworth (2007). It is noted that the value of 1,500 μM for the concentration of Ca/Mg-binding sites on parvalbumin (from Baylor and Hollingworth, 2007) was obtained from a measured value in frog muscle. This value for frog should approximate that for fast-twitch mammalian muscle, as it is close to the estimate of 1,300 μM determined from the value of 4.4 g parvalbumin per kilogram of EDL muscle from mouse measured by Heizmann et al. (1982; the value of 1,300 μM assumed a molecular weight for parvalbumin of 12 kD and the factor of 0.58 above for converting from whole-muscle weight to myoplasmic water volume, and noting that there are two metal-binding sites per parvalbumin molecule). The assumed values for $K_{d,Ca}$ and $K_{d,Mg}$ for parvalbumin were, respectively, 0.012 and 91.0 μM (Baylor and Hollingworth, 1998).

The concentration of the Ca/Mg-binding sites on troponin is the same as that for the Ca-regulatory sites on troponin (Robertson et al., 1981). As done in Robertson et al. (1981), this same concentration is assumed for the Ca/Mg sites on myosin. The values assumed for the K_ds for Ca and Mg binding to these sites were, respectively, 0.002 and 20 μM for troponin and 0.033 and 3.6 μM for myosin (from Table 1 of Robertson et al., 1981).

As seen in the last two sections in Table 2, Ca binding to the Ca/Mg sites on the three proteins were calculating with no Mg present and with $[Mg^{2+}]$ = 2 mM. From the results in column 6 of Table 2 with no Mg present (the situation with the usual measurement solution used with the BAPTA method), the estimated fraction of Ca bound to the three proteins relative to that captured by BAPTA was 0.414 (0.33 + 0.055 + 0.029), with 80% of this because of parvalbumin (80% = 100 × 0.33 ÷ 0.414). The reason for this is the much higher affinities (lower K_ds) of the three proteins compared with that of BAPTA in the absence of Mg (Table 2, column 4). The main reason BAPTA captures most (∼70%) of the total Ca is that the total concentration of Ca/Mg-binding sites on these proteins is less than the concentration of total Ca in the muscle.

One way to minimize Ca bound to the Ca/Mg sites on parvalbumin, troponin, and myosin would be to add Mg to the measurement solution to reduce their apparent affinities for Ca. The last section of Table 2 (last three rows) indicates that the addition of 2 mM Mg to the measurement solution greatly reduces the affinities (increases the $K_{Dapp,Ca}$ values given in column 4) for the three proteins so that BAPTA would be able to capture much more of the Ca so that much less Ca would be undetected (or "lost") by BAPTA. As indicated by the results shown in column 6, almost no Ca would be lost to troponin and myosin, and the predicted loss of Ca to parvalbumin would be reduced from 33 to 5% of that Ca captured by BAPTA. As indicated in the text associated with the experimental results with 2 mM Mg present, there is reason to suspect that the protein-denaturing effect of the SDS treatment of the muscle would have eliminated or greatly reduced parvalbumin's ability to bind Ca, in which case "loss" of Ca to parvalbumin would not have occurred. To test this, experiments with the BAPTA method were performed with and without 2 mM Mg present. The section after the next section simulates possible outcomes of these experiments depending on whether or not the Ca/Mg sites on parvalbumin (and also troponin and myosin) were able to bind Ca after SDS treatment.

Published January 26, 2015

Estimation of Ca bound in the resting state to parvalbumin and other intracellular, non-SR sites

It was of interest to estimate the concentration of Ca bound to parvalbumin and other myoplasmic components in the resting state in muscles from mice. The estimates here assume that resting myoplasmic concentrations of Ca^{2+} and Mg^{2+} in the myoplasm are 0.05 µM and 1 mM, respectively, the values assumed in Baylor and Hollingworth (2007). With this value of $[Mg^{2+}]$, the value for $K_{Dapp,Ca}$ for parvalbumin from Eq. A2 is 0.144 µM ($0.144 = 0.012 \times (1 + 1{,}000/91)$). With this value of $K_{Dapp,Ca}$ along with the above value of $[Ca^{2+}]$ and a value for $[Parv_T]$ of 1,500 µM from Table 2, [CaParv] from Eq. A1 is estimated to be 387 µM (concentration referred to myoplasmic volume; $387 = 1{,}500 \times 0.05/(0.05 + 0.144)$). With the factor of 0.58 kg myoplasm per kilogram of muscle (from Baylor et al., 1983), the concentration of CaParvalbumin referred to whole-muscle weight is 0.224 mmoles/kg of muscle ($0.224 = 387/1{,}000 \times 0.58$). Following the same procedure just given for parvalbumin, the estimated concentrations of Ca on the Ca/Mg sites on troponin and myosin at rest are, respectively, 79 and 1 mmoles/kg of muscle (calculated with their concentration values in Table 2 with the apparent K_ds in Eqs. A2 and A4 determined with their Ca and Mg K_ds given above). Ca bound to myosin at rest is therefore negligible. The estimated concentration of Ca bound to the Ca/Mg sites on troponin at rest is 0.046 mmoles/kg of muscle ($0.046 = 79/1{,}000 \times 0.58$). The resting values of Ca bound to parvalbumin and troponin are used with Eqs. 23c and 23d in the Discussion and in Section 7 of the supplemental text to provide a predicted value of total Ca in muscle minus the amount of Ca bound to CSQ.

Following the same procedure with values from Table 2 for Ca bound to the Ca-regulatory sites on troponin and SERCA in the resting state gave concentrations for these two components of 0.0089 and 0.025 mM, respectively (volumes referred to myoplasmic volume). The same procedure gave a resting concentration of 0.0002 mM for CaATP (using ATP's concentration and apparent K_d for Ca binding with $[Mg^{2+}]$ = 1 mM from Table 1 of Baylor and Hollingworth, 1998). Ca binding to calmodulin should be much less than that to troponin, as the affinity for Ca binding to calmodulin is similar or lower than that to troponin, and calmodulin's concentration is much lower than that of troponin (Robertson et al., 1981; Baylor et al., 1983). Based on these results, Ca bound to parvalbumin and the Ca/Mg sites on troponin are expected to be the only nonnegligible myoplasmic Ca components of total Ca in resting muscle.

This paragraph assesses the possible contribution of Ca in mitochondria to the total Ca content of muscle. Scorzeto et al. (2013) reported values for the concentration of free Ca^{2+} in mitochondria ($[Ca^{2+}]_{mito}$) of fast-twitch muscles from mice (*flexor digitalis brevis*) of 0.16 µM with WT mice and 0.23 µM with both isoforms of CSQ knocked out. They also gave estimates of the volume fraction of fibers occupied by mitochondria just below the sarcolemma and the rest of the fiber or "intermyofibrillar" region, regions taking up ∼10 and 90% of the fiber volume, respectively. The volume fraction of mitochondria (with respect to fiber volume) in the intermyofibrillar region averaged 4.3 and 7.2% in WT and the double-KO muscles, respectively. The corresponding averages in the subsarcolemmal regions averaged 5.8 and 4.7%, respectively. Therefore, the average volume fraction of mitochondria in the whole fibers increased from 4.5% in WT muscles to 7.0% in double-KO muscles (e.g., $4.5\% = 0.9 \times 4.3\% + 0.1 \times 5.8\%$). With double-KO muscles, which had the largest values of $[Ca^{2+}]_{mito}$ and mitochondrial volume fractions, the concentration of free Ca^{2+} in mitochondria with respect to fiber volume was 0.000016 mM, which is negligible (0.000016 mM = 0.00023 mM × 0.07; concentration referred to fiber volume). The only way total Ca in mitochondria could have a nonnegligible resting Ca content is if mitochondria contained a high concentration of Ca-binding sites (a Ca-binding capacity comparable to that of CSQ) that had very high affinities for binding Ca^{2+} (like parvalbumin's). No such protein has been reported, so we conclude with near certainty that the contribution of mitochondria to non-SR Ca is negligible in both WT and double-KO muscles.

Simulations of BAPTA experiments and assessment of whether or not Ca was lost to parvalbumin

Table 3 simulates experimental results with the BAPTA method under three cases: Case 1: parvalbumin is unable to bind metals (Ca or Mg), and no Mg is present in the measurement solution; Case 2: parvalbumin can bind metals, and no Mg is present in the measurement solution; and Case 3: parvalbumin can bind metals and 2 mM of total Mg is present in the measurement solution. Based on the results from the section above with Table 2, Ca binding to SERCA, CSQ, and the Ca-regulatory sites on troponin should be negligible and is ignored. Although the simulations do not consider Ca binding to the Ca/Mg sites on troponin and myosin, similar results would be expected for these proteins, although significantly less than for parvalbumin (see Table 2). In brief, starting with assumed values for the total concentrations of the relevant ions and substances, the simulations calculate the concentrations of the Ca-bound, Mg-bound, and metal-free forms of the relevant substances before and after adding 1 mM EGTA. For each case, the predicted changes in concentration are then used to predict the associated absorbance changes, which are then summed to give the predicted, experimentally accessible value of $A_0 - A_M$ and its associated, predicted value of $[Ca_T]$.

Rows 1–5 of Table 3 give the assumed total concentrations of Ca, BAPTA, EGTA, parvalbumin, and Mg,

Published January 26, 2015

respectively, in terms of the concentrations in the final solution. Some of the starting assumptions are the same as those used and detailed above for Table 2. The concentration of 120 µM for total BAPTA was the same as that used for Table 2. The value of 21.234 µM for the concentration of total Ca was the sum of the concentrations of Ca bound to BAPTA (16 µm), free Ca (0.034 µM), and Ca bound to parvalbumin (5.2 µM) given in column 5 of Table 2. The value of 7.0 µM for the concentration of total parvalbumin (Table 3, row 4) is from column 3 of Table 2. Columns 2, 4, and 6 give the concentrations for all of the components considered for the simulated A_M aliquot for cases 1–3, respectively. Columns 3, 5, and 7 give concentrations and related values with 1 mM EGTA added (row 3) for cases 1–3, respectively; these columns correspond to the A_0 aliquots associated with columns 2, 4, and, 6, respectively. As seen in row 5, 2 mM of total Mg was present for case 3. The simulations involved adjusting the concentration of free Ca^{2+} to give the concentration of total Ca in row 1; the values of $[Ca^{2+}]$ are given in row 6. For case 3, the similarly adjusted values of $[Mg^{2+}]$ are given in row 7. The calculated

TABLE 3

Simulations of possible results of experiments to help assess if Ca was "lost" to parvalbumin

	1	2	3	4	5	6	7
		Case 1: No Mg and no parvalbumin		Case 2: No Mg and with parvalbumin		Case 3: With both Mg and parvalbumin	
		Muscle solution	With EGTA	Muscle solution	With EGTA	Muscle solution	With EGTA
		(*all concentrations in µM*)					
		Rows 1–5 are assumed (typical or expected total values for sample)					
1	Ca_T	21.234	21.234	21.234	21.234	21.234	21.234
2	$BAPTA_T$	120.0	120.0	120.0	120.0	120.0	120.0
3	$EGTA_T$		1,000.0		1,000.0		1,000.0
4	$Parv_T$			7.0	7.0	7.0	7.0
5	Mg_T					2,000.0	2,000.0
		Ca^{2+} and Mg^{2+} values adjusted to give Ca_T and Mg_T values above					
6	Ca^{2+}	0.0472	8.9×10^{-5}	0.0339	8.9×10^{-5}	0.0495	0.000149
7	Mg^{2+}					1,983.893	1590.948
		Rows 8–17 determined with above values for Ca^{2+} and Mg^{2+}					
8	BAPTA	98.8132	119.9513	103.9706	119.9514	89.449	109.663
10	CaBAPTA	21.1868	0.0487	16.0294	0.0486	20.113	0.074
11	MgBAPTA					10.439	10.263
12	EGTA		978.8149		978.8664		586.676
13	CaEGTA		21.1851		21.1336		21.152
14	MgEGTA						392.173
15	Parvalbumin			1.8293	6.9484	0.260	0.379
16	CaParvalbumin			5.1707	0.0516	1.072	0.005
17	MgParvalbumin					5.668	6.617
		Differences between values with and without EGTA					
18	ΔBAPTA		21.1381		15.9808		20.214
19	ΔCaBAPTA		−21.1381		−15.9808		−20.039
20	ΔMgBAPTA						−0.176
		Rows 21–24: Absorbance changes at 292 nm calculated from rows 18–20					
21	ΔA_{BAPTA}		0.1059		0.0800		0.1013
22	$\Delta A_{CaBAPTA}$		−0.0067		−0.0051		−0.0064
23	$\Delta A_{MgBAPTA}$						−0.0005
24	ΔA_{total} or A_0-A_M		0.0992		0.0749		0.0944
		Predicted $[Ca_T] = (A_0 - A_M)/(\Delta\varepsilon \cdot l)$					
25	Predicted Ca_T		21.151		15.970		20.132
		Row 26 gives the value in row 25 divided by that in row 1					
26	Predicted/actual		0.996		0.752		0.948

This table provides simulations of experimentally predicted values of $[Ca_T]$ with and without Mg present and with and without metal binding to parvalbumin. The text provides most of the details for the assumed and predicted values. For the case of parvalbumin, Ca and Mg binding was calculated as described with Table 2. Relationships used to calculate Ca and Mg binding to BAPTA and EGTA are given in Section 1 of the supplemental text. For rows 21 and 22, values of 5,009 and 320 M^{-1} cm^{-1}, respectively, were used for the extinction coefficients at 292 nm of the metal-free and Ca-bound forms of BAPTA (ε_B and ε_{CaB}, respectively; see Materials and methods). The value of 2,665 M^{-1} cm^{-1} assumed for the extinction coefficient for the Mg-bound form of BAPTA (ε_{MgB}) in row 23 was based on the observation of Tsien (1980) that the decrease in absorbance of BAPTA with Mg binding was about half of that produced by Ca binding (2,665 = 320 + 0.5 × (5,009 − 320)). As used throughout, the value of $\Delta\varepsilon$ used to calculate $[Ca_T]$ (row 25) from $A_0 - A_M$ (row 24) was $\varepsilon_{CaB} - \varepsilon_B$, i.e., −4,689 M^{-1} cm^{-1} (−4,689 = 320 − 5,009). Row 26 gives the ratios of the values in row 25 to those in row 1.

Published January 26, 2015

values of the metal-free, Ca-bound, and Mg-bound forms are given in rows 8–17. For these rows, Section 1 of the supplemental text gives the relationships used for the BAPTA and EGTA components, and Eqs. A1–A4 above give the relationships used for the parvalbumin components. Rows 18–20 give the changes in concentration of the BAPTA components, the only components giving measurable absorbance differences. The corresponding absorbance changes are given in rows 21–23, and the sum of these absorbance differences, given in row 24, is the predicted value for the absorbance difference ($A_0 - A_M$) that would be measured for each case. Row 25 gives the predicted value of the concentration of total Ca that would be reported with the BAPTA method, and row 26 gives the ratio of this reported value to the actual concentration of total Ca in row 1.

The main conclusions from the results in row 26 (also given in the last section of Results) are that the BAPTA method should report almost all (>99%) of the total Ca if parvalbumin is unable to bind Ca (case 1). If the high affinity of parvalbumin for Ca was unaffected by the denaturing effect of the SDS treatment and Mg is not added, the BAPTA method is predicted to underestimate [Ca_T] by ~25% because of "loss" of Ca to parvalbumin (case 2). Adding 2 mM Mg to the solution would greatly minimize this loss with a prediction of ~95% of the total Ca being reported (case 3). Another result from the simulations is that EGTA competes essentially all (>99.5%) of the Ca from BAPTA and parvalbumin, if the latter is able to bind Ca (compare values in row 13 with those in rows 10 and 16).

The contribution of Mg from muscle samples is negligible

This section justifies ignoring Mg from the muscle sample for the simulations in Table 3 and for the BAPTA method in general. Assuming that the high-end estimate of 15.5 mmoles/kg for total Mg in frog muscle (Godt and Maughan, 1988) applies to mouse muscle, the concentration of total Mg in the final volume for the example above (the value that would go in row 5 of Table 3) would be 0.10 mM (0.10 mM = 15.5 mmoles/kg × 8 mg × 10^{-6} kg/kg ÷ 1.2 ml × 10^3 ml/L). As shown by comparing the value in column 7 for row 23 to that for row 24 in Table 3, the contribution of the added 2.0 mM of total Mg for Case 3 would lead to an underestimate of ΔA for BAPTA of only 0.5% (−0.5% = 100 × −0.0005 ÷ 0.0944). Because the 0.1 mM of Mg from the muscle is 1/20,000th of the added 2.0 mM for Case 3, the error would be ~2,000-fold less than 0.5% and, therefore, negligible.

We thank Marc-André Bonin for his helpful discussions about how protons might interact with BAPTA (Section 2 of the supplemental text).

This work was supported by grants from the Canadian Institutes of Health Research (MOP-62959 to P.C. Pape), National Sciences and Engineering Research Council of Canada (341980 to P.C. Pape), Italian Telethon ONLUS (GGP13213 to F. Protasi), and National Institutes of Health (AR059646 to R.T. Dirksen and F. Protasi).

The authors declare no competing financial interests.

Richard L. Moss served as editor.

Submitted: 24 June 2014
Accepted: 6 January 2015

REFERENCES

Baylor, S.M., and S. Hollingworth. 1998. Model of sarcomeric Ca^{2+} movements, including ATP Ca^{2+} binding and diffusion, during activation of frog skeletal muscle. *J. Gen. Physiol.* 112:297–316. http://dx.doi.org/10.1085/jgp.112.3.297

Baylor, S.M., and S. Hollingworth. 2007. Simulation of Ca^{2+} movements within the sarcomere of fast-twitch mouse fibers stimulated by action potentials. *J. Gen. Physiol.* 130:283–302. http://dx.doi.org/10.1085/jgp.200709827

Baylor, S.M., W.K. Chandler, and M.W. Marshall. 1983. Sarcoplasmic reticulum calcium release in frog skeletal muscle fibres estimated from Arsenazo III calcium transients. *J. Physiol.* 344:625–666. http://dx.doi.org/10.1113/jphysiol.1983.sp014959

Canato, M., M. Scorzeto, M. Giacomello, F. Protasi, C. Reggiani, and G.J.M. Stienen. 2010. Massive alterations of sarcoplasmic reticulum free calcium in skeletal muscle fibers lacking calsequestrin revealed by a genetically encoded probe. *Proc. Natl. Acad. Sci. USA.* 107:22326–22331. http://dx.doi.org/10.1073/pnas.1009168108

Caputo, C., and P. Bolaños. 1994. Fluo-3 signals associated with potassium contractures in single amphibian muscle fibres. *J. Physiol.* 481:119–128. http://dx.doi.org/10.1113/jphysiol.1994.sp020423

Celichowski, J., and K. Grottel. 1993. Twitch/tetanus ratio and its relation to other properties of motor units. *Neuroreport.* 5:201–204. http://dx.doi.org/10.1097/00001756-199312000-00003

Cieslar, J., M.T. Huang, and G.P. Dobson. 1998. Tissue spaces in rat heart, liver, and skeletal muscle in vivo. *Am. J. Physiol.* 275:R1530–R1536.

Cota, G., and C.M. Armstrong. 1988. Potassium channel "inactivation" induced by soft-glass patch pipettes. *Biophys. J.* 53:107–109. http://dx.doi.org/10.1016/S0006-3495(88)83071-6

Cox, J.A., D.R. Winge, and E.A. Stein. 1979. Calcium, magnesium and the conformation of parvalbumin during muscular activity. *Biochimie.* 61:601–605. http://dx.doi.org/10.1016/S0300-9084(79)80157-1

Everts, M.E., T. Lømo, and T. Clausen. 1993. Changes in K^+, Na^+ and calcium contents during in vivo stimulation of rat skeletal muscle. *Acta Physiol. Scand.* 147:357–368. http://dx.doi.org/10.1111/j.1748-1716.1993.tb09512.x

Fénelon, K., C.R.H. Lamboley, N. Carrier, and P.C. Pape. 2012. Calcium buffering properties of sarcoplasmic reticulum and calcium-induced Ca^{2+} release during the quasi-steady level of release in twitch fibers from frog skeletal muscle. *J. Gen. Physiol.* 140:403–419. http://dx.doi.org/10.1085/jgp.201110730

Fenn, W.O. 1936. Electrolytes in muscle. *Physiol. Rev.* 16:450–486.

Fryer, M.W., and D.G. Stephenson. 1996. Total and sarcoplasmic reticulum calcium contents of skinned fibres from rat skeletal muscle. *J. Physiol.* 493:357–370. http://dx.doi.org/10.1113/jphysiol.1996.sp021388

Gissel, H., and T. Clausen. 1999. Excitation-induced Ca^{2+} uptake in rat skeletal muscle. *Am. J. Physiol.* 276:R331–R339.

Glesby, M.J., E. Rosenmann, E.G. Nylen, and K. Wrogemann. 1988. Serum CK, calcium, magnesium, and oxidative phosphorylation in mdx mouse muscular dystrophy. *Muscle Nerve.* 11:852–856. http://dx.doi.org/10.1002/mus.880110809

Godt, R.E., and D.W. Maughan. 1988. On the composition of the cytosol of relaxed skeletal muscle of the frog. *Am. J. Physiol.* 254:C591–C604.

Harrison, S.M., and D.M. Bers. 1987. The effect of temperature and ionic strength on the apparent Ca-affinity of EGTA and the analogous Ca-chelators BAPTA and dibromo-BAPTA. *Biochim. Biophys. Acta.* 925:133–143. http://dx.doi.org/10.1016/0304-4165(87)90102-4

Heizmann, C.W., M.W. Berchtold, and A.M. Rowlerson. 1982. Correlation of parvalbumin concentration with relaxation speed in mammalian muscles. *Proc. Natl. Acad. Sci. USA.* 79:7243–7247. http://dx.doi.org/10.1073/pnas.79.23.7243

Hollingworth, S., M.M. Kim, and S.M. Baylor. 2012. Measurement and simulation of myoplasmic calcium transients in mouse slow-twitch muscle fibres. *J. Physiol.* 590:575–594. http://dx.doi.org/10.1113/jphysiol.2011.220780

Inesi, G., M. Kurzmack, C. Coan, and D.E. Lewis. 1980. Cooperative calcium binding and ATPase activation in sarcoplasmic reticulum vesicles. *J. Biol. Chem.* 255:3025–3031.

Irving, M., J. Maylie, N.L. Sizto, and W.K. Chandler. 1987. Intrinsic optical and passive electrical properties of cut frog twitch fibers. *J. Gen. Physiol.* 89:1–40. http://dx.doi.org/10.1085/jgp.89.1.1

Kake-Guena, S.A., C.R.H. Lamboley, P. Bouchard, J. Frenette, E. Rousseau, R.T. Dirksen, F. Protasi, and P.C. Pape. 2014. New method for determining the total calcium content of tissue applied to whole skeletal muscles from mice with and without calsequestrin knocked out. *Biophys. J.* 102:731a.

Kirby, A.C., B.D. Lindley, and J.R. Picken. 1975. Calcium content and exchange in frog skeletal muscle. *J. Physiol.* 253:37–52. http://dx.doi.org/10.1113/jphysiol.1975.sp011178

Lamboley, C.R., R.M. Murphy, M.J. McKenna, and G.D. Lamb. 2013b. Endogenous and maximal sarcoplasmic reticulum calcium content and calsequestrin expression in type I and type II human skeletal muscle fibres. *J. Physiol.* 591:6053–6068. http://dx.doi.org/10.1113/jphysiol.2013.265900

MacLennan, D.H., and P.T.S. Wong. 1971. Isolation of a calcium-sequestering protein from sarcoplasmic reticulum. *Proc. Natl. Acad. Sci. USA.* 68:1231–1235. http://dx.doi.org/10.1073/pnas.68.6.1231

Mendez, J., and A. Keys. 1960. Density and composition of mammalian muscle. *Metabolism.* 9:184–188.

Murphy, R.M., N.T. Larkins, J.P. Mollica, N.A. Beard, and G.D. Lamb. 2009. Calsequestrin content and SERCA determine normal and maximal Ca^{2+} storage levels in sarcoplasmic reticulum of fast- and slow-twitch fibres of rat. *J. Physiol.* 587:443–460. http://dx.doi.org/10.1113/jphysiol.2008.163162

Paolini, C., M. Quarta, A. Nori, S. Boncompagni, M. Canato, P. Volpe, P.D. Allen, C. Reggiani, and F. Protasi. 2007. Reorganized stores and impaired calcium handling in skeletal muscle of mice lacking calsequestrin-1. *J. Physiol.* 583:767–784. http://dx.doi.org/10.1113/jphysiol.2007.138024

Paolini, C., M. Quarta, L. D'Onofrio, C. Reggiani, and F. Protasi. 2011. Differential effect of calsequestrin ablation on structure and function of fast and slow skeletal muscle fibers. *J. Biomed. Biotechnol.* 2011:1–10. http://dx.doi.org/10.1155/2011/634075

Pape, P.C., D.-S. Jong, and W.K. Chandler. 1995. Calcium release and its voltage dependence in frog cut muscle fibers equilibrated with 20 mM EGTA. *J. Gen. Physiol.* 106:259–336. http://dx.doi.org/10.1085/jgp.106.2.259

Pape, P.C., K. Fénelon, C.R.H. Lamboley, and D. Stachura. 2007. Role of calsequestrin evaluated from changes in free and total calcium concentrations in the sarcoplasmic reticulum of frog cut skeletal muscle fibres. *J. Physiol.* 581:319–367. http://dx.doi.org/10.1113/jphysiol.2006.126474

Peachey, L.D., and A.F. Huxley. 1962. Structural identification of twitch and slow striated muscle fibers of the frog. *J. Cell Biol.* 13:177–180. http://dx.doi.org/10.1083/jcb.13.1.177

Posterino, G.S., and G.D. Lamb. 2003. Effect of sarcoplasmic reticulum Ca^{2+} content on action potential-induced Ca^{2+} release in rat skeletal muscle fibres. *J. Physiol.* 551:219–237. http://dx.doi.org/10.1113/jphysiol.2003.040022

Protasi, F., C. Paolini, and M. Dainese. 2009. Calsequestrin-1: a new candidate gene for malignant hyperthermia and exertional/environmental heat stroke. *J. Physiol.* 587:3095–3100. http://dx.doi.org/10.1113/jphysiol.2009.171967

Ringer, S. 1883. A further contribution regarding the influence of the different constituents of the blood on the contraction of the heart. *J. Physiol.* 4:29–42. http://dx.doi.org/10.1113/jphysiol.1883.sp000120

Robertson, S.P., J.D. Johnson, and J.D. Potter. 1981. The time-course of Ca^{2+} exchange with calmodulin, troponin, parvalbumin, and myosin in response to transient increases in Ca^{2+}. *Biophys. J.* 34:559–569. http://dx.doi.org/10.1016/S0006-3495(81)84868-0

Rojas, L., and C. Zuazaga. 1988. Influence of the patch pipette glass on single acetylcholine channels recorded from *Xenopus* myocytes. *Neurosci. Lett.* 88:39–44. http://dx.doi.org/10.1016/0304-3940(88)90312-6

Scorzeto, M., M. Giacomello, L. Toniolo, M. Canato, B. Blaauw, C. Paolini, F. Protasi, C. Reggiani, and G.J.M. Stienen. 2013. Mitochondrial Ca^{2+}-handling in fast skeletal muscle fibers from wild type and calsequestrin-null mice. *PLoS ONE.* 8:e74919. http://dx.doi.org/10.1371/journal.pone.0074919

Sztretye, M., J. Yi, L. Figueroa, J. Zhou, L. Royer, P. Allen, G. Brum, and E. Ríos. 2011. Measurement of RyR permeability reveals a role of calsequestrin in termination of SR Ca^{2+} release in skeletal muscle. *J. Gen. Physiol.* 138:231–247. http://dx.doi.org/10.1085/jgp.201010592

Tsien, R.Y. 1980. New calcium indicators and buffers with high selectivity against magnesium and protons: design, synthesis, and properties of prototype structures. *Biochemistry.* 19:2396–2404. http://dx.doi.org/10.1021/bi00552a018

Yoshida, M., A. Yonetani, T. Shirasaki, and K. Wada. 2006. Dietary NaCl supplementation prevents muscle necrosis in a mouse model of Duchenne muscular dystrophy. *Am. J. Physiol. Regul. Integr. Comp. Physiol.* 290:R449–R455. http://dx.doi.org/10.1152/ajpregu.00684.2004

Zhang, L., J. Kelley, G. Schmeisser, Y.M. Kobayashi, and L.R. Jones. 1997. Complex formation between junctin, triadin, calsequestrin, and the ryanodine receptor. Proteins of the cardiac junctional sarcoplasmic reticulum membrane. *J. Biol. Chem.* 272:23389–23397. http://dx.doi.org/10.1074/jbc.272.37.23389

Lamboley et al., http://www.jgp.org/cgi/content/full/jgp.201411250/DC1

Section1: Summary of divalent-ion and proton binding to BAPTA and EGTA

This section starts with a review of relationships for proton and divalent binding to the Ca^{2+} chelators EGTA and BAPTA (most of which is also described in Pape et al., 1995, and Harrison and Bers, 1987). In both cases, the Ca^{2+} chelation site has four carboxyl groups in close proximity (Tsien, 1980). The four groups can bind protons with decreasing affinities as the number of protons already bound increases. The reaction schemes for binding of the first and second protons are given, respectively, by

$$H^+ + X^{4-} \leftrightarrow HX^{3-} \tag{S1}$$

and

$$H^+ + HX^{3-} \leftrightarrow H_2X^{2-}, \tag{S2}$$

where X, for purposes of this study, is either EGTA or BAPTA. At equilibrium, the fraction of divalent-free chelator with one and two protons bound, f_1 and f_2, respectively, are given by

$$f_1 \equiv \frac{\left[HX^{3-}\right]}{[X]} = \frac{10^{pK_1 - pH}}{1 + 10^{pK_1 - pH} + 10^{pK_1 + pK_2 - 2pH}} \tag{S3}$$

and

$$f_2 \equiv \frac{\left[H_2X^{2-}\right]}{[X]} = \frac{10^{pK_1 + pK_2 - 2pH}}{1 + 10^{pK_1 - pH} + 10^{pK_1 + pK_2 - 2pH}}, \tag{S4}$$

where [X] is the sum of concentrations of the divalent-free forms, i.e.,

$$[X] = \left[X^{4-}\right] + \left[HX^{3-}\right] + \left[H_2X^{2-}\right], \tag{S5}$$

and pK_1 and pK_2 are the pKa values for the binding of the first and second protons, respectively. (A pKa value is $-\log_{10}$ of the K_d of the associated proton-binding reaction.) The fraction of divalent-free chelator that is also proton free, f_0, is given by

$$f_0 = 1 - f_1 - f_2 = \frac{1}{1 + 10^{pK_1 - pH} + 10^{pK_1 + pK_2 - 2pH}}. \tag{S6}$$

For both BAPTA and EGTA, the values of pK_3 and pK_4 are very low, so that the forms with three and four protons bound can be neglected for the range of pH values for results in this study (pH ≥6). (All results in this study were obtained at pH 8, except those with BAPTA shown in Fig. S1 in the next section, which includes results from pH 6.0–8.) All of the binding constants given below were measured—or were interpolated to give values—at room temperature (near 22°C) with physiological ionic strength (100–200 mM). For EGTA, the values of 9.48 and 8.81 for pK_1 and pK_2, respectively, were obtained from the tabulated stability constants in Godt and Lindley (1982). With these values of pK_1 and pK_2, the values of f_0, f_1, and f_2 for EGTA at pH 8.0 are 0.0044, 0.1335, and 0.8621. For BAPTA, titration experiments of Tsien (1980) gave values of 6.36 and 5.47 for pK_1 and pK_2, respectively (100 mM KCl; 22 ± 2°C). With these values, the fractional values of $BAPTA^{4-}$, $HBAPTA^{3-}$, and H_2BAPTA^{2-} (f_0, f_1, and f_2) are, respectively, 0.252, 0.577, and 0.171 at pH 6; 0.809, 0.185, and 0.005 at pH 7; and 0.978, 0.022, and 6.6×10^{-5} at pH 8. The main reasons for choosing pH 8.0 for the usual measurement solution was to minimize the protonated forms of BAPTA and to increase the affinity of EGTA for Ca^{2+} (see below), which is important for the step in the method in which EGTA displaces Ca from BAPTA.

The combination of divalent (denoted "Dv^{2+}," where Dv^{2+} could be either Ca^{2+} or Mg^{2+} in this case) with the three forms of divalent-free chelator above are given by the reactions

$$Dv^{2+} + X^{4-} \xleftrightarrow{K_D} DvX^{2-}, \tag{S7}$$

$$Dv^{2+} + HX^{3-} \xleftrightarrow{K_D'} DvX^{2-} + H^+, \tag{S8}$$

and

$$Dv^{2+} + H_2X^{2-} \xleftrightarrow{K_D''} DvX^{2-} + 2H^+. \tag{S9}$$

(The K_d for each of the reactions is shown above the connecting symbol.)

Using the equilibrium relationships above for the divalent-free forms of the chelators, it is readily shown that these three reactions at equilibrium can be combined to give the reaction

$$Dv^{2+} + X \xleftrightarrow{K'_{Dapp,Dv}} DvX^{2-}, \tag{S10}$$

where

$$K'_{Dapp,Dv} = K_D\left(1 + 10^{pK_1 - pH} + 10^{pK_1 + pK_2 - 2pH}\right) \tag{S11}$$

and the associated equilibrium relationship is given by

$$\frac{[DvX^{2-}]}{[X]} = \frac{[Dv^{2+}]}{K'_{Dapp,Dv}}. \tag{S12}$$

As above, $[X]$ is the sum of concentrations of the divalent-free forms. (Note that Eq. S10 is the same as Eq. A9

in Pape et al., 1995, except that $K'_{Dapp,Dv}$ replaces K_{Dapp} for Ca.) The prime symbol in $K'_{Dapp,Dv}$ indicates that the apparent K_d is restricted to the case that only one divalent is present. It is readily shown that in the presence of both Ca^{2+} and Mg^{2+}, the fraction of total chelator occupied by Ca (f_{Ca}) is given by

$$f_{Ca} = \frac{[Ca^{2+}]}{[Ca^{2+}] + K_{Dapp,Ca}}, \quad \text{(S13)}$$

where the apparent K_d for Ca binding to the chelator is given by

$$K_{Dapp,Ca} = K'_{Dapp,Ca}\left(1 + [Mg^{2+}] \Big/ K'_{Dapp,Mg}\right). \quad \text{(S14)}$$

Likewise, the fraction of total chelator occupied by Mg is given by

$$f_{Mg} = \frac{[Mg^{2+}]}{[Mg^{2+}] + K_{Dapp,Mg}}, \quad \text{(S15)}$$

where the apparent K_d for Mg binding to chelator X is given by

$$K_{Dapp,Mg} = K'_{Dapp,Mg}\left(1 + [Ca^{2+}] \Big/ K'_{Dapp,Ca}\right). \quad \text{(S16)}$$

The fraction of chelator in the divalent-free form is given by $1 - f_{Ca} - f_{Mg}$, and the fractions of divalent-free chelator in nonprotonated, singly protonated, and doubly protonated forms (f_0, f_1, and f_2, respectively) are given, respectively, by Eqs. S6, S3, and S4.

Determination of the apparent affinities for Mg and Ca binding to EGTA and BAPTA with Eq. S11 requires values for their associated K_d values (the K_ds with no protons present). For EGTA, values assumed for the K_ds of Ca and Mg were 1.13×10^{-11} M and 6.173×10^{-6} M, respectively (from Godt and Lindley, 1982). With the values of pK_1 and pK_2 for EGTA, the corresponding values for $K'_{Dapp,Ca}$ and $K'_{Dapp,Mg}$ at pH 8.00 for EGTA are 0.00256 and 1,400 µM, respectively. The value of 0.215 µM assumed for the K_d for Ca binding to BAPTA was calculated with Eq. S11 to give the value of 0.22 µM for $K'_{Dapp,Ca}$ at pH 8.00 determined with Fig. 1 in the main text. The value of 16,100 µM assumed for the K_d for Mg binding to BAPTA was calculated with Eq. S11 to give the value of 17,000 µM for $K'_{Dapp,Mg}$ at pH 7.60 reported by Tsien (1980). With the values of pK_1 and pK_2 for BAPTA, the corresponding values for $K'_{Dapp,Ca}$ and $K'_{Dapp,Mg}$ at pH 8.00 for BAPTA are 0.220 and 16,500 µM, respectively.

In summary, this section gives all of the relationships needed to calculate all of the forms of EGTA and BAPTA present in nonnegligible concentrations for the conditions in this study.

Section 2: Absorbance spectra of BAPTA at different pH values

Fig. S1 A plots UV absorbance spectra for divalent-free BAPTA at pH 6, 7, and 8, and another spectrum at pH 8.0 with Ca added to the solution to give a concentration of 1 mM Ca (22.5°C; 120 mM KCl, 2 mM HEPES, and nominal concentration of 0.15 mM for BAPTA; absorbance values were corrected for the slight dilution associated with adjusting pH and adding Ca).Consistent with the observation of Tsien (1980) that there was "very little effect on the spectrum until the pH drops below 6.5 or so," the spectrum at pH 7.0 is very close to that at pH 8.

Fig. S1 B shows five difference spectra derived from the spectra in A. The solid curve (labeled 1) shows the difference spectrum for Ca binding to essentially all of the BAPTA that was present (the 0-Ca curve used for the difference is the pH 8 data shown in A). The dot–dash curve (curve indicated with arrow; because of limited space, the label "2" is not shown) gives the difference between the spectra at pH 8.0 and that at pH 7.0, and the dashed curve gives the difference between

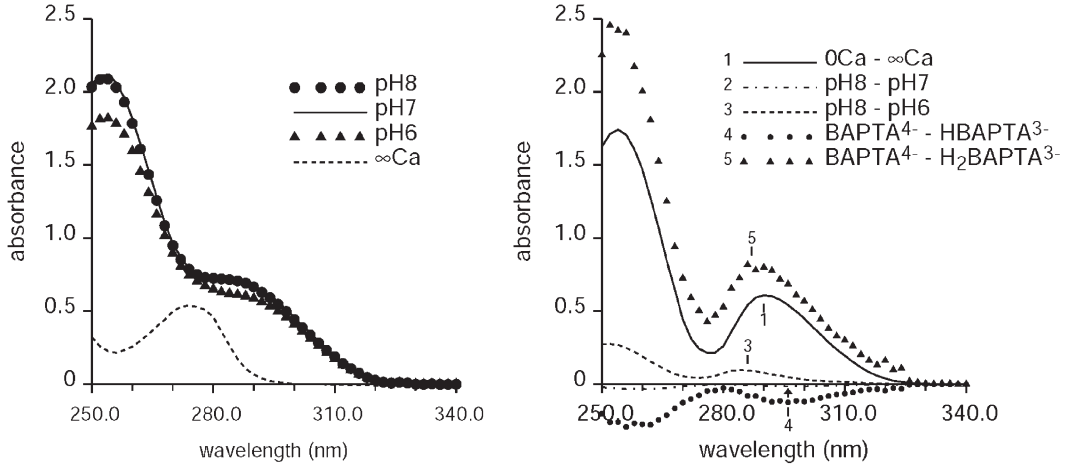

Figure S1. Effects of pH on the absorbance spectra of BAPTA. See text for details.

the spectra at pH 8.0 and pH 6.0 (curve 3). To aid in comparisons with the difference spectrum with Ca binding (curve 1), the difference spectra with binding of one or two protons were calculated as described here. An absorbance spectrum of BAPTA at a particular pH and with no divalent present—like those in A (excluding the curve with Ca present)—should be made up of the sum of absorbance spectra of the different forms of divalent-free BAPTA, as given by the following relationship:

$$A(pH) = A_0 \cdot f_0(pH) + A_1 \cdot f_1(pH) + A_2 \cdot f_2(pH). \quad \text{(S17)}$$

A_0, A_1, and A_2 are the absorbance spectra if all of the BAPTA was bound, respectively, with 0, one, or two protons. The three forms of Eq. S17 corresponding to the three measured spectra (three pH levels in Fig. S1 A) give a set of three linear equations that can be used to solve for the three unknown spectra (A_0, A_1, and A_2) in the usual way, using the values of f_0, f_1, and f_2 for the three pH levels given in the preceding section. The difference spectrum expected if all of the BAPTA was initially present in the singly protonated form and it all became converted to the proton-free form is given by $A_0 - A_1$ and is plotted as closed circles (curve 4) in Fig. S1 B. Interestingly, this has the opposite sign for the difference spectrum going from the Ca-bound to Ca-free form (curve 1). Likewise, the closed triangles give $A_0 - A_2$ (curve 5), the spectrum for conversion between H_2BAPTA^{2-} and $BAPTA^{4-}$. Although this difference spectrum is greater than that of the difference spectrum with Ca removal from BAPTA (curve 1), the two are quite similar. Moreover, because a relatively small error (such as a small error in the scaling factors used to correct for dilution of BAPTA that occurred when adjusting the pH of the solution) would have a relatively large effect on the magnitude of the derived difference spectra, it seems reasonable to suppose that the difference is caused by such an error, and that the binding of two protons to $BAPTA^{4-}$ has about the same effect on the absorbance spectrum as Ca binding.

As discussed in Tsien (1980), BAPTA is composed of the combination of two identical halves, with each half containing an amine group composed of a nitrogen attached to a benzene ring and two carboxylic acid groups, and most of the UV absorbance in the wavelength range of interest of the $BAPTA^{4-}$ form arises from the conjugation between the amine and benzene ring. Tsien (1980) attributed the large absorbance change upon Ca binding to the loss of this conjugation caused by twisting of the nitrogen-benzene ring bonds when the BAPTA molecule rearranges itself to accommodate Ca^{2+} in the chelation pocket formed by the four carboxyl groups. Tsien (1980) proposed that the similarity of the effect of proton binding to BAPTA to that of Ca^{2+} binding was caused by loss of the amine-benzene ring conjugation when a proton binds to the amine group. This explanation, however, does not explain the relative lack of effect on the difference spectrum when only one proton binds and the observation here that the absorbance change was in the opposite direction to that associated with Ca binding (curve 4 vs. curve 1 in Fig. S1 B). If proton binding to the amine group was correct, the expected difference spectrum should have been about half that associated with Ca binding. A more likely explanation is that the first proton binds to one of the carboxyl groups somehow helping with the conjugation between the amine and benzene ring. With two protons bound, an energetically favorable chelation pocket forms (similar to that with Ca bound) with hydrogen bonds linking the four reoriented carboxyl groups, again disrupting the amine-benzene ring conjugation in both halves of the BAPTA molecule. (We wish to acknowledge and thank Marc-André Bonin for suggesting this explanation.)

For the purpose of the experiments in this study (performed at pH 8), the reason for examining the effect of pH on BAPTA absorbance was to assess absorbance changes arising from changes of concentration of proton-bound BAPTA when adding EGTA or Ca standard (changes that would be attributed to changes in the Ca-bound form of BAPTA). Contribution from the doubly protonated form, H_2BAPTA^{2-} can be neglected, as <1 in 10^4 divalent-free BAPTA molecules are present as H_2BAPTA^{2-} at pH 8.0 (previous section). Changes in the contribution of the singly protonated form are expected to be almost negligible because of the calculation in the preceding section showing that only 0.022 of the divalent-free BAPTA is present as $HBAPTA^{3-}$ at pH 8.0, and because the fractional change in $HBAPTA^{3-}$ from the A_M to the A_0 aliquot would be severalfold <0.022, and because the results in Fig. S1 B indicate a relatively small difference in absorbance between the $HBAPTA^{3-}$ and $BAPTA^{4-}$ forms (compare curves 4 and 1).

Section 3: Deviation between measured and actual absorbance caused by stray light

For a substance known to obey Beer's law measured with an ideal spectrophotometer, the reported absorbance versus concentration relationship should be linear. As shown in this section, the spectrophotometer used in this study displayed a significant variation from this ideal behavior, a result attributable to stray light. Stray light in this context appears as an added light intensity (denoted "I_S") recorded by the detector, either from light that doesn't pass through the sample or from light at wavelengths outside of the range nominally set by the spectrophotometer's monochronometer. Evidence (not depicted) indicates that the latter is the case for the spectrophotometer used in this study (Pharmacia Ultraspec 2000). This section shows how the stray

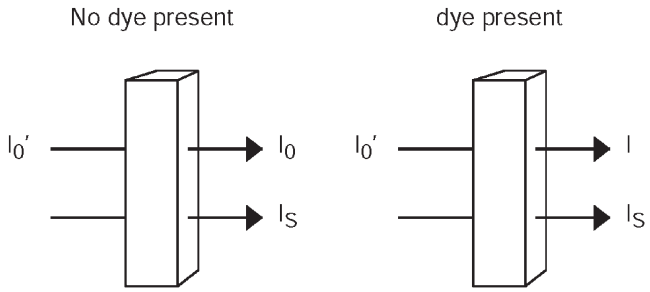

Figure S2. Schematics illustrating the components of light used to determine the absorbance of a substance in a cuvette and the unwanted stray light that is not absorbed. See text for details.

light component was assessed, and how measured absorbance values were corrected to give the true absorbance of the substance(s) of interest in the sample.

With the light intensities depicted in Fig. S2 and defined below, the measured absorbance of the blank and raw absorbance of the sample are given, respectively, by

$$A_{blank} = \log_{10}\left(\frac{I_0^{'} + I_S}{I_0 + I_S}\right) \tag{S18}$$

and

$$A_{raw\_sample} = \log_{10}\left(\frac{I_0^{'} + I_S}{I + I_S}\right), \tag{S19}$$

where $I_0^{'}$ is the intensity of incident, absorbable light and I_0 and I are the intensities of absorbable light leaving the blank (cuvette with water or solution only) and sample, respectively, all at the nominal wavelength set by the monochronometer. The blank-corrected absorbance, denoted "A_{sample}," is given by the difference between A_{raw_sample} and A_{blank}, yielding the relationship

$$A_{sample} = \log_{10}\left(\frac{I_0 + I_S}{I + I_S}\right). \tag{S20}$$

The true absorbance (denoted "A_{true}")—the value sought, i.e., the absorbance attributable to substances in the sample not present in the blank—is given by

$$A_{true} = \log_{10}\left(\frac{I_0}{I}\right). \tag{S21}$$

In general, A_{true} could include the sum of absorbances from several components. In the case of an absorbance

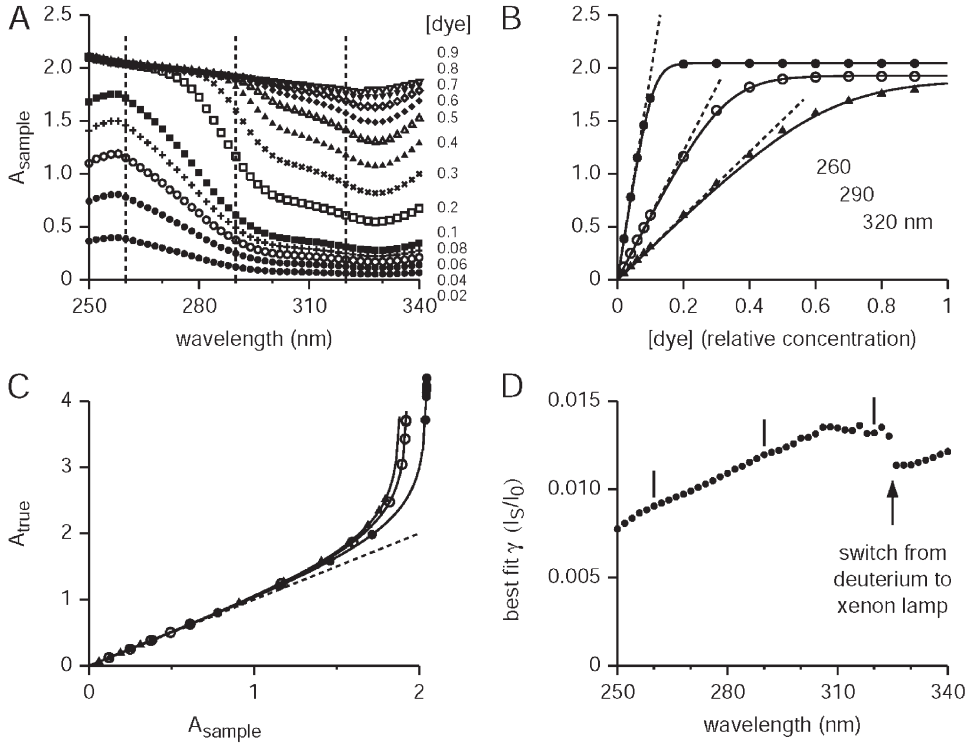

Figure S3. Characterization of the stray light on the absorbance spectra of green dye and illustration of the determination of I_S/I_0 values. (A–D) See text for details.

associated with a muscle sample in this study, A_{true} generally includes a contribution from muscle components and the Ca-free and/or the Ca-bound forms of BAPTA.

Dividing the numerator and denominator in Eq. S20 by I_0 and then substituting in Eq. S21 gives

$$A_{sample} = \log_{10}\left(\frac{1+\gamma}{I/I_0+\gamma}\right) = \log_{10}\left(\frac{1+\gamma}{10^{-A_{true}}+\gamma}\right), \quad \text{(S22)}$$

where

$$\gamma \equiv \frac{I_S}{I_0}. \quad \text{(S23)}$$

The first use of Eq. S22 was to determine γ by measuring A_{sample} at known values of A_{true} using a dye known to obey Beer's law. Fig. S3 A shows 13 absorbance spectra measured at different concentrations of green food–coloring dye, a dye known to obey Beer's law and one of the dyes generally recommended for calibrating spectrophotometers based on this property (e.g., Frings and Broussard, 1979). Each symbol represents a different relative concentration of the dye, as indicated on the right-hand side of A. A solution corresponding to the value 1 was obtained by adding 200 drops of green food coloring (Club House brand purchased in a grocery store) in 100 ml water; the other concentrations were obtained by dilution of this stock solution with water. (A spectrum for the stock solution is not shown because we forgot to do it.) The symbols in Fig. S3 B plot A_{sample} versus [dye] values from the data in A, with each symbol representing a different wavelength, either 260, 290, or 320 nm, as indicated. These wavelengths are also indicated by the vertical dashed lines in A. The dashed lines in B are the expected A_{true} versus $[dye]$ relationships. These lines pass through the points (0, 0) and the point with the lowest dye concentration so that they are given by the linear relationship

$$A_{true}([dye]) = \frac{[dye]}{[dye]_{lowest}} A_{true}([dye]_{lowest}), \quad \text{(S24)}$$

where $[dye]_{lowest}$ is the lowest dye concentration (relative dye concentration = 0.02). Eq. S24 is justified because the errors caused by the stray light are negligible at this lowest concentration, as detailed below, and because the green food–coloring dye is known to obey Beer's law. The solid lines in B are given by Eq. S22 using A_{true} values from Eq. S24 and the least-squares best-fit value of γ (obtained by minimizing the sum of squares of the difference between measured values of A_{sample} and values of A_{sample} predicted with Eq. S22).

Eq. S22 can be rearranged to give

$$A_{true} = A_{sample} + \log_{10}\left(\frac{1}{1+\gamma(1-10^{A_{sample}})}\right). \quad \text{(S25)}$$

Eq. S25 can be used to correct a blank-corrected measured absorbance (A_{sample}) to give the actual absorbance, provided that the value of γ is known. It is noted that A_{true} is always $\geq A_{sample}$ as long as $A_{true} < \infty$. Fig. S3 C shows application of Eq. S25 for the same three sets of data and associated values of γ shown in B. It is seen from these curves that A_{true} starts to noticeably deviate from A_{sample} starting at absorbance values near 1, with the difference between A_{true} and A_{sample} progressively increasing with increasing absorbance values. The curves approach asymptotic values as A_{true} and $[dye]$ approach relatively large values. An asymptotic value is given by

$$A_{sample}([dye] \to \infty) = \log_{10}\left(1+\frac{1}{\gamma}\right),$$

obtained by combining Eq. S23 with Eq. S20 and setting $I = 0$. Based on visual inspection of the curves, it seems reasonable to conclude that the correction procedure is reliable for our spectrophotometer for A_{sample} values up to 1.5–1.8, depending on the wavelength. Although the correction procedure appeared to work for all of the points measured, its reliability is expected to significantly diminish as the asymptotic value for A_{sample} is approached.

Fig. S3 D plots all of the values of γ for the full wavelength range of 250–340 nm used in this study. The vertical line segments mark the value of γ obtained at the wavelengths shown in B and C. There is some deviation in the progressively increasing value of γ with wavelength at the point marked by the arrow. As indicated, this arrow marks the wavelength where the spectrophotometer switches from its deuterium to its xenon lamp. The increasing values of γ with wavelength are likely caused by the fact that light intensity from the deuterium lamp decreases with increasing wavelength in this wavelength range.

In summary, the calibration and correction procedures shown here enabled us to extend the useful wavelength range of our spectrophotometer from a maximum A_{sample} value of ~1 to values approaching 1.5–1.8. Although it was previously well established that green food–coloring dye or related dyes can be used to assess the nonlinearity in spectrophotometers, to our knowledge, this is the first description of how information from such dyes can be used to correct absorbance values thereby extending the useful range of a spectrophotometer.

Section 4: Ca leaching from labware affected Ca standard measurements but should not have affected the $[Ca_T]_{WM}$ results based on Beer's law

Results in this section show that significant differences were often observed between measured and expected values of $[CaB]_S$, and that these differences were caused entirely, or in large part, by Ca leaching from two labware sources. Fig. S4 A plots the measured value of $[CaB]_S$ with no muscle present (Eq. 19b) versus the number of days after making the nominal 1.5-mM $CaCl_2$ solution used for the standard measurements. For the

Ca standard measurements for the results in Fig. S4 A, 9 µl of the nominal 1.5-mM $CaCl_2$ solution was added to a 0.45-ml sample (S_M) to give a nominal (or "expected") increase in [CaB] of 0.03 mM (as elsewhere, this concentration refers to the volume before adding the 9 µl). The nominal 1.5-mM $CaCl_2$ solution was made by multiple dilutions using highly purified water (>18 MΩ-cm) starting with a 0.1-M $CaCl_2$ standard (Fluka/Sigma-Aldrich), and it was stored in a glass scintillation vial at ∽4°C. Despite some scatter in the data, it is clear that measured values of $[CaB]_S$ near the start were close to, but somewhat greater than, the expected value of 0.03 mM, and then the values progressively increased with time, reaching values >33% (>0.04 mM) of the expected value within 120 d. As no other explanation seems plausible, the progressive increase is almost certainly caused by Ca leaching from the glass scintillation vial, increasing the $CaCl_2$ concentration by >33% (i.e., from ∽1.5 to >2.0 mM).

As an example of the scatter in the reported values of $[CaB]_S$ made on one day, the open circles on the right-hand side of Fig. S4 A plot $[CaB]_S$ values obtained with muscle present (Eq. 19a) along with their associated value of $[CaB]_S$ determined without muscle present (shown as a closed circle and plus symbol, the same closed circle and plus symbol that were plotted at 42 d). This result shows that there was significant scatter in the $[CaB]_S$ values even though they were expected to all have the same value. Similar variability in $[CaB]_S$ was observed in all of the experiments in which glass Pasteur pipettes were used to mix the added 9 µl of Ca standard with the A_M solution to give the A_S aliquot. (This was the mixing procedure used for all of the experiments in this Methods and Approaches article except for a couple of experiments performed after the discovery of this problem.) As described next, Ca was later found to leach from Pasteur pipettes during the mixing process, a source of Ca responsible, at least in part, for the variability of $[CaB]_S$ values.

Fig. S4 B plots the BAPTA absorbance at 292 nm of the usual measurement solution versus the number of exchanges of the solution with a Pasteur pipette. A single exchange consists of taking up almost all of the 0.45 ml of solution into the pipette and expelling it back into the cuvette. (Several exchanges of this type were used to convectively mix in the cuvette added EGTA so-

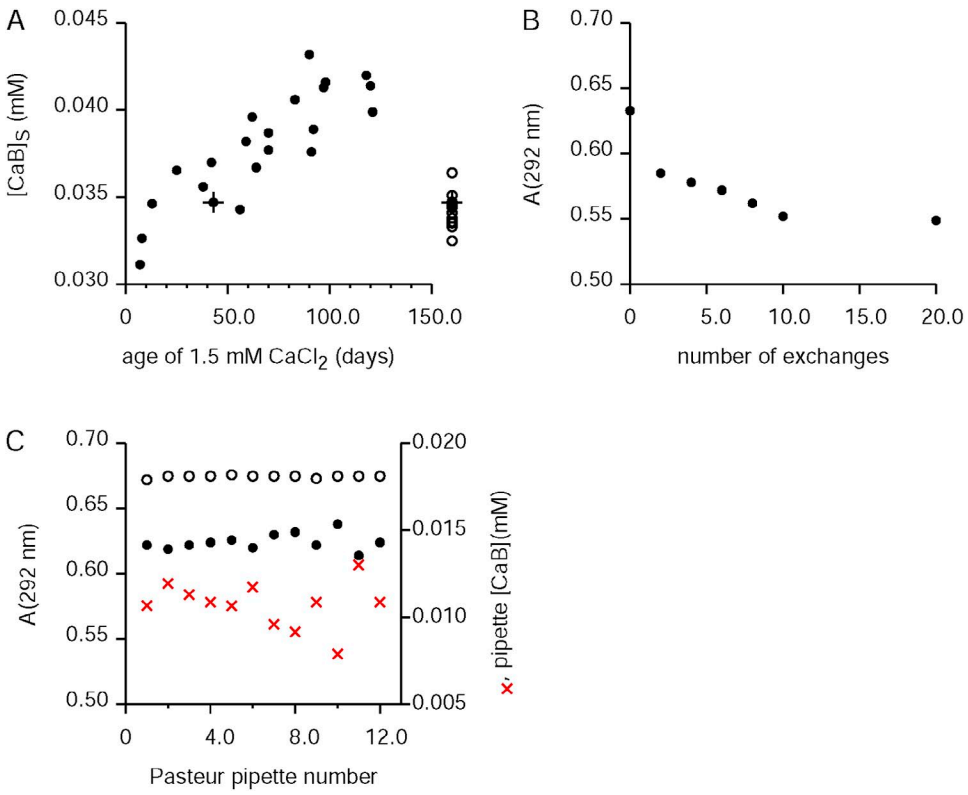

Figure S4. Ca leaching from labware used for Ca standard measurements. (A) The amount of Ca added with the Ca standard increased with time, an effect attributed to Ca leaching from the glass scintillation vial in which the 1.5-mM Ca standard was stored. (B) The decrease in BAPTA absorbance at 292 nm (increase in CaBAPTA concentration) versus the number of exchanges of the solution in the cuvette. An exchange is defined as taking the solution up into a glass Pasteur pipette and returning it to the cuvette. Several (two to four) such "exchanges" were generally used to mix added components (EGTA or Ca) into the cuvette, although nothing was added in this case. The decreased absorbance is attributable to Ca leaching from the Pasteur pipette. (C) The amount of Ca leached varies from pipette to pipette. See text for additional details.

lution, for the A_0 and S_0 aliquots, or added Ca solution, for the A_S, S_S, A_∞, and S_∞ aliquots.) There was a clear, progressive decrease in absorbance attributable to an increase in Ca attributable to Ca leaching from the Pasteur pipette, as it was made of soda-lime glass, which contains Ca.

The results in Fig. S4 C show tests of 12 different Pasteur pipettes to assess whether the amount of Ca leaching varies from one pipette to another. The open circles in Fig. S4 C show absorbance values of the usual measurement solution. The closed circles show the absorbance after two exchanges with the Pasteur pipette. The red X symbols plot the [CaB] value determined from the absorbance change (see Eq. 19b). The scatter in red X-symbol data can be explained by variation in the amount of Ca leached from the different Pasteur pipettes. The range of this scatter is similar to that seen with the open and closed symbols in Fig. S4 A (for the closed symbols, the scatter is not associated with the progressive increase in $[CaB]_S$), so it is likely that these variations are also caused by different degrees of Ca leaching from Pasteur pipettes.

It is noted that the average value for [CaB] caused by Ca leaching from the pipettes in Fig. S4 C was >0.01

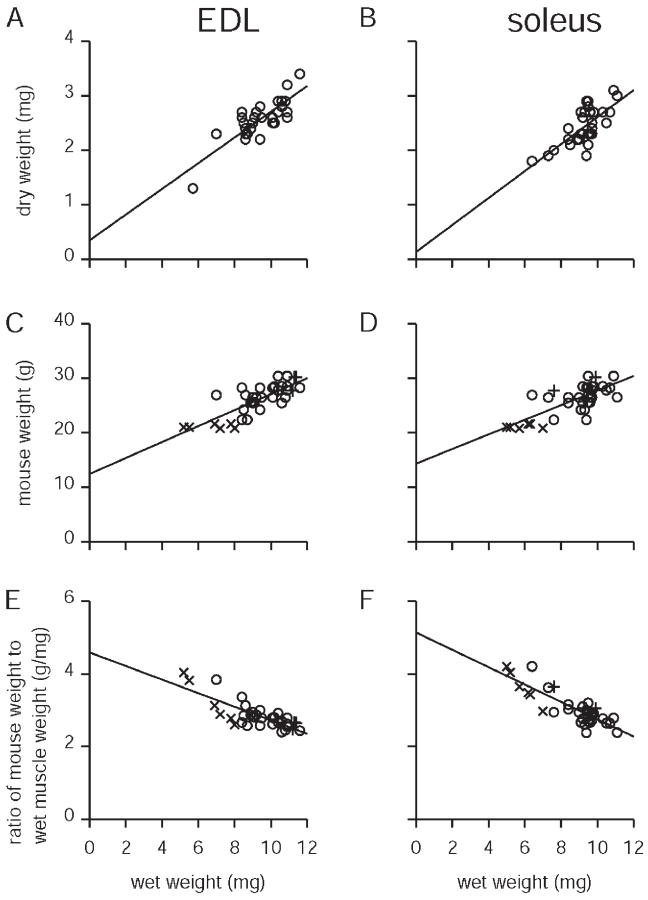

Figure S5. Plots versus wet muscle weights of dry muscle weight, whole mouse weight, and the ratio of whole mouse weight to wet muscle weight. As indicated, the panels on the left and right sides were obtained with mouse EDL and soleus muscles, respectively. The open circles in all six panels were taken from the same set of C57BL/6 mice ordered at the same time. The + and × symbols in C–F were from two other sets of mice plotted with the same symbols in Fig. 6. (See the legend of Fig. 6 for details about the mice used for these two sets.) All panels plot some variable with respect to the wet weight of the muscle on the abscissa. The top (A and B), middle (C and D), and bottom panels (E and F) plot, respectively, dry muscle weight, weight of the mouse from which the muscles were taken, and the ratio of mouse weight to wet muscle weight. Each panel shows the least-squares best-fit line to the data. The slopes (intercepts; p-values) of these lines are: (A) 0.236 mg/mg (0.347 mg; $P < 0.0001$), (B) 0.247 mg/mg (0.133 mg; $P < 0.0001$), (C) 1.464 g/mg (12.43 g; $P = 0.0054$, (D) 1.341 g/mg (14.32 g; $P = 0.0263$), (E) -0.187 g/mg^2 (4.59 g/mg; $P < 0.0001$), and (F) -0.239 g/mg^2 (5.14 g/mg; $P < 0.0001$). The average values (SEM; *n* values) for the variable plotted on the ordinates for the six panels are: (A) 2.57 mg (0.24 mg; 29), (B) 2.44 mg (0.06 mg; 32), (C) 26.1 g (0.5 g; 36), (D) 26.2 g (0.5 g; 38), (E) 2.85 g/mg (0.06 g/mg; 36), and (F) 3.03 g/mg (0.07 g/mg; 38). For the wet muscle weights (abscissa values) in A and B, the average values (SEM; *n* values) for EDL and soleus muscles were 9.43 mg (0.24 mg; 29) and 9.33 mg (0.18 mg; 32), respectively. For the wet muscle weights (abscissa values) in C and D (and E and F), the average values (SEM; *n* values) for EDL and soleus muscles were 9.32 mg (0.27 mg; 36) and 8.82 mg (0.26 mg; 38), respectively. The average ratios (SEM; *n* values) of dry to wet muscle weights for EDL and soleus muscles were, respectively, 0.242 (0.016; 29) and 0.262 (0.004; 32) mg/mg.

mM, which is about the magnitude of the largest unexpected increase in $[CaB]_S$ in A. This >0.01-mM magnitude is not readily reconciled with the early results in Fig. S4 A showing that the measured values of $[CaB]_S$ were close to the expected value of 0.03 mM, unless there was some difference in the Pasteur pipettes used for the experiments in A and C. This was likely the case, as the Pasteur pipettes used in C were purchased after all the data in A was obtained.

Fortunately, the problem of Ca leaching from Pasteur pipettes should not have impacted the main results in this study, as explained here. As noted above, because of this problem, the value of $[B_T]$ needed for obtaining the amount of Ca in a muscle sample was determined with the approach based on Beer's law (Eq. 6) instead of the approach based on the Ca standard (Eq. 8). Very importantly, the A_m and S_m aliquots did not require mixing, so they had no contact with a Pasteur pipette. Pasteur pipettes were used for mixing the A_0 and S_0 aliquots, but these involved adding excess EGTA, which would have bound essentially all of the Ca leached from the Pasteur pipette. In the case of the A_∞ and S_∞ aliquots, the extra Ca would not have been a problem, as the aim of these aliquots was to add excess Ca so that essentially all of the BAPTA was in the Ca-bound form. For the purpose in the article of comparing $A_M - A_S$ with $S_M - S_S$ to assess whether muscle affects the ability of BAPTA to detect Ca, the fact that Ca leached from the pipette should not be important (other than the added random variability) because samples with and without muscle were treated in the same way, including mixing of the A_S and S_S samples with Pasteur pipettes.

Section 5a: The inverse relationship between $[Ca_T]_{WM}$ and wet muscle weight is not caused by differences in fractional water content

As noted with Fig. 6, $[Ca_T]_{WM}$ (units of millimoles of Ca per kilogram of wet muscle weight) approximately doubled when wet muscle weight was halved over most of the range of muscle weights (from 12 to 6 mg) for both mouse EDL and soleus muscle samples. This means that the total Ca content of the muscle (product of $[Ca_T]_{WM}$ and wet muscle weight) did not change much. One possible explanation is that all of the muscle samples had about the same amount of solids (protein, lipids, and any other nonaqueous components), so that the greater wet weights were caused by greater fractional water contents in the muscle samples, a result of excess extracellular and/or intracellular water fractions, perhaps caused by the way the muscle samples were processed. For example, differences in the extracellular fractional water content could be caused by differences in the extent that water is removed from the muscle during the step of blotting the muscle sample on tissue just before weighing it, although such differences are expected to be minor. Because this explanation means dry muscle weight would remain constant and therefore not depend on wet muscle weight, the experiments in this section were performed to assess the possibility of variability in the fractional water content by adding dry muscle weight to the usual measurements.

The results in this section were from experiments performed in the usual way and with the same type and age range (4–6 mo) of the mice used in Fig. 6 (A and C), except that the muscle samples were dried. After measuring the wet muscle weight in the usual way, muscle samples were placed on squares of aluminum foil (⌣2-cm sides) and dried in an oven at 70°C for 42 h. A and B in Fig. S5 plot the dried muscle weights versus wet muscle weights for EDL and soleus muscle samples, respectively. The least-squares best-fit lines for both muscle types have y intercepts close to zero, indicating that the dry muscle weight is approximately proportional to wet muscle weight. If the range of muscle weights was totally attributable to differences in the fractional water content with no change in the total mass of proteins and other solids, the fitted lines in A and B would have been horizontal. This was not the case, as the slopes of the fitted lines were significantly different than zero (see legend to Fig. S5). Moreover, the y intercepts are very close to zero, indicating a proportional relationship between dry and wet muscle weights. This proportionality means that the inverse relationships between $[Ca_T]_{WM}$ and wet muscle weight in Fig. 6 were not caused by differences in the fractional water content.

Section 5b: Muscle weight versus mouse weight: Smaller muscles need to propel fractionally greater mouse body weights

C and D in Fig. S5 plot the weight of the mice from which the EDL and soleus muscles, respectively, were taken versus wet muscle weight. The positive slopes were again significantly different than zero, indicating that a lighter muscle weight tended to be associated with a lighter mouse. The positive y intercepts indicate that the muscle weights are not proportional to mouse weights; rather, the muscle weights vary over a fractionally greater range than the mouse weights.

E and F in Fig. S5 plot the ratio of mouse weight to wet muscle weight versus wet muscle weight for the same data points shown in C and D, respectively. Again, the least-squares best-fit slopes are significantly different than zero. These results support the explanation for the inverse relationship between $[Ca_T]_{WM}$ versus muscle weight given with Fig. 6 in the main text. The muscle fibers in the smaller muscles would tend to have a higher relative workload because of their greater mouse weight to muscle weight ratio and that some, as yet unknown, mechanism sensing this greater workload somehow increases the concentration of total Ca in the muscle fibers to produce a greater specific force.

The lines in E and F in Fig. S5 were used to generate the linear scales at the top of the panels in Fig. 6 in the main text. The reason for this is that mouse weights were not measured for most of the points in Fig. 6, with the important exception of the data points plotted with + and × symbols in B and D of Fig. 6 (plotted with the same symbols in Fig. S5, C–F), as the values of *R* and muscle weights associated with these points span most of the ranges for these parameters. The linear relationships are expected to apply to the data in Fig. 6, even though more than half of the *R* versus muscle weight data points used for these relationships (the open circle symbols) were from a different set of mice. As seen in E and F of Fig. S5, the least-squares best-fit lines provide a good fit to all of the *R* versus muscle weight data. Moreover, the same relationship between *R* and muscle weight would be expected, as the muscle strains were the same or very similar, and the age of the mice were in the same range, 3–6 mo.

Section 5c: Apparent nonreproducibility in $[Ca_T]_{WM}$ results is attributable to contamination of the muscle samples by aluminum

A and B in Fig. S6 plot $[Ca_T]_{WM}$ versus wet muscle weight for most of the muscles reported in Fig. S5 (not all of the muscles were analyzed). As in Fig. 6 in the main text, the least-squares best-fit lines again show marked inverse relationships between $[Ca_T]_{WM}$ and muscle weight. However, as described here, there were problems with the set of $[Ca_T]_{WM}$ values shown in these panels that are likely caused by contamination with aluminum from the aluminum foil used to dry the muscle. The solid line in A and B show the least-squares best-fit line to the plotted points. The hashed line in A and B shows the least-squares best-fit line to the data in Fig. 6 (A and C, respectively). To help with the comparison, these best-fit lines and the data from Fig. 6 (A and C) are also plotted in C and D, respectively, of Fig. S6. Despite the fact that the sets of mice used for the top and bottom panels were from the same strain (C57BL/6) and were within the same age range (4–6 mo), the results for the two sets were significantly different. The main differences are: (a) the slopes of the fitted lines (see legend to Fig. S6) for the points in the top panels are three to four times greater than those in the bottom panels; (b) the average values (see legend to Fig. S6) are 61 and 93% greater for the EDL and soleus muscles data, respectively; and (c) the data points are much more scattered. As seen in Fig. 6 (B and D), the $[Ca_T]_{WM}$ versus muscle weight results from several different sets

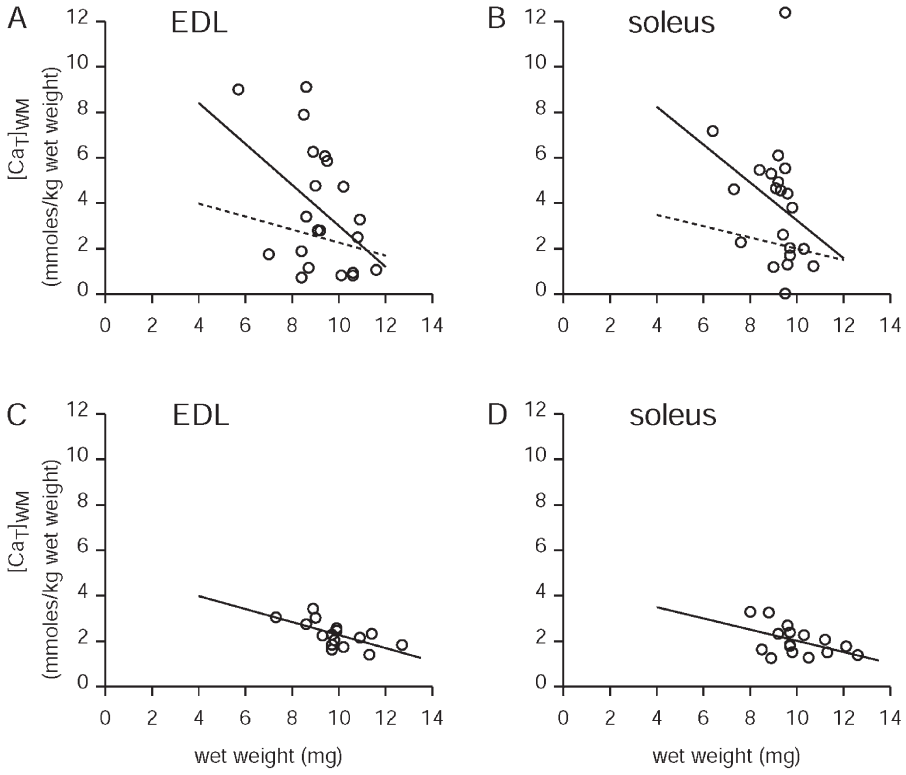

Figure S6. Plots of $[Ca_T]_{WM}$ values versus wet muscle weights for EDL (A and C) and soleus muscles (B and D). The results in A and B are from the set of mice used for the experiments in Section 5. The results in C and D are from the set of results plotted in Fig. 6 (A and C, respectively). The solid line in each panel shows the least-squares best-fit line to the data. The slopes in units of millimoles/kilogram wet weight per milligram wet weight (intercepts in units of millimoles/kilogram wet weight) of these lines are: (A) −0.902 (12.02), (B) −0.834 (11.58), (C) −0.287 (5.13), and (D) −0.247 (4.48). The average values of $[Ca_T]_{WM}$ for the four panels are: (A) 3.70, (B) 3.97, (C) 2.30, and 2.06 mmoles/kg wet weight. See text for additional details.

of muscles were reasonably well described by the same fitted line, indicating that the results were reproducible. Because the results with the dried muscle samples in Fig. S6 (A and B) are markedly different, this indicates that the BAPTA method is either nonreproducible or that something else occurred with these experiments. Results given next show that the $[Ca_T]_{WM}$ values with the dried muscles are unreliable. Results discussed afterward indicate that the greater apparent $[Ca_T]_{WM}$ values are very likely the result of contamination by aluminum ions (Al^{3+}). Collectively, these results mean that the discrepancies between the top and bottom panels in Fig. S6 are not caused by nonreproducibility with the BAPTA method.

Each point in Fig. S7 plots $[Ca_T]_{WM}$ for a muscle taken from the right side of a mouse versus $[Ca_T]_{WM}$ for the muscle sample taken from the left side of the same mouse (i.e., paired samples). A and C were obtained with EDL muscles, and B and D were obtained with soleus muscles. The muscles for the top panels (A and B) were not dried, whereas those for the bottom panels (C and D) were dried on aluminum foil. The lines in each panel correspond to the situation that the left- and right-side values exactly match (i.e., they have slopes of 1 and intercepts of 0). The data in A and the corresponding data for soleus muscles from the same mice shown in B are from the set of results shown in Fig. 6, also shown above in Fig. S6 (C and D). Although there is some deviation from equality, the data without drying do approach the expectation of equality between $[Ca_T]_{WM}$ between paired left and right muscle samples. In contrast to the expectation of approximately equal values for left and right muscle samples from the same mouse, the data obtained with drying on aluminum foil in the bottom panels are very scattered. (Note the greater than twofold difference in the scales in the bottom vs. top panels in Fig. S7, so that the discrepancy is even greater than it appears by a visual comparison between the bottom and top panels.) The lack of equality between the $[Ca_T]_{WM}$ values for the paired dried muscle samples is considered as evidence that the results are unreliable.

As noted above, the experiments with the dried muscle samples were performed as those in Fig. 6 were, with the exception of the drying process. The only difference that we can think of that could reasonably explain the results is that Al^{3+} from the aluminum foil leached into the muscle samples during the drying process. The possibility that Al^{3+} could interact with BAPTA was assessed by adding Al^{3+} in the same way used for Ca standard measurements (9-µl additions of 45 mM aluminum sulfate introduced into 0.45-ml samples of the usual measurement solution, resulting in an addition of 0.9 mM of Al^{3+}). This maneuver resulted in an initial decrease in BAPTA absorbance measured at 292 nm (de-

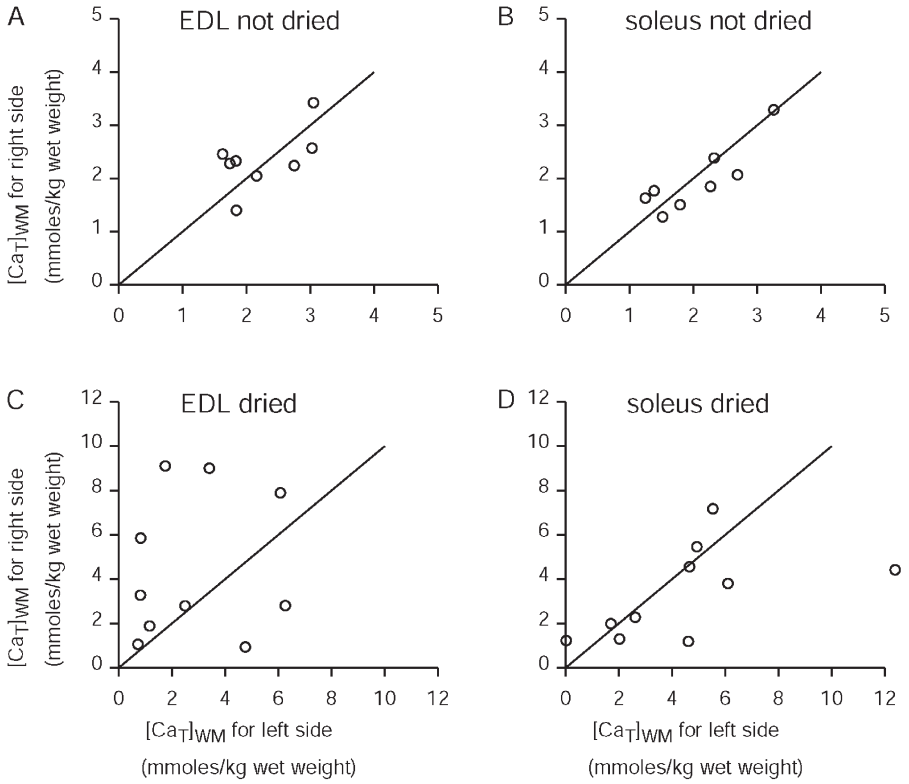

Figure S7. Plots of $[Ca_T]_{WM}$ values from muscles taken from the right side of a mouse versus the left side. A and B are from the results for EDL and soleus muscles, respectively, in Fig. 6 (A and B) in the main text. C and D are from EDL and soleus muscles, respectively, from the set of mice used for Section 5. See text for additional details.

noted "A(292)") to significantly less than half of the initial value. Curiously, A(292) increased approximately exponentially, approaching a steady level within a few minutes that was ∼10% less than the initial value of A(292) before adding Al^{3+}. Subsequent additions of the same amount of Al^{3+} displayed decreases in A(292) of about the same magnitude (by ∼10%) as that produced in the steady level with the first 9-µl addition of aluminum sulfate, although without the initial, much larger decrease in A(292) and subsequent recovery. We do not have a simple explanation for the initial decrease and subsequent recovery seen only with the first 9-µl addition, although it may have something to do with the precipitation of Al^{3+} as aluminum hydroxide known to occur at neutral and basic pH levels. If the value of the initial large decrease in A(292) to less than half of the initial was the correct value to use for the purpose of estimating the K_d for Al^{3+} binding to BAPTA, a very rough estimate for this K_d would be near, although somewhat <1 mM. If the steady levels are the appropriate values to use, the results above give a very rough estimate for the K_d of ∼5 mM (5 mM is the approximate concentration needed to reduce the steady value of A(292) to about half its initial value). As with Ca binding, adding EGTA reverses the decrease in BAPTA absorbance. Because the addition of 1 mM EGTA (9-µl addition of 50 mM EGTA into 0.45-ml cuvette) completely or nearly completely reverses the decrease in A(292) by 0.9 mM aluminum sulfate, these preliminary results indicate that EGTA binds Al^{3+} with high affinity. In regards to the initial aim of these experiments, the main conclusion from these preliminary results is that Al^{3+} does appear to bind to BAPTA, reducing its absorbance, and EGTA competes the Al^{3+} off BAPTA. Therefore, contamination by Al^{3+} could be interpreted as Ca^{2+} binding with the BAPTA method. We conclude with near certainty that this is what occurred with the dried muscle samples caused by leaching from the aluminum foil used in the drying procedure. Different degrees of leaching would explain the greater scatter in the data compared with the earlier results (top vs. bottom panels in Fig. S6) and the marked non-equality of $[Ca_T]_{WM}$ values from paired left and right muscles (bottom panels in Fig. S7). The three- to fourfold steeper slopes of the least-squares best-fit lines in the top panels in Fig. S6, giving the appearance of more pronounced inverse relationships between $[Ca_T]_{WM}$ and muscle weight, could be explained by greater Al^{3+} leaching into smaller muscles as a result of their greater surface to volume ratios.

Section 6: Possible explanation for two outlier points and criterion used to reject them

Two $[Ca_T]_{WM}$ data points, termed outliers, were considered unreliable and were rejected because their values were significantly out of the range of the other values in their set, and because there is a reasonable explanation for why this might have occurred (of the total number of points in this study from 148, 31, and 16 from, respectively, mouse, frog, and rat muscle samples, only one point from the mouse and one point from the frog muscle samples were rejected). The criterion for rejecting the points was that their values were greater than three standard deviations than the mean of the remaining points in their group. There was no reason to suspect any bimodal distribution in the data, as sets of data had normal distributions as assessed by approximately linear normal probability plots (not depicted; for the sets with the outlier points, their distributions also appear normal without the outlier points). Neither of the outliers was from the main set of control muscles, and each of these points is discussed in the main text. The two outliers were not included in the final averages for the dataset to which they belonged (one point is in Fig. 7 A, and the other is from a frog muscle exposed to normal Ringer's solution for 1 h). Part of the justification for rejecting these points from the final averages is that it is quite possible that they occurred because of experimental error as explained here. For a given muscle sample, the four aliquots were measured in the order A_M, A_0, A_S, and A_∞, and similarly for the background solution measurements, S_M, S_0, S_S, and S_∞. As a result, the first measurement in the next sample (A_M or S_M) came after the sample with excess Ca from the preceding sample. Although care was taken to thoroughly rinse the cuvette before introducing a new aliquot, it is possible that a small amount of the high Ca solution in the A_∞ (or S_∞) aliquot was not removed, thereby increasing the Ca in the following A_M (or S_M) aliquot.

Section 7: Predictions of the degrees to which $[Ca_T]_{WM}$ would be reduced by CSQ KO

To interpret the results with CSQ knocked out in EDL muscle, it is helpful to first estimate the total Ca present in normal muscle minus that bound to CSQ. This estimate, to follow, gives the predicted value of $[Ca_T]_{WM}$ with CSQ KO assuming that the only effect of the KO was to remove the Ca component bound to CSQ. For this purpose, the SR component of total Ca ($[Ca_T]_{SR}$) for Eqs. 23a in the main text is separated into free Ca^{2+} ($[Ca^{2+}]_{SR}$) and bound Ca ($[CaBound]_{SR}$), as given by the following equations:

$$[Ca_T]_{WM} = [Ca_T]_{EC} + [Ca_T]_{NonSR} + [Ca^{2+}]_{SR} + [CaBound]_{SR}. \quad \text{(S26a)}$$

Similar to Eqs. 23b–23d in the main text, this relationship in fractional terms is given by

$$1.0 = f_{EC} + f_{NonSR} + f_{SR\_free} + f_{SR\_bound}. \quad \text{(S26b)}$$

$$\text{EDL muscle: } 1.0 = 0.11 + 0.12 + 0.026 + 0.744 \quad \text{(S26c)}$$

$$\text{soleus muscle: } 1.0 = 0.11 + 0.02 + 0.030 + 0.840 \quad \text{(S26d)}$$

As with Eqs. 23c and 23d, Eqs. S26c and S26d give estimated values for the fractions of $[Ca_T]_{WM}$ associated with the different components in EDL and soleus muscles, respectively. The sums of f_{SR_free} and f_{SR_bound} are 0.77 and 0.87 for Eqs. S26c and S26d, respectively, the same values given for f_{SR} in Eqs. 23c and 23d, respectively. The ratios of f_{SR_free} and f_{SR_bound} were determined from the estimated ratio of 1 free Ca^{2+} ion for 28 bound Ca atoms in the SR (Fénelon et al., 2012). As covered in the Introduction of the main text, results of Fénelon et al. (2012) with frog twitch muscle indicate that at least 80% of the Ca in the SR at rest is bound to CSQ, although this percentage would be closer to 97% if CSQ were the only source of bound Ca in the SR CSQ. (97% is from the ratio of 1:28 for free Ca^{2+} to bound Ca.) Based on results with mammalian skinned fibers, Murphy et al. (2009) concluded that Ca-binding sites on CSQ account for all of the maximal bound Ca in the SR, indicating that Ca-binding sites on CSQ are, in fact, the only nonnegligible sites for bound Ca in the SR. With the bound form of Ca in the SR all attributed to CSQ and with the above assumptions, CSQ KO is predicted to reduce $[Ca_T]_{WM}$ to 0.256 (1 − 0.744) and 0.160 (1 − 0.840), respectively, of the values for EDL and soleus muscles from WT mice.

REFERENCES

Fénelon, K., C.R.H. Lamboley, N. Carrier, and P.C. Pape. 2012. Calcium buffering properties of sarcoplasmic reticulum and calcium-induced Ca^{2+} release during the quasi-steady level of release in twitch fibers from frog skeletal muscle. *J. Gen. Physiol.* 140:403–419. http://dx.doi.org/10.1085/jgp.201110730

Frings, C.S., and L.A. Broussard. 1979. Calibration and monitoring of spectrometers and spectrophotometers. *Clin. Chem.* 25:1013–1017.

Godt, R.E., and B.D. Lindley. 1982. Influence of temperature upon contractile activation and isometric force production in mechanically skinned muscle fibers of the frog. *J. Gen. Physiol.* 80:279–297. http://dx.doi.org/10.1085/jgp.80.2.279

Harrison, S.M., and D.M. Bers. 1987. The effect of temperature and ionic strength on the apparent Ca-affinity of EGTA and the analogous Ca-chelators BAPTA and dibromo-BAPTA. *Biochim. Biophys. Acta.* 925:133–143. http://dx.doi.org/10.1016/0304-4165(87)90102-4

Murphy, R.M., N.T. Larkins, J.P. Mollica, N.A. Beard, and G.D. Lamb. 2009. Calsequestrin content and SERCA determine normal and maximal Ca^{2+} storage levels in sarcoplasmic reticulum of fast- and slow-twitch fibres of rat. *J. Physiol.* 587:443–460. http://dx.doi.org/10.1113/jphysiol.2008.163162

Pape, P.C., D.-S. Jong, and W.K. Chandler. 1995. Calcium release and its voltage dependence in frog cut muscle fibers equilibrated with 20 mM EGTA. *J. Gen. Physiol.* 106:259–336. http://dx.doi.org/10.1085/jgp.106.2.259

Tsien, R.Y. 1980. New calcium indicators and buffers with high selectivity against magnesium and protons: design, synthesis, and properties of prototype structures. *Biochemistry.* 19:2396–2404. http://dx.doi.org/10.1021/bi00552a018